

UNIVERSITÀ DEGLI STUDI DI PADOVA

Corso di Laurea in Medicina e Chirurgia

Dipartimento di Scienze Cardio-Toraco-Vascolari

e Sanità Pubblica

Direttore: Prof. Federico Rea

U.O.C. Cardiocirurgia Pediatrica e Cardiopatie Congenite

Direttore: Prof. Vladimiro Vida

TESI DI LAUREA

Congenital TrainHeart:
development of a fully 3D printed simulator
for hands-on surgical training

Relatore: Prof. Vladimiro Vida

Laureando: Francesco Galliotto

ANNO ACCADEMICO: 2021/2022

TABLE OF CONTENTS

<i>ABSTRACT</i>	1
<i>RIASSUNTO</i>	2
<i>I. INTRODUCTION</i>	3
1. Congenital Heart Disease	3
1.1 Premises.....	3
1.2 Cardiovascular Embryology.....	5
1.3 Classification	11
1.4 Clinical Presentation	17
1.5 Diagnosis.....	18
1.6 Treatment	22
2. 3D technologies	24
2.1 3D segmentation and Computer-Aided Design (CAD)	24
2.2 3D printing	25
2.3. 3D bioprinting	28
2.4. Usage of 3D printing in cardiovascular sciences	32
3. Surgical simulation in Congenital Heart surgery	36
3.1 Premises.....	36
3.2 Animal-based Simulation and wet Lab	36
3.3 3D printed simulators.....	38
3.4 “Hybrid” simulation.....	40
<i>II. AIM OF THE THESIS</i>	41
4. Rationale of the study	41
5. Purpose of the study	41
<i>III. MATERIALS AND METHODS</i>	43
6. Chest wall simulator development	43
6.1 Crucial aspects	43
7. Procedure-specific model development	49
7.1 Low fidelity models.....	49
7.2 Intermediate fidelity models.....	50
8. Printing process and materials	56
<i>IV. RESULTS</i>	61

9. Chest wall simulator	61
9.1 Evolution.....	61
9.2 Final version: “Congenital TrainHeart”	63
9.3 Accessories	65
9.4 Future directions.....	69
10. Models and surgical procedures.....	70
10.1 Purse strings and central cannulation	70
10.2 Patch positioning.....	72
10.3 Vascular anastomosis	73
10.5 Sinus venosus ASD.....	77
10.6 Coarctation of the aorta	79
10.7 CABG platform for distal anastomosis.....	80
10.8 Surgical aortic valve replacement	83
10.9 Surgical Planning	85
<i>V. DISCUSSION</i>	<i>89</i>
11. A new era for Congenital heart surgery training	89
12. Advantages	91
13. Disadvantages and Limitations	92
14. Cost analysis.....	94
<i>VI. CONCLUSIONS</i>	<i>97</i>
<i>BIBLIOGRAPHY</i>	<i>99</i>
<i>Ringraziamenti</i>	<i>107</i>

ABSTRACT

Background: With the growing expectation of a perfect outcome for patients undergoing cardiac surgery, it is now imperative to find alternative surgical training methods for residents and fellows. However, surgical simulation usually requires a fair amount of funds and manpower to establish a reliable program. For this reason, the increasing interest in the 3D printing field allowed the development of new technologies that found immediate application in surgical simulation.

Aim of the study: This thesis illustrates the development of a low-cost 3D printed simulator for congenital and acquired cardiac surgery.

Materials and methods: A simulator was designed to replicate position, view, and exposure of the heart within the chest wall using different approaches (median sternotomy, mini-sternotomy, subaxillary, and posterior mini-thoracotomy). All components were designed using a 3D modeling software and printed using a stereolithography 3D printer. All models that come with the simulator were designed using the same CAD software used for the chest simulator or using 3D reconstruction software for CT or MRI scans.

Results: The simulator consists of a chest wall cavity with an oval opening on the top simulating a median sternotomy. The simulator can be attached to a tripod, allowing for height adjustments and pitch-and-roll movements. In addition, five different covers were designed to modify the opening, thus allowing to replicate minimally-invasive surgical approaches. The fully printed design made it possible to significantly reduce the cost of the entire product. All models are printed with a special elastic resin which makes it possible to cut and suture all structures.

Conclusion:

A novel low-cost fully 3D printed simulator was developed. This may represent a valid tool for high fidelity simulation programs in congenital and acquired cardiac surgery in addition to a patient-specific surgical planning.

RIASSUNTO

Introduzione: Con la crescente aspettativa di un perfetto outcome per i pazienti sottoposti a interventi di cardiocirurgia, risulta fondamentale sviluppare e utilizzare nuove modalità per la formazione dei giovani chirurghi. Tuttavia, ad oggi, l'organizzazione di corsi di simulazione risulta dispendioso sia in termini di risorse economiche che di personale. Proprio per questo, il crescente interesse collettivo verso la stampa 3D ha permesso di sviluppare nuove tecnologie che possono essere efficacemente utilizzate nell'ambito della simulazione cardiocirurgica.

Obiettivo dello studio: Questa tesi descrive lo sviluppo di un simulatore a basso costo stampato in 3D che può essere utilizzato sia nell'ambito delle cardiopatie congenite che di quelle acquisite

Materiali e metodi: Il simulatore è stato sviluppato in modo tale da simulare posizione, visuale ed esposizione del cuore all'interno del torace in diversi approcci chirurgici. Tutte le componenti del simulatore sono state progettate tramite un software di modellazione 3D e stampati con stampante 3D a stereolitografia. I modellini da inserire all'interno dello stesso simulatore sono stati a loro volta sviluppati o tramite l'utilizzo dello stesso software o sfruttando tecniche di ricostruzione 3D a partenza da immagini TC o RMN.

Risultati: Il simulatore si compone di una struttura che simula la cavità toracica con una apertura ellittica nella parte superiore atta a simulare una sternotomia mediana. Il simulatore può essere fissato ad un treppiede permettendo aggiustamenti per quanto concerne l'altezza, nonché movimenti di inclinazione e rotazione. In aggiunta, sono state realizzate quattro cover che permettono di modificare l'apertura sulla parte superiore del simulatore, al fine di simulare accessi di tipo mininvasivo. I modellini sono stati invece stampati con una resina elastica che, date le sue caratteristiche, può essere tagliata e suturata.

Conclusioni: Il nuovo simulatore stampabile in 3D che è stato sviluppato potrebbe rappresentare uno strumento estremamente valido per le simulazioni cardiocirurgiche ad alta fedeltà e per il planning personalizzato di una procedura.

I. INTRODUCTION

1. Congenital Heart Disease

1.1 Premises

Congenital heart disease (CHD), also known as congenital heart defects, includes a broad spectrum of anomalies of the heart and great vessels that arise before birth and derive from an altered embryological development of the cardiovascular tract. When referring to CHD, defects such as conduction system anomalies or cardiomyopathies are excluded, even if these are present at birth, because of the different clinical presentations.

For what concerns epidemiology, Congenital Heart Disease can be found in 19-75 of every 1.000 live birth, with incidence increasing if fetuses who do not survive to the end of the pregnancy are included (1). To all newborns with CHD is estimated that 50-60% of them will need at least one surgical operation, with 30% requiring medical procedures right after birth. The peak of deaths is represented by the first 28 days, with, on the other hand, 97% of the patients surviving at least to the age of 1, and 95% at least to the age of 18. All these patients can suffer from secondary heart disease later in life due to the surgical procedures needed to fix the heart in the first place (2).

The most common CHD is Ventricular Septal Defect (VSD), followed by Transposition of the Great Arteries (TGA) and Tetralogy of Fallot (TOF).

Nowadays, these conditions are considered multifactorial as long as specific causes haven't been found yet, reducing our possibility of preventing them during or before pregnancy. However, thanks to the improvement of ultrasound imaging, prenatal diagnosis is widespread in the most advanced countries, reducing mortality due to late postnatal diagnosis.

In the devolvement of these conditions, the main drive is represented by mutations of the regulators of heart development during embryogenesis but, also environmental factors are implied (3). For what concerns the latter, infection such as the ones included in the TORCH complex (Toxoplasma, Rubella, Cytomegalovirus, Herpes Simplex) or exposure to specific drugs such as Thalidomide or Angiotensin Receptors Blockers, should be considered; also, one

other significant risk factor is the presence in the family of close relatives with a CHD showing how genetic plays a critical role in the etiology of these conditions(4). Thanks to development made in the understanding of how heart cells develop, nowadays it is known that all cells type in the cardiovascular lineage (Myocardial, endocardial and smooth muscle) come from common precursors that differentiate into specific cell types. Regulation and expansion of all these cell types are driven by the WNT families of secreted molecules (5,6).

Genetics studies have identified numerous genes responsible for inherited and sporadic heart diseases, most of them encoding for transcription factors implied in specific events in cardiac development such as ventricular separation or formation of the outflow tract. Also, signaling protein defects are involved in the development of some CHD and in particular, these anomalies can underlie valvular diseases. A notable example is the NOTCH pathway: this signaling protein is expressed in the endocardium of the great vessels where it plays an important role in determining valve formation. Some studies showed how NOTCH1 mutation could lead to a broad spectrum of conditions such as aortic stenosis, VSD, and TOF (7)

Stated that some genes have a strong association with CHD, it should be considered how also some aneuploidy syndromes are strongly related to congenital heart defects. In particular, Down syndrome (Trisomy 21) has shown to have a strong association with CHD (40-50%), most commonly with the atrioventricular septal defect (AVSD), patent ductus arteriosus, and Tetralogy of Fallot. Turner syndrome is associated in most cases with Aortic Coarctation or anomalies of the aortic valve, such as a bicuspid aortic valve. Williams syndrome (Deletion of 7q11) correlates to supravalvular aortic stenosis, while Trisomy 18 (Edwards syndrome) and trisomy 13 (Patau syndrome) are associated with atrial septal defect, ventricular septal defect, and patent ductus arteriosus.

One other consideration that must be done is that the heart is functioning while developing, resulting in the fact that also hemodynamic modification inside the heart can lead to an altered evolution of the organ itself. The concept of “No flow- No growth” is widely known, underlying the fact that a reduction of the blood flow through a structure determines a much slower or incomplete formation of the structure itself. To exemplify, an altered mitral valve with a reduced orifice lumen can lead to an underdevelopment of the left ventricle and the ascending aorta.

All developmental defects described can occur at any stage of heart formation resulting in a broad spectrum of morphological abnormalities that sometimes are incompatible with life itself, resulting in the termination of pregnancy. Moreover, the fact that many genetic and environmental factors are implied can partially explain the high variability of CHD.

1.2 Cardiovascular Embryology

The cardiovascular system of the embryo starts its development from the lateral mesoderm, around the third week of gestation, when the nutrition of the embryo itself cannot be guaranteed by the diffusion mechanism anymore. Cardiac cells precursor, which commitment is induced by signals from the adjacent endoderm (MBP, FGF, Hedgehog, Wit ligands, and TGF family), at this point migrate and form the Primary heart field (PHF), from which the heart chambers develop, and the secondary heart field (SHF) from which the conotruncus arises. Cells in the SHF show laterality, with the right-sided cells being responsible for the formation of the left part of the conotruncus and the left ones accountable for the formation of its right part. This property derives from the same molecular signals responsible for laterality in the whole embryo, such as 5HT and expression of transcription factor PITX2. Lineage analysis has demonstrated that cells in the caudal cardiogenic mesoderm contribute to the atria, whereas cells in the rostral cardiogenic mesoderm contribute to the ventricles (8).

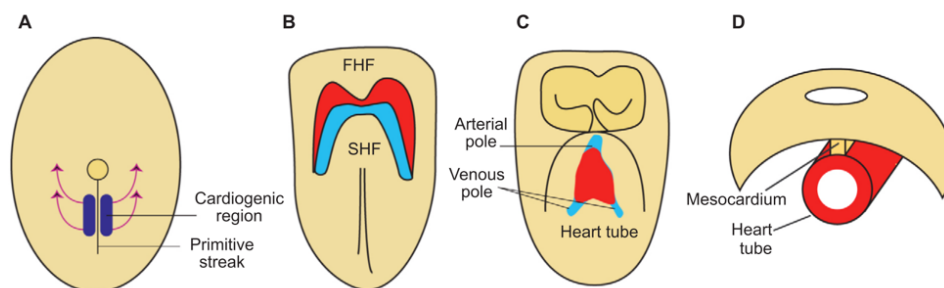


Figure 1 - First developmental steps of the cardiocirculatory tract. (A) Cardiac progenitors migrate cranially along the primary streak. (B) Formation of the Primary/First Heart Field (FHF) and Secondary heart field (SHF). (C) and (D) Formation of the heart tube. (From “Lin C-J, Lin C-Y, Chen C-H, Zhou B, Chang C-P. Partitioning the heart: mechanisms of cardiac septation and valve development. *Development*. 2012;139(18):3277-3299”).

Both heart fields appear as islands of cardiogenic precursor cells that get together to form a horseshoe-shaped region called “cardiac crescent” or “cardiogenic field”. At this point, bilateral cardiac primordia occur in a rostral to caudal direction forming the primitive linear heart tube with the addition of the pericardial mesoderm at its caudal end (9,10).

After the formation, the heart tube, which presents an internal coating made of endothelial cells and an external one made of myocardial cells, undergoes a process of elongation due to the recruiting of cells coming from the SHF; this process is fundamental to the normal development of the conotruncus and part of the right ventricle. Anomalies of this elongation process can result in CHD such as DORV, VSD, and Tetralogy of Fallot.

Around the 23rd day of gestation, a folding process begins. The heart tube assumes an S-shaped form with asymmetry about the anterior-posterior, left-right, and dorsal-ventral axes in a rightward looping. During this process, local enlargements of the tube are visible. The atrial portion forms a common atrium, the AV junction remains narrow, while the primitive ventricle, divided in a cranial part from which derives the right ventricle and a caudal area from which derives the left one, appears enlarged as well. At this point, two more segments can be visualized in the cranial portion, conotruncus, and aortic sac. In the first place, all structures appear smooth on the inside except for the portion from which the left ventricle arises that appears trabeculated.

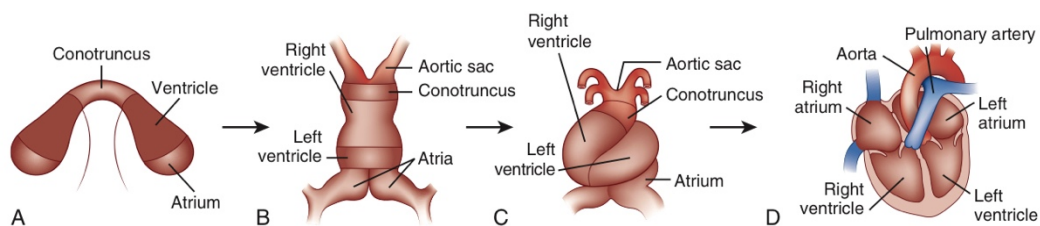


Figure 2 - Model of cardiogenesis. Cardiogenic precursors, bilaterally positioned in the lateral plate mesoderm, contain pre patterned information regarding their ultimate positional identity and cell fate, as modeled by color code (A). The convergence and fusion of the cardiac primordia form a linear heart tube (B), which undergoes rightward or D looping (C). Rightward looping appropriately aligns the cardiac chambers for morphogenesis into the mature four-chambered structure (D). (Adapted from Allen HD, Gutgesell HP, Clark EB, et al, editors: Moss and Adams' heart disease in infants, children, and adolescents: including the fetus and young adult, ed 6, Philadelphia, 2001, Lippincott Williams & Wilkins, p 4, Figure 1.1.)

Cardiac septation begins around the 27th and 37th day of gestation and can be defined as the process that leads to the formation of the four heart chambers, two

atria and two ventricles, and the division of the conotruncus in the Aorta and Pulmonary artery. In order to achieve a correct separation, four main structures must develop correctly: atrial septum, atrioventricular junction, ventricular septum, and outflow tract of the infundibular septum. In this morphogenetical process, a correct formation of the so-called atrioventricular cushions must occur as these structures are involved in the formation of the atrial and ventricular septum as well as in the formation of the AV valves resulting, if altered, in CHD like Atrial Septal defect (ASD), ventricular septal defect (VSD) or defects of the great vessels like Tetralogy of Fallot or Transposition of the great arteries. It's important to underline that complete septation of the heart is not necessary for the embryo's survival, which may in part explain the high incidence of septation defects seen in clinical practice. The atrial separation process sees, at first, around the fifth week of gestation, the formation of the septum primum that develops from the dorsal wall of the atrium and grows toward the AV cushions. This septum is not complete due to the presence of the ostium primum, a fenestration on the lower part of the septum (the one close to the AV cushions), resulting in a maintained communication between the atria, which is necessary to allow the oxygen-rich blood coming from the inferior vena cava, to shunt from the right side to left side of the heart. With the development of the AV cushions, the septum primum closes; however, before this process completes, a second fenestration in the central/upper part of the septum, called Ostium Secundum, appears. At this point, septum secundum develops. However, this structure does not completely divide the atria allowing blood to shunt between the right and left atrium as in the previous step. After birth, when lungs expand and pulmonary resistances decrease, the shunt reverses, and the septum secundum collapses on the septum primum, resulting in the closure of the atrial communication.

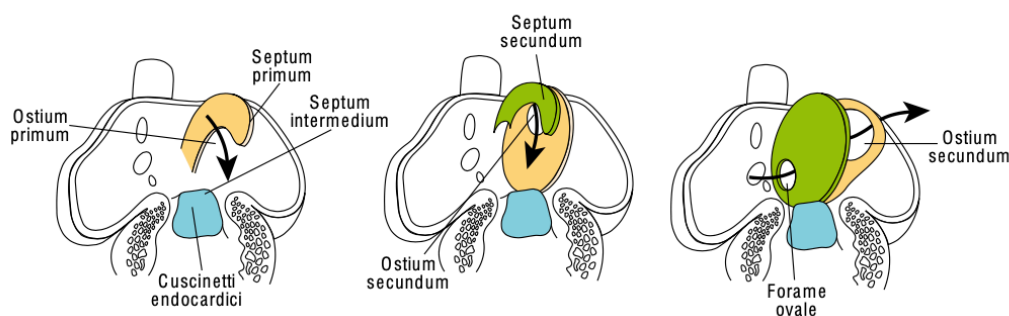


Figure 3 - Formation of the interatrial septum (From “De Felici M, Boitani C, Bouché M, et al. *Embriologia Umana. III edizione. PICCIN Nuova Libreria; 2020*”).

Ventricular septation starts from the fourth week of gestation when both primitive ventricles increase their volume by the continuous growth of the myocardium in the external portion. The medial walls of both growing ventricles gradually join, thus forming the muscular septum that does not entirely separate the right and left cavities as long as the cranial part of the septum itself develops afterward from atrioventricular cushions during the atrioventricular junction formation.

To complete heart separation also the atrioventricular junction should develop correctly. Endocardial cushions play a fundamental role in this process as they contribute to both atrial and ventricular separation, with an abnormality resulting in an ostium primum atrial septal defect, in an inlet type ventricular septal defect or, in an Atrioventricular canal defect.

Of primary importance is also the correct development of the outflow tract. In the first place, the outflow tract appears as a tubular structure that connects the primary right ventricle and the aortic sac, and, in order for the pulmonary artery and the aorta to develop, septation must occur. In addition, considering that at first, this structure communicates only with the right ventricle, continuity with the left ventricle must be gained. During this process, called wedging, the subaortic conus undergo remodeling allowing the aortic valve to reach its final position (11). For what concerns separation, two crests arise from the conotruncus, the right conotruncal crest and the left conotruncal crest; simultaneously, the anterior atrioventricular cushion grows towards the outflow tract, combining with both conotruncal crests thus dividing pulmonary artery and aorta. Also, the cardiac outflow tract receives a significant contribution of cells from the neural crest, a population of migratory pluripotent cells that arise adjacent to the developing neural tube (12).

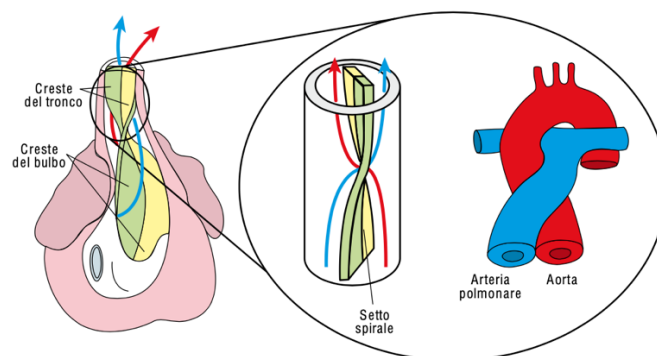


Figure 4 - Formation of the aortopulmonary septum (From “De Felici M, Boitani C, Bouché M, et al. *Embriologia Umana*. III edizione. PICCIN Nuova Libreria; 2020”).

Supporting this theory, murine and avian models where the neural crest was ablated resulted in abnormalities of the heart and great arteries, while the murine one developing CHD such as persistent truncus arteriosus, Double outlet right ventricle (DORV), and Tetralogy of Fallot (12,13). Alongside genetic factors, also environmental factors play an important role in outflow tract formation; one of the most important is retinoic acid, the active derivative of vitamin A, as shown on murine models with knockout of retinoic acid receptor, which mimics the neural crest ablation phenotype. (14–16)

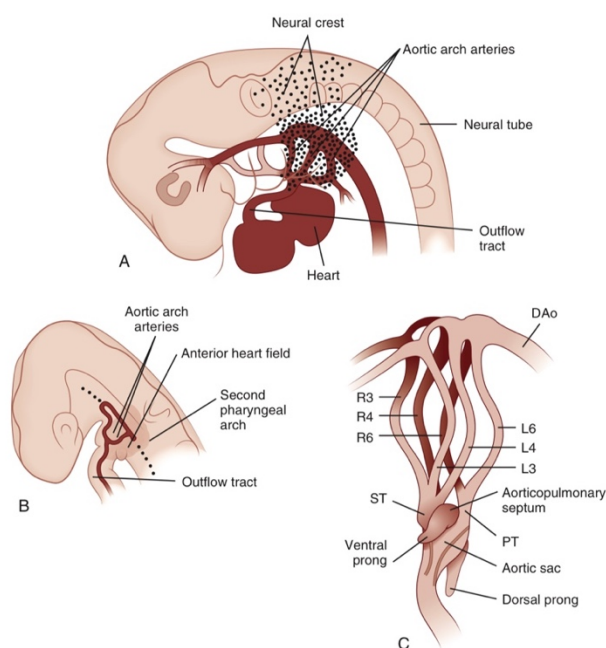


Figure 5 - Development of neural crest, anterior heart field, and outflow tract. (A) The cardiac neural crest migrates into pharyngeal arches 3, 4, and 6, where it plays a crucial role in patterning the paired aortic arch arteries by preventing the regression of aortic arch arteries 3, 4, and 6, the precursors of the definitive great arteries. (B) The anterior heart field is a recently described and separate migratory population of cells that originate near the second pharyngeal arch and contribute to cardiac outflow tract development. (C) Aortic Arches.

(A and C from “Harvey RP, Rosenthal N, editors: *Heart development*, San Diego, 1999, Academic Press, pp 180, 182”; B modified from “Waldo KL, Kumiski DH, Wallis KT, et al: *Conotruncal myocardium arises from a secondary heart field. Development* 128:3179–3188, 2001”).

Between the fourth and fifth week of gestation, five pairs of arteries arise from the aortic sac, a dilated portion in the cranial part of the truncus arteriosus. Since the fifth pair usually does not develop, aortic arches are named I, II, III, IV, and VI. After the first month, the first and the second arches regress, leaving residues that will form small arteries in the head. From the III aortic arch internal and external carotid arteries arise, while the fourth is implied in the formation of the common

carotid and subclavian in the left part and subclavian artery on the right side. From the sixth aortic arch, also called “pulmonary arch,” arises the proximal portion of the pulmonary artery on the right side, whether the left side forms the ductus arteriosus, the structure that allows blood to shunt between the aorta and the pulmonary artery.

For what concern valves, atrioventricular and semilunar evolve from different structures. The former develops after the fusion of the endocardial cushions from areas of mesenchymal tissue in the upper part of the ventricles, whether the latter arises during the outflow tract septation process.

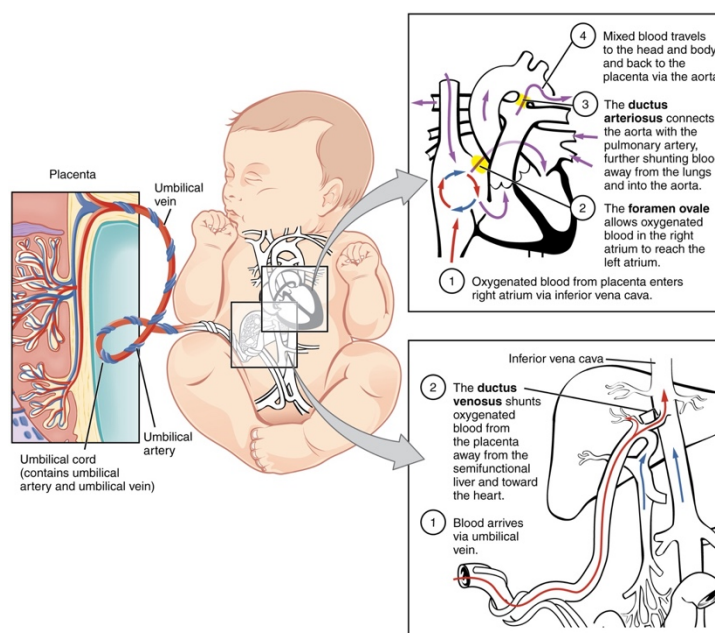


Figure 6 - Development of Blood Vessels and Fetal Circulation - Anatomy and Physiology
(From “OpenStax Accessed: 2022-03-27).

After describing the morphogenesis of the heart, it’s important to underline how fetal circulation differs from postnatal. In the fetus, oxygen-rich blood coming from the placenta through the umbilical vein shunts the liver thanks to the Ductus Venosus, and reaches the right atrium through the inferior vena cava. The right atrium also collects the oxygen-poor blood coming from the superior vena cava. Once in the right atrium, blood can flow in two directions: towards the left atrium, passing through the foramen ovale or towards the right ventricle. Due to the fact that pulmonary vascular resistance is high in the fetus, most of the blood reaches the left ventricle, passes the mitral valve, and is ejected in the ascending aorta. The smaller amount of blood that gets into the right ventricle is ejected in the pulmonary artery but shunts to the aorta thanks to the presence of the ductus arteriosus. Closure

of the Ductus arteriosus generally occurs a few hours after birth due to contraction of its walls; this step is mediated by bradykinin, whether definitive obliteration occurs by intimal proliferation between the first and the third month after birth in most cases. In some patients, an alteration of this process can lead to a condition called Patent Ductus Arteriosus. Closure of the foramen ovale occurs as well a few hours after birth due to the increased pressure in the left atrium in association with a reduction in the right one, deriving from the lowered pulmonary resistance.

1.3 Classification

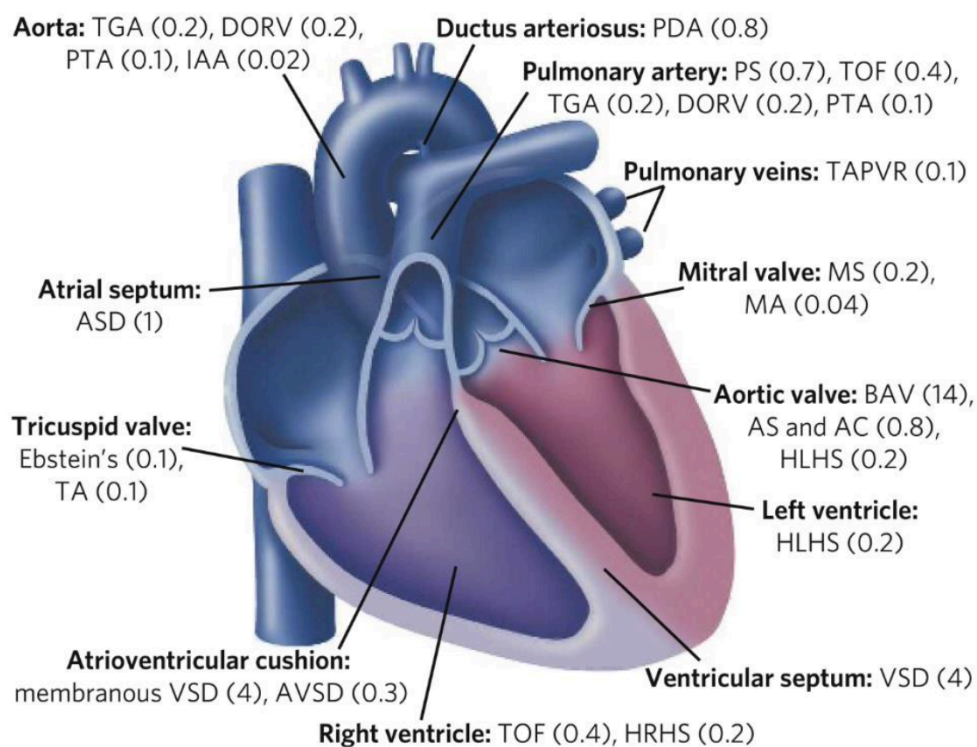


Figure 7 - Congenital heart defects. This adult heart diagram illustrates the structures affected by congenital heart diseases, with the estimated incidence of each disease per 1,000 live births indicated in parentheses. AC, aortic coarctation; AS, aortic stenosis; ASD, atrial septal defect; AVSD, atrioventricular septal defect; BAV, bicuspid aortic valve; DORV, double outlet right ventricle; HLHS, hypoplastic left heart syndrome; HRHS, hypoplastic right heart; IAA, interrupted aortic arch; MA, mitral atresia; MS, mitral stenosis; PDA, patent ductus arteriosus; PS, pulmonary artery stenosis; PTA, persistent truncus arteriosus; TA, tricuspid atresia; TAPVR, total anomalous pulmonary venous return; TGA, transposition of the great arteries; TOF, tetralogy of Fallot; VSD, ventricular septal defect. (Adapted from "Bruneau BG. The developmental genetics of congenital heart disease. *Nature*. 2008;451(7181):943-948").

Congenital heart disease (CHD) consists of anomalies of the heart which can affect venous drainage, septation or connection between its segments, and the function of the valve apparatuses. Typically, the heart is composed of three main segments, atria, ventricles, and great arteries, which connection allows oxygen-poor blood to flow through the pulmonary artery into the lungs and oxygen-rich blood to return from the lungs and flow through the aorta into the systemic circulation thus forming small and great circulation. The disposition of the segments listed above is characterized by no communication between the two circulations, with the exception of the pulmonary capillaries.

Being CHD a vast spectrum of conditions with high intra and inter-individual variability, this section will describe two ways of classifying congenital heart defects: the anatomical and the pathophysiological.

The morphological classification is based on a sequential approach, describing the characteristics of all three heart segments, atria ventricles and arterial trunks, and their reciprocal connections. Two independent groups coordinated by Richard Van Praagh in the US and Maria Victoria de la Cruz in Mexico City developed this system.

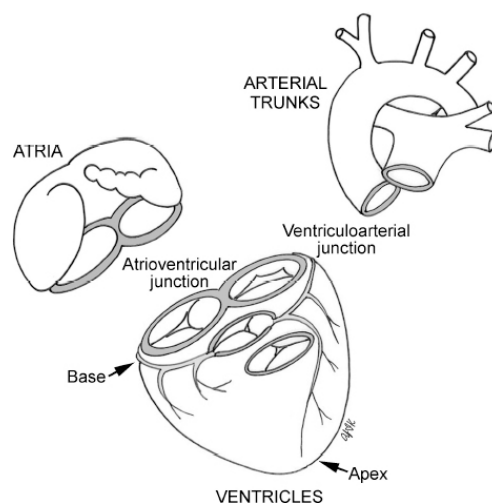


Figure 8 -The three segments: Atria, Ventricles and arterial trunks. (From “G. Thiene and C. Frescura, “Anatomical and pathophysiological classification of congenital heart disease,” in *Cardiovascular Pathology*, Sep. 2010, vol. 19, no. 5, pp. 259–274. doi: 10.1016/j.carpath.2010.02.006”).

The first step of this approach consists of describing each cardiac segment's situs. In the “Situs solitus”, the most common condition, the morphologically right atrium is located on the right side of the heart while the morphologically left atrium is on

the left side. In this condition, the trilobate lung is positioned on the right side of the chest while the bilobate one is on the left side. In the “Situs Inversus” however, the disposition is mirrored. In addition, conditions where there is no laterality can be identified, creating the category of the "Situs Ambiguus”. In this case, both atria and lungs can show isomerism. Isomerism can be right or left, with the former condition characterized by two atria that appear morphologically right and the latter where atria appear both morphologically left; in this case, also lungs can be both bilobate (as the left one) or trilobate (as the right one). Isomerism can also associate with polysplenia or asplenia, with heterotaxy of the abdominal organs. It’s also interesting to highlight how right isomerism is frequently associated with anomalous pulmonary venous drainage while the left one, with a persistent left superior vena cava draining in the coronary sinus.

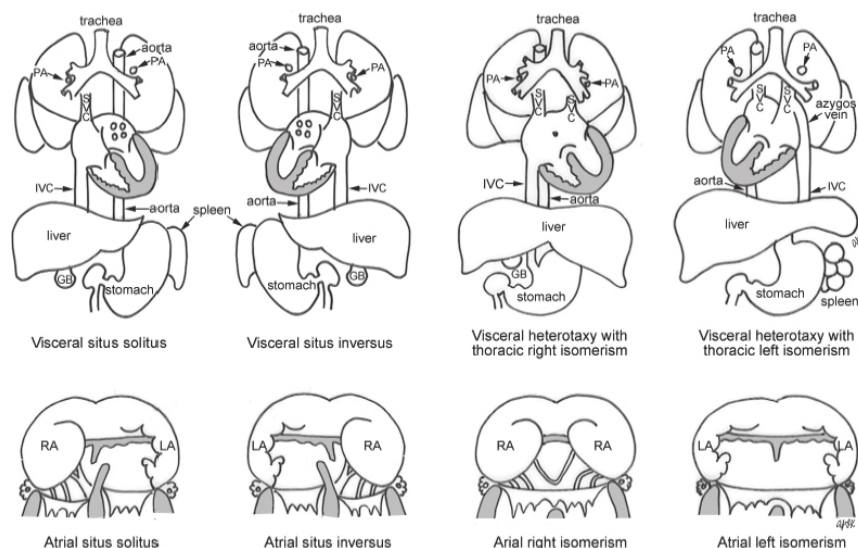


Figure 9 – Representation of the different patterns of atrial and visceral situs. (From “G. Thiene and C. Frescura, “Anatomical and pathophysiological classification of congenital heart disease,” in *Cardiovascular Pathology*, Sep. 2010, vol. 19, no. 5, pp. 259–274. doi: 10.1016/j.carpath.2010.02.006”).

Once atria localization has been established, the second step consists in determining atrioventricular connection that can be biventricular or univentricular. In the first case, each atrium connects with one ventricle in a way that can be concordant or discordant. In the concordant AV connection, the right ventricle is connected with a morphologically right ventricle, with the same happening for the left atrium and ventricle. In the discordant AV connection, as it happened in the L-TGA, the right atrium relates to a morphologically left ventricle, with the same happening on the other side of the hearth. In univentricular AV connection, both atria communicate

with only one ventricle, which can be morphologically right or left due to the absence of AV valves or abnormal/absent development of one of the two ventricles. The last step aims to describe ventriculoarterial connection (VA connection). As described for AV connection, also in this case we can identify two main conditions: VA concordance and VA discordance. In the first case, the pulmonary artery arises from the morphologically right ventricle while the left one is connected with the Aorta. In the second scenario, the right ventricle connects with the aorta while the left one with the pulmonary artery, resulting in the two circulations, great and small, being parallel.

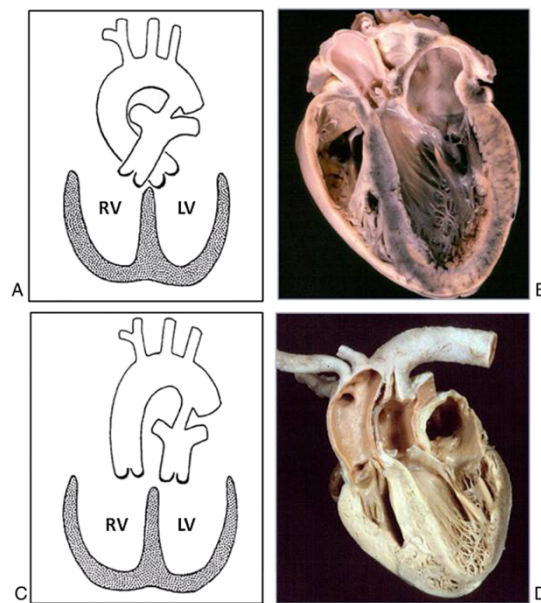


Figure 10 - VA connection. (A and B) Schematic representation and anatomical specimen of discordant VA connection. LV: left ventricle; RV: specimen of concordant VA connection. (C and D) Schematic representation and right ventricle. (From “G. Thiene and C. Frescura, “Anatomical and pathophysiological classification of congenital heart disease,” in *Cardiovascular Pathology*, Sep. 2010, vol. 19, no. 5, pp. 259–274. doi: 10.1016/j.carpath.2010.02.006”)

In addition, two more conditions can be described: Double outlet and single outlet VA connection. In the double outlet VA connection both great arteries arise from one ventricle while in the Single outlet, only one great artery originates from the heart. After describing the structural classification, the pathophysiological classification, based on the clinical consequences of the heart anomalies, will be described in the next paragraph. Five main categories of CHD can be identified: increased pulmonary blood flow, decreased pulmonary blood flow, obstruction to blood

progression with no septal defects, conditions so severe to be incompatible with postnatal blood circulation, and CHD silent till adult age.

The first category, CHD with increased pulmonary blood flow, is characterized by communication between the right and the left side of the heart resulting in a left to right shunt. These communications can occur on various sites, including the venous pole, as in the partial anomalous pulmonary venous return (PAPVR), atria (ASD), AV junctions, as in the Atrio-Ventricular septal defects both partial and complete (AVSD), Ventricles (VSD), Aortopulmonary septum as in Persistent Truncus Arteriosus or in the aortopulmonary window, with the last one being a communication between the great arteries just above semilunar valves. Also, Patent ductus arteriosus can be added to this category.

The increased pulmonary blood flow results in various consequences on the lungs. In the first place, patients presenting these heart anomalies are more likely to develop lungs infection that can severely impact their survival. On the other hand, the pulmonary overload, both from pressure and volume, determines intimal proliferation in lungs vessels, increasing pulmonary resistance, which, in the most severe condition named "Eisenmerger syndrome", can lead to a reversion of the shunt (from left to right to right to left shunt) resulting in cyanosis. Due to all these considerations, it appears clear why these CHDs should be surgically corrected early in life, usually within the first two years.

The second category includes CHDs characterized by decreased blood flow to the lungs, usually resulting in a right to left shunt, which leads to cyanosis because oxygen-rich blood mixes with oxygen-poor blood, decreasing its oxygen saturation before being ejected into the systemic circulation.

In this group of anomalies, we can find Isolated pulmonary artery stenosis, Tetralogy of Fallot (TOF), Tricuspid Atresia, Ebstein's anomaly of the tricuspid valve, and single ventricles with pulmonary stenosis.

TOF can present itself in a broad spectrum of severity from slight pulmonary stenosis to pulmonary atresia. In this last case, blood reaches the lungs through a reverse flow through PFO or thanks to systemic collateral arteries arising from the descending aorta; this second scenario can lead to an increased pulmonary blood flow due to left to right shunt established, causing obstructive pulmonary vascular disease. In Tricuspid atresia, blood shunts from the right to the left atrium, through the Foramen Oval, reaches the left ventricle, and is forwarded to the Aorta, while a

small part reaches the pulmonary circulation thanks to the presence of a restrictive VSD that allows left to right shunting.

The third group, CHD with obstruction to blood progression and no septal defect, includes Pulmonary stenosis, Aortic stenosis, both classifiable in subvalvular, valvular, and supra-valvular, and Coarctation of the Aorta. This last CHD is characterized by the presence of a plication right after the insertion of the ductus arteriosus at the isthmus level, which determines an obstruction to blood flow. The plication itself seems to be caused by an excess of ductal tissue that wraps the isthmus aorta; this tissue shrinks, responding to bradykinin stimulation a few hours after birth, resulting in a reduction of the aortic lumen. In this scenario, additive blood flow to the lower part of the body is granted by collateral circulation through the internal mammary arteries and intercostal arteries. It's interesting to underline how symptoms can occur in the first days after birth or, in the less severe forms, in adults according to the severity of the obstruction.

The fourth category includes three main types of CHD joined by incompatibility with postnatal blood circulation. The first group, Ductal-Dependent CHD, includes Pulmonary atresia, Mitral or Aortic atresia, and Severe coarctation of the aorta or hypoplastic/interrupted aortic arch. In all these cases, blood flow to the descending aorta is granted by ductus arteriosus, and prostaglandins therapy right after birth is mandatory for the patient's survival. In the same category also CHD with parallel systemic and pulmonary circulation are present, including complete transposition of the great arteries (TGA), where the pulmonary artery arises from the left ventricle while the aorta arises from the right one. In TGA it's fundamental to have connections between the two circulations to allow deoxygenated and oxygenated blood to mix. In addition to maintaining the ductus arteriosus opened with prostaglandins, if no defects such as ASD or VSD are present, the patient must undergo an endovascular procedure a few hours after birth, called Rashkind procedure, with the aim of creating a communication between the right and left atrium. The third group that can be found in this category is the Anomalous connection/obstruction of the pulmonary veins, as in the Total Anomalous Pulmonary venous return, a condition that can be classified into supra cardiac, infra cardiac and intracardiac, and Scimitar syndrome.

The peculiarity of this category is that all conditions included are perfectly compatible with intrauterine life due to the function of the placenta and the fact that lungs do not function, and the pulmonary circulation is almost entirely bypassed.

One last category is represented by CHDs which remains silent until adult age like Bicuspid Aortic Valve, the most common CHD with an incidence of 2% in live births, Anomalies of the coronary arteries, and Congenitally corrected transposition of the great arteries. This last condition is characterized by both Atrioventricular and Ventriculoarterial discordance resulting in a morphologically right ventricle receiving blood from the left atrium and ejecting it into the aorta, with a morphologically left ventricle receiving blood from the right atrium and pumping it into the pulmonary artery.

In addition to these two anomalies also Wolf Parkinson White syndrome can be classified in this category as well (17).

1.4 Clinical Presentation

Clinical presentations of CHD are highly heterogeneous and are directly related to the type of anomaly involved and its severity. In some cases, when the heart defect is not severe, symptoms can appear only in adult age.

CHD characterized by an increased blood flow to the lungs, like VSD, ASD or AVSD, usually determines an increased probability of developing pulmonary infection. In addition, patients can present signs of congestive heart failure. In these cases, dyspnea and tachycardia can usually be found. Another symptom is the fatigue that, in newborns, makes feeding much more difficult, leading to a low caloric intake, generally determining a regular growth in height but not in weight. Peripheral edema can also be present. It should also be considered how, if these patients are treated late in life, a pulmonary hypertensive crisis can happen right after the surgery due to the long-term remodeling of the pulmonary vessels.

CHD characterized by low blood flow to the lungs or right to left shunt are usually associated with cyanosis, a change in body tissue color to a bluish-purple that appear when oxygen levels in the arterial blood are low. More specifically, this condition can be encountered when deoxygenated hemoglobin levels are higher than 5g/100 ml in venous capillary blood. In heart anomalies where the pulmonary valve or the RVOT is stenotic, the right ventricle is overloaded and, if the anomaly

is not corrected, hypertrophy of ventricular myocardium with an increased risk to developing heart failure can occur.

In the same way, conditions characterized by a stenotic left efflux determine hypertrophy of the left ventricle and, in addition, reduced peripheral perfusion, also leading to dyspnea, chest pain due to the reduction of the blood flow into coronaries arteries, and syncopation.

For what concern auscultation is interesting to underline, for what concern septal defects like ASD or VSD, how in evaluating the severity of the condition, duration of the murmur is way more important than its intensity. For example, in the VSD case, high-intensity murmurs, but with a short duration, are usually associated with small defects due to the high gradient between the right and left ventricle. On the other hand, huge septal defects determine an equilibrium between the two chambers' pressure, leading to a low-intensity murmur but with a longer duration.

1.5 Diagnosis

At the end of the 19th century, Sir William Osler, in his classic textbook, in the five pages dedicated to “Congenital Affections of the Heart,” sentenced that “these [disorders] have only limited clinical interest, as in a large proportion of cases the anomaly is not compatible with life, and in others, nothing can be done to remedy the defect or even to relieve symptoms” (18).

This statement resulted in little attention given to CHD diagnosis that, at the time, was mainly based on physical examination, auscultation, electrocardiography, and chest x-Ray, until the 1960s when also cardiac catheterization and angiography were introduced. With the evolution of medicine and the progressive improvement of surgical techniques, CHD gained more interest and diagnostic tools were developed in order to identify these conditions not only in postnatal life but also during intrauterine life, resulting in a significant improvement in patient's survival. One of the most important tools, Ultrasound, a technology developed by sonar used in submarines during WWII, was used at first in the 1970s. At this point, however, this technology was rudimental, and only M-mode was available, and this imaging technique proved to be insufficient in identifying the CHDs. However, due to the rapid evolution of Ultrasound technologies, allowing two-dimensional visualization

of cardiac structures, diagnosis of CHD was finally possible. Also, thanks to the introduction of the Doppler ultrasound, a deeper analysis of blood flow and hemodynamics was made possible. Nowadays, Ultrasound is used for both prenatal and postnatal diagnosis, and also for surgical planning. In the last twenty years, two new technologies entered the spectrum of available tools for CHD diagnosis: Computer Tomography (CT) and Magnetic Resonance Imaging (MRI).

For what concerns prenatal diagnosis of CHD, it usually occurs between the 18th and the 22nd week of gestation, a period when all structures are completely formed, and the fetus is big enough to adequately evaluate all organs. In exploring the heart's morphology with ultrasound, four main projections must be obtained: four chambers, three vessels (with trachea when possible) and the equivalent of the parasternal long axis (PLAX) and parasternal short-axis (PSAX) in post-natal evaluation.

The four-chamber view allows the visualization of both ventricles and both atria and can be used to evaluate the presence of ASD, VSD, and AVSD. This view also assesses whether the pulmonary veins are connected to the right or to the left atrium. In this specific view, sometimes also the coronary sinus can be visualized. In the three-vessels view, superior vena cava, ascending aorta, and the main pulmonary artery in a transverse section can be visualized, defining their reciprocal anatomical relationship and the one with the airways. The three vessels view is also used to compare aortic and Pulmonary artery diameters to identify conditions where one of the two vessels is underdeveloped, like in Hypoplastic Left Heart Syndrome where the ascending aorta is usually very small or enlarged, as it can happen due to stenosis of one of the two semilunar valves and the consequent accelerated and turbulent blood flow.

The parasternal long-axis (PLAX) is used to evaluate the left ventricular inflow and outflow tract as it allows the visualization of the left atrium, mitral valve, left ventricle, aortic valve, and ascending aorta. For what concerns the equivalent of the PSAX in the adult, this view shows, when correctly archived, in its center the aortic valve while, all around it, the left and right atria, Right AV continuity with the tricuspid valve, right ventricle inflow and outflow tract, and the main pulmonary artery bifurcating into the left and right pulmonary branches. This particular view can also help, using the color-doppler, to identify subaortic VSD and pulmonary stenosis/obstruction or underdevelopment of the pulmonary artery or of its

branches. It should be considered that fetal cardiac ultrasound is usually utilized in all cases where a CHD is suspected because of the presence of risk factors such as maternal drug usage during the first trimester or genetic abnormalities diagnosed with other exams such as amniocentesis or chorionic villus sampling. Even if technology has improved a lot in the last year, it should be considered that this imaging technique presents some limitation, mainly due to the fact that all structure examined are very small and located quite far from the transducer (ultrasound have to trespass maternal abdominal walls, uterine wall, amniotic sac and fluid, in addition to the fetus's chest), with minor defects that cannot be adequately identified. With the constant improvement of Ultrasound technology, it is possible nowadays to obtain a 3D reconstruction of the fetus's heart that can be used to help parents understand the CHD of their baby; the medical staff can also use the same model to confirm the diagnosis or in by teachers for teaching purposes. Even if, to this days it's challenging to create these patient-specific models, software to rapidly reconstruct cardiac anatomy will likely be available soon. Research is also moving rapidly for what concerns the application of Artificial Intelligence (AI) to the prenatal diagnosis of CHD to make this process easier and less operator-dependent. Since Ultrasound is a sensible technique that doesn't expose the patient to ionizing radiation, it appears to be one of the most used imaging tools in the primary diagnosis or confirmation of congenital heart defect also in postnatal life.

One other imaging technique currently used in the evaluation of patients with CHD is CT. This technique uses a rotating X-ray tube and a row of detectors placed in the gantry to measure X-ray attenuations by different tissues inside the body. Due to the fact that CT exposes patients to ionizing radiation or, in some cases, to contrast medium, the usage of this imaging technique should be tailored and used only when necessary for the diagnosis or for surgical planning. Moreover, the American College of Cardiology sees cardioTC as the only option when there are contraindications to the MRI exam, such as the presence of a pacemaker or an ICD or even claustrophobia (19).

Nowadays, ECG-gated spiral scans are employed for CHD imaging, a technique that synchronizes the tomographic acquisition with the cardiac cycle to obtain still images of the heart. The temporal resolution appears to be one of the most critical parameters to obtain usable images since patients with CHD usually present a high heart rate and a limited ability to cooperate.

CardioTC is also used, in association with the intravenous injection of iodine-based contrast medium, to study the morphology of the coronary arteries, representing a quicker way to evaluate the presence of congenital or acquired anomalies in comparison to cardiac angiography, which is still in use mainly for patients with a high chance of also needing a therapeutic intervention (20).

In addition to cardioTC and Echocardiography, also MRI is widely used for CHD evaluation. This technique has been widely adopted in this field because it can characterize anatomy, function, blood flow, and tissue dynamics using protocols that include cine acquisitions in various orientations, flow quantitation using phase-contrast velocity encoding, and angiographic data after administration of intravenous contrast (21). One of the main advantages of cardiac MRI is the total absence of radiation, which makes it suitable for young patients decreasing their risk associated with ionizing radiation, in addition to its flexibility in comparison to other imaging techniques as it allows the production of an infinite number of projections, including custom ones to address any special clinical needs.

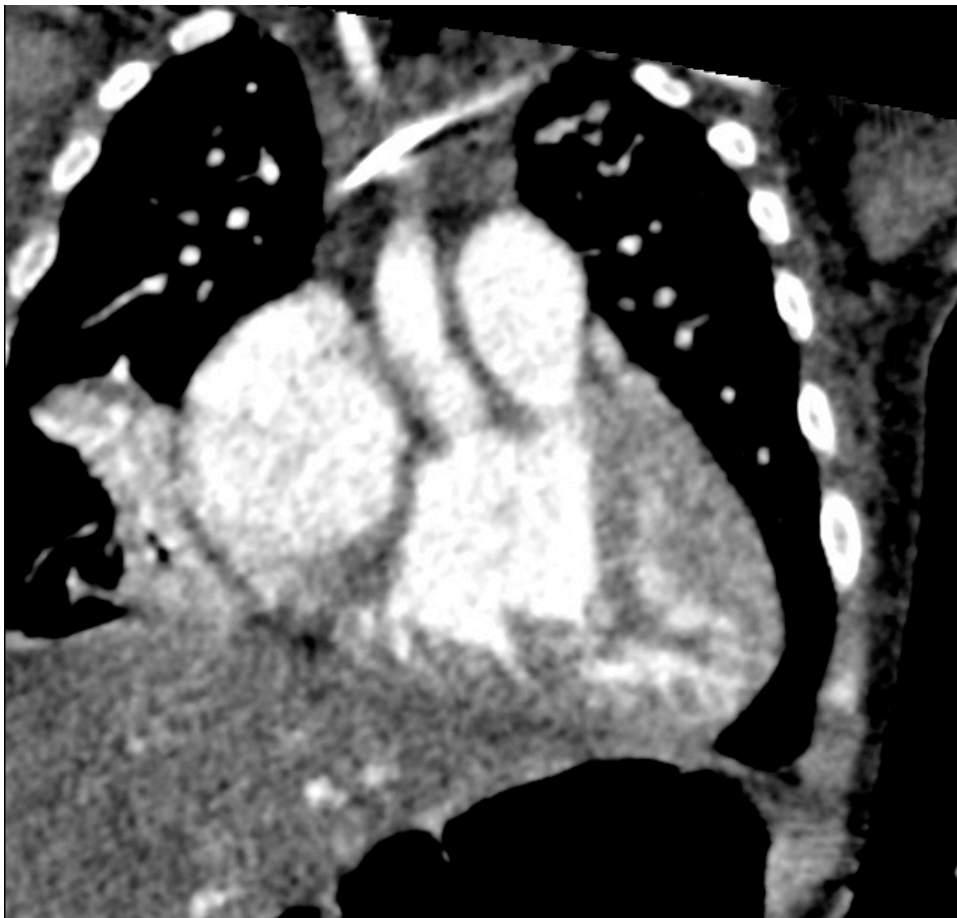


Figure 11 – TC frame showing a double outlet right ventricle: Aorta and Pulmonary Artery are both arising from the right ventricle. The right atrium is also visible.

1.6 Treatment

Even if transcatheter procedures are rising as an interesting tool to approach these conditions, the treatment of Congenital Heart disease remains mainly surgical. A third option is also available, the "watch and wait", applied to small septal defects, both atrial or ventricular, that, due to their dimension, have a high probability of closing spontaneously. The same approach can be applied to all L-TGA cases where the patient is asymptomatic and has no need for a surgical procedure. For what concerns open heart surgery, most procedures are run with the usage of cardiopulmonary bypass, which is necessary to oxygenate and pump blood while the patient's heart is arrested, allowing the surgeon to open atria or ventricles and repair the defect. The heart-lung machine isn't always used, as it happened for some palliative procedures, like in the modified BT shunt positioning.

In describing the different approaches used to access cardiac structures, it's possible to identify many ways to reach the heart and great vessels. The first approach is the median sternotomy, the most commonly used incision to enter the anterior mediastinum. For what concern minimally invasive approaches, we can find mini-sternotomy, where the incision is made from the mid-portion of the sternum to the tip of the xiphoid process, and anterior or anterolateral thoracotomy, an approach used mainly for ASD or VSD repair (22–24).

In CHD surgery is fundamental to divide procedures into two categories: Palliative and Corrective. Palliative procedures include operations to reduce the patient's symptoms or elongate the patient's life expectancy without however leading to normal heart morphology or circulatory physiology.

This group includes the Modified Black Taussig shunt, a conduit connecting the right subclavian artery to one branch of the pulmonary artery, used in newborns with CHD characterized by insufficient blood flow to the lungs due to RVOTO, PA stenosis or PA atresia. In the same category, the Fontan procedure is included.

This three-step intervention is mainly used for palliation of Univentricular hearts and leads to the connection of both Venae Cavae to the right pulmonary branch allowing oxygen-poor blood to reach the lungs bypassing the hearth.

When using the term "Correction", all surgeries with the aim of re-establish a normal morphology or circulatory physiology are included. Correction or palliation of CHD can occur with different timing after birth depending on the heart anomaly of the patient and can be achieved after a few days from delivery, as it happened

for the Arterial Switch operation in babies with TGA, or after a few years as in the correction of some ASD. In this last case, it's usually helpful to delay the procedure to operate on a bigger heart, improving patient outcomes and reducing the probability of complications. Of course, in the period before the surgery, the patient is constantly evaluated, and if necessary, the correction can be anticipated.

For what concerns the Trans Catheter approach, Rashkind and Miller reported the first balloon atrial septostomy in 1966, describing a new means of palliating the cyanotic child with transposition of the great arteries and launching the field of interventional congenital catheterization (25). Today these innovative techniques allow treating many conditions. One of the primary use in CHD is represented by defect occlusion for both pediatric and adult patients. The percutaneous approach can be used to close the PDA, collaterals, or shunts placing metal coils inside the structure, or can be used to close ASD or VSD. Also, valves can be targeted with the endovascular approach: transcatheter balloon valvotomy is now the primary therapy in many centers for pulmonary or aortic stenosis. In addition, also valvuloplasty or valve replacement can be performed; however, it should be considered that the usage of valve prostheses is limited for pediatric patients since the implanted valve doesn't grow with the patient. To overcome this problem, research in the 3D bioprinting field is advancing rapidly.

Surgery for CHD dramatically changed the outcomes for patients with even complex defects, and surgical mortality has significantly decreased over time (26–30). Some studies reported that the higher risk of premature death up to thirty years after surgery was more notable in moderate and severe lesions, but mild lesions were not spared. Nevertheless, for many CHDs, most patients survive into adulthood with an overall 25-year survival of about 90% after CHS (31).

One crucial aspect that should be taken under consideration is the fact that the constant improvement of techniques to address the correction of CHD (developed in the last fifty years) is generating a vast population of adults with congenital heart diseases, the so-called “Grown Up Congenital Heart” (GUCH), that will represent a challenge for cardiac surgeons to come.

2. 3D technologies

2.1 3D segmentation and Computer-Aided Design (CAD)

To obtain a 3D model from medical imaging such as CT, MRI, or 3D ultrasound, Image segmentation and Computer-Aided (CAD) design are fundamental technologies.

Image segmentation is the process of partitioning a digital image into multiple segments with the aim of changing the representation of the image into something more meaningful and easier to analyze. To be more specific, we can intend segmentation as the process which assigns the same label to all pixels which share the same characteristic in terms of computer properties such as color, intensity, or texture. For example, for what concerns CT image processing, the X-Ray absorption rate is measured, normalized to the absorption rate of water, given in so call Hounsfield Units (HU); with image segmentation, all pixels with the same HU can be selected and with the help of interpolation algorithm like marching cubes, a 3D reconstruction can be obtained (32).

One of the methods that better fit medical imaging processing is the so-called thresholding method that, after assigning a threshold value, turns the grayscale image, typical of medical imaging, into a binary image where all pixels with values above the thresholded line are selected whether the others aren't. The thresholding interval is generally chosen from a histogram showing all pixel distribution in the intensity range. One of the facts that makes this particular segmentation method suitable for medical imaging is that in a CT scan, the HU value directly correlates with electron density, so by segmenting pixels with the same grey values, isolating a specific region of interest (ROI), we can isolate structures of similar nature. The same process can be applied to 3D ultrasound sequences since the echogenicity of the structures depends on the density and mechanical properties whether for MRI it differs because, in this case, the grayscale differs between sequences and weighting applied. However, with bright blood sequences, the result is similar to standard contrast-enhanced CT scans and the process is almost the same. What should be considered is that, in order to obtain the 3D reconstruction of the desired structure, the ROI must be selected in all slices of the sequence and then interpolated. As a direct consequence, the smallest structures that can be reconstructed from such

images depend on the image resolution determined by the thickness of the slices: the less thick they are, the more the resolution increase.

For heart segmentation we usually require a minimum thickness of 1.5 mm, with optimal thickness ranging from 0.5 to 1 mm.

In order to print the 3D model obtained, a post-processing step through CAD software it's necessary. This software allows describing the 3D object obtained from the segmentation process using bidimensional geometrical shapes such as triangles that are the most commonly used due to their more efficient handling and easy tessellation of complex shapes creating a so-called triangle mesh which consists of three elements: vertices, edges, and triangles. Vertices are points in 3D space, edges are connections between pairs of vertices, while triangles are triplets of vertices.

In our case, CAD software such as Meshmixer™ (Autodesk Inc, San Rafael, CA, USA), was mainly used to perfect the heart model for the printing process, correcting small errors, smoothing the surfaces, cutting the models, and defining wall thickness.

A second CAD software, Shapr3D, was used to design the chest wall simulator.

2.2 3D printing

3D printing, or Additive Manufacturing (AM), is the process that allows the creation of solid objects from a CAD model or a 3D model. The term “3D printing” can refer to various processes in which materials are deposited, joined, or solidified under computer control to create a three-dimensional object, with the material being added together, typically layer by layer. Whether after its invention, this technology was considered mainly helpful for the development of prototypes and was referred to as “Rapid prototyping”, to these days, this technology, thanks to the continuous development regarding both materials and the 3D printing process itself, is considered an industrial production technology. This technology, first developed and patented by Charles Hull in 1986, has started growing since then and, according to Forbes, in 2024, will account for a market of 35 billion dollars(33). This revolutionary method was almost immediately employed in the biomedical field, with the first reports of its application in dentistry and maxillo-facial surgery published in 1994. The main areas of medicine in which 3D printing is currently

applied and researched are dentistry, regenerative medicine, tissue engineering, drug production, prosthesis design, and the production of custom-made devices and anatomical models for teaching or preoperative planning (34,35).

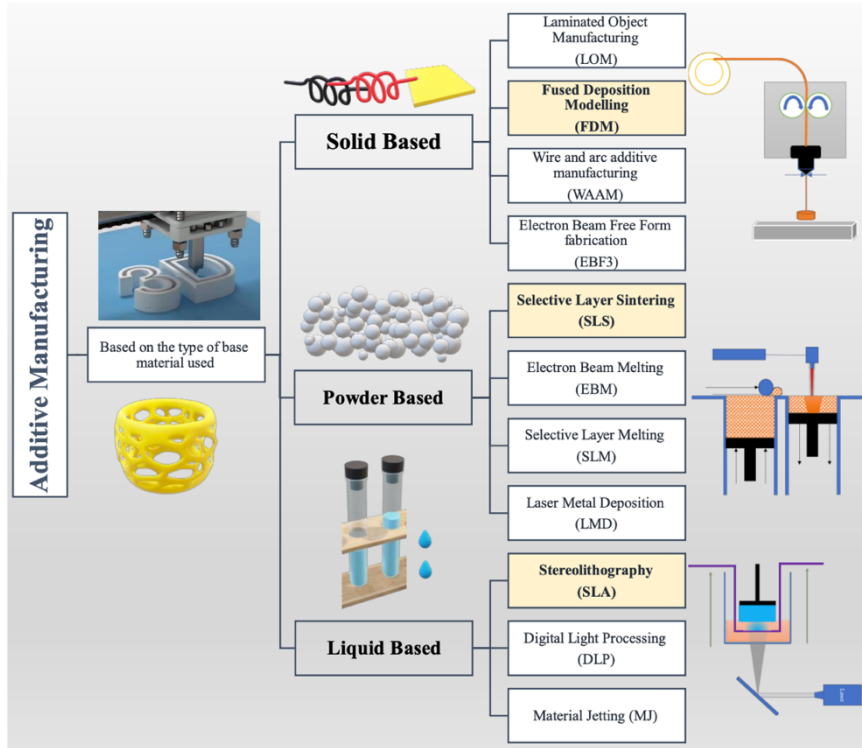


Figure 12 - Classification of AM techniques based on the type of base materials used. (From “Anderson, T. The Application of 3D Printing for Healthcare. Available online: <https://www.itij.com/latest/long-read/application-3d-printing-healthcare> “.

A variety of AM methods are available to 3D print a large number of materials: material jetting, binder jetting, vat photopolymerization, powder bed fusion, material extrusion, direct energy deposition, and sheet lamination. Moreover, AM can be grouped into three categories based on the type of base material used: solid-based, powder-based, and liquid-based. For the purpose of this study, I will describe only stereolithography (SLA), a liquid-based technology, as this is the one we use to develop our models.

The workflow of the 3D printing process is illustrated in Fig.12. First, the CAD model is created, then the standard tessellation language (.stl) file of the CAD is generated; the STL file creation process consists of the convention of the continuous geometry in the CAD file into small triangles. The .stl file is then exported in a model slicing software, in our case PreForm (Formlabs Inc., Somerville, MA,

USA), which creates a tool path for the 3D printer. Here, the 3D model is translated into 2D slices containing the cross-sections information.

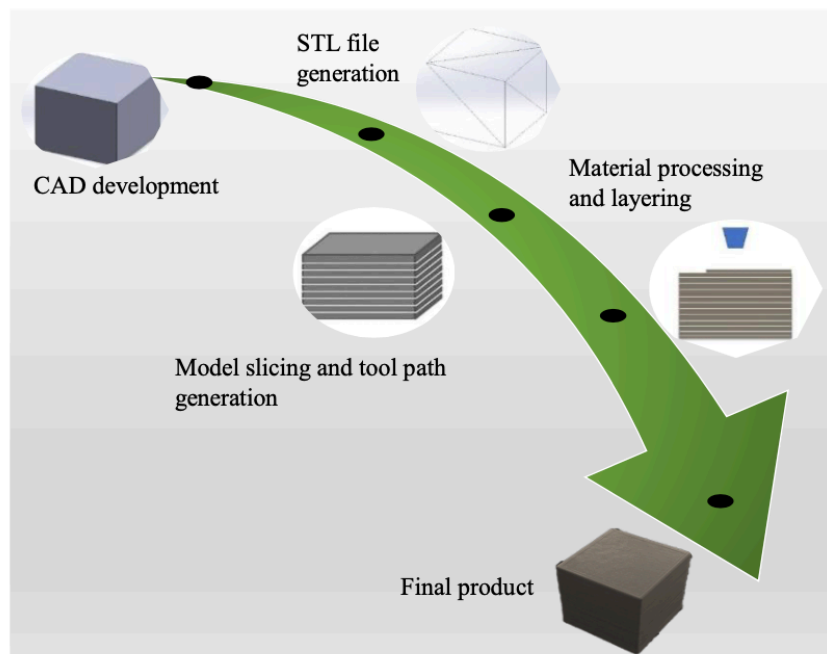


Figure 13 -3D printing process workflow. (From B. Derby, “Printing and prototyping of tissues and scaffolds,” *Science (New York, N.Y.)*, vol. 338, no. 6109, pp. 921–926, Nov. 2012, doi: 10.1126/SCIENCE.1226340”).

The 3D printer then starts the material processing and layering process. Our 3D printers, a Formlabs Form2™ and a Formlabs Form3L™ (Formlabs Inc., Somerville, MA, USA), are DLP Vat-photopolymerization based printers that work on the process of photopolymerization in which the solidification of the photo sensitive resin is induced through the action of a laser beam. An SL device typically consists of a container filled with liquid resin (acrylic or epoxy resin), a moveable elevator platform inside the container, an ultraviolet laser with beam focusing optics on top, and a deflecting mirror system to control the laser beam which draws onto the surface of the resin stimulating the local polymerization of the liquid. The laser solidifies at first the object borders, then the internal parts. When the layer is polymerized, the elevator platform goes down a defined distance, typically a layer thickness of 0.1–0.5 mm, submerging the model in the liquid resin bath. A sweeper smooths out the surface, and the resin levels out. Thus the hardened layer is covered with a new liquid layer, and the drawing continues. In this way, a model is built layer by layer. To prevent the sagging of isolated and overhanging parts during the building process, supporting structures (supports) must be provided in the

production process and are automatically generated by the slicing software which analyses the model identifying all parts that are more likely to collapse during the printing process. After the completion of the printing process, the model is detached from the printing platform and washed into a solvent bath to remove all non-photopolymerized resin residues, and then cured under UV floodlights or using a photothermal process. The duration of the printing and curing process is widely variable, depending mainly on the volume and complexity of the model that is being printed, and can vary between a few hours and several days. These same aspects impact resin consumption, going from using a few ml for printing small models like, in our case, fetal hearts, to almost 1 L for bigger models. The advantages of SL are the high geometrical accuracy and the transparency of the used material that allows looking into the model. The disadvantage of SL is the complex and time-consuming postprocessing and the costly cleaning process.

2.3. 3D bioprinting

3D bioprinting can be considered a consequence of the growing interest in AM applications in the medical field as advances enabled the usage of biocompatible materials, cells and supporting components. This technology consists of a layer-by-layer precise positioning of biological materials, biochemicals, and living cells, with spatial control of the placement of functional components, leading to the fabrication of 3D structures. Three main approaches can be identified: biomimicry, autonomous self-assembly, and mini tissue building blocks.

Biomimicry consists in reproducing cellular and extracellular components of tissues and organs and needs, to be effective, a deep knowledge of the biological tissue. On the other hand, autonomous self-assembly is an approach that uses embryonic organ development as a guide and relies on the cell as the primary driver of histogenesis, directing composition, localization, functional and structural properties of the tissue. It requires an intimate knowledge of the developmental mechanisms of embryonic tissue genesis and organogenesis as well as the ability to manipulate the environment to drive embryonic mechanisms in printed tissue. At last, the concept of mini tissues should be analyzed: these can be defined as the smallest structural and functional components of a tissue. Mini tissues can be fabricated and assembled into larger constructs using the previously described techniques.

For what concerns tissue bioprinting it's possible to identify three main strategies: inkjet bioprinting, micro extrusion bioprinting, and laser-assisted bioprinting.

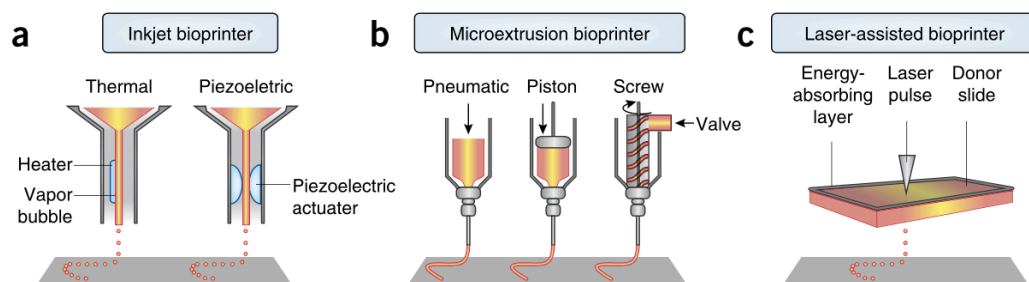


Figure 14 -Components of inkjet, micro extrusion, and laser-assisted bioprinters. (a) Thermal inkjet printers electrically heat the printhead to produce air-pressure pulses that force droplets from the nozzle, whereas acoustic printers use pulses formed by piezoelectric or ultrasound pressure. (b) Micro extrusion printers use pneumatic or mechanical dispensing systems to extrude continuous beads of material and/or cells. (c) Laser-assisted printers use lasers focused on an absorbing substrate to generate pressures that propel cell-containing materials onto a collector substrate. “Figure adapted from “Malda, J. et al. 25th-anniversary article: engineering hydrogels for biofabrication. *Adv. Mater.* 25, 5011–5028 (2013)”.

The former, also known as drop-on-demand printing, sees a controlled volume of liquid delivered to predefined locations using thermal or acoustic forces. Thermal printers electrically heat the head to produce pressure pulses that force droplets from the nozzle. The advantage of this technique includes high printing speed, low cost, and wide availability. On the other hand, some negative factors, such as the risk of exposing cells and materials to thermal and mechanical stress, are present. The acoustic ones contain a piezoelectric crystal that creates an acoustic wave that breaks the liquid into droplets; in this case, the advantages consist of reducing heat and pressure stress (36–38).

In order to use inkjet bioprinting biological material has to be in liquid form to enable droplet formation; whether the biocompatible scaffold needs to be solid; to overcome this limitation, materials used for this method of printing can be cross-linked after their deposition using chemical, pH or UV light.

Nowadays, inkjet bioprinting has been used to regenerate functional skin and cartilage in situ (39,40).

Microextrusion bioprinting consists of a temperature-controlled material-handling

and dispensing system and stage. Small quantities of material are deposited in two dimensions with the micro extrusion head moving along the z-axis with the deposits layer serving as a foundation for the next layer. The main advantage of this printing technique is the ability to deposit very high cell densities even if it is reported that the cell viability after micro extrusion bioprinting is lower than in inkjet-based bioprinting, probably due to the shear stress cells encounter during the deposition process. Microextrusion bioprinters have been used to fabricate multiple tissue types, including aortic valves (41), branched vascular trees [38], and *in vitro* pharmacokinetic [39] as well as tumor models [40]

The last bioprinting technique consists of Laser-assisted bioprinting, based on the laser-induced forward transfer. A typical LAB device consists of a pulsed laser beam, a focusing system, a 'ribbon' that has a donor transport support usually made from glass that is covered with a laser-energy-absorbing layer (e.g., gold or titanium) and a layer of biological material (e.g., cells and/or hydrogel) prepared in a liquid solution, and a receiving substrate facing the ribbon. The focused laser pulses on the absorbing layer of the ribbon to generate high-pressure bubbles that propel the biological material (45).

One other technique emerging in bioprinting is Melt Electrowriting (MEW). This technology sees the usage of voltage stabilized jets to accurately place low-micrometer scale fibers in pre-defined locations in 3D space (46). MEW enables the development of highly porous sophisticated biometric scaffolds, and it has been used for example, to mimic the collagen network in the cartilage (47,48).

3D bioprinting is based on the rationale that the printing scaffold should degrade in order to be replaced by the cellular ECM; materials currently used in this field are based on either naturally derived polymers (like alginate, gelatin, collagen, chitosan, or hyaluronic acid) or synthetic molecules; the latter can be better tailored with specific physical properties presenting however the negative of poor biocompatibility, toxic degradation products and loss of mechanical properties during degradation. All materials used must have some characteristics such as short-term stability, required to maintain initially their mechanical properties, and the ability to support cellular attachment, proliferation, and function.

As the scaffold degrades, cells inside it produce proteases and then ECM proteins that define the new tissue(49). About this process it appears important to consider

several aspects. First of all, the ability to control degradation rates in order to give cells a sufficient amount of time to replace the lost volume with their own ECM proteins; in addition, degradation products should be non-toxic and rapidly clear from the body.

For what concerns cell sources, current options for printing cells involve either the deposition of multiple primary cell types into patterns that faithfully represent the native tissue or printing stem cells that can proliferate and differentiate into required cell types. As with any transplanted tissues or organs, rejection of bioprinted constructs by the host immune system is a potential problem that can be overcome by using an autologous source of cells or by using tolerance-induction strategies. Autologous sources of cells may be obtained from biopsies, from the generation and differentiation of autologous stem cells, or through reprogramming approaches. Bioprinting technologies have been used in many fields, including cardiovascular. Whether research aims to develop a technology able to print fully functioning human organs, including hearts, to these days, it's only possible to print personalized thick and perfusable cardiac patches as described by Dvir et al. (50). To produce these patches, they started from a biopsy of rat omentum, extracting cells and processing the remaining material to eliminate all cells; this material was then used to obtain a 2.5% thermoresponsive hydrogel serving as a bionik for 3D printing. Two cellular bionic were generated: one containing cardiac cells for printing parenchyma tissue and a bio-ink containing blood vessels forming cells. It's very interesting how a mathematical model was used to design the vascular pattern to ensure enough oxygen to each part of the printed patch. The obtained patch was then transplanted and secured between two layers of rat omentum and, after seven days, located and extracted to be analyzed, showing how cells were elongated and aligned, with massive striation, indicating their contractility potential. As a proof of concept, the same group was able to print a miniature human heart starting from human myocardial cells. This heart was not functional but anatomically complete (50).

Moreover, the same group suggested a new concept of tissue engineering, producing 3D printed heart patches with a build-in soft electronic having both the capacity of recording tissue function and activating cells, providing pacing stimuli.

By doing so they were able to demonstrate the ability to accurately place different cell types and different electronic components in the 3D space, technology that will lead in the future to engineer complex tissues and control their function. Such systems would also allow the physician to monitor the function of an engineered tissue after transplantation and, if needed, to intervene from afar efficiently (51).

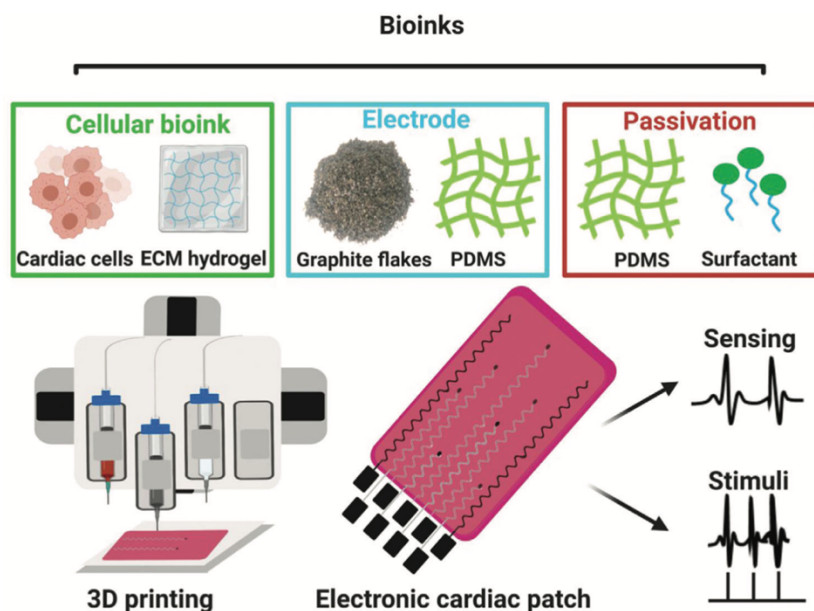


Figure 15 -Schematics of the concept. Three distinct bioinks were produced: A bioink composed of cardiac cell-containing ECM hydrogel to form the tissue, a bioink composed of the conducting material of the electronics, and a bioink containing the dielectric material which passivates the electrodes, leaving open conducting pads for point-sensing and stimulation. The three bioinks were 3D printed together to engineer the electronic cardiac patch. The electronics within the patch can provide sensing of extracellular signals and stimulation for pacing. (From [52])

2.4. Usage of 3D printing in cardiovascular sciences

Nowadays, 3D printing technologies in cardiovascular sciences are mainly used in four areas: prenatal and postnatal counseling, teaching, surgical planning, and training.

Prenatal diagnosis of CHD is fundamental to grant correct pregnancy management and adequately plan delivery and medical procedure right after it.

In addition to a correct diagnosis, prenatal counseling is fundamental to help parents understand the congenital heart disease of the fetus, making them more aware of the condition and of all procedures needed after birth. Nowadays, 2D cartoons and

drawings are mainly used to explain cardiac defects. In our center, in the last two years, a protocol to obtain and print patient-specific fetal 3D heart models was developed and utilized in prenatal counseling showing an increase in knowledge and awareness for what concerns the CHD of the future newborn.



Figure 16 - Reconstruction of a fetal heart affected by Tetralogy of Fallot. The two models are the 1:1 scale and the 5:1 scale.

Fetal 3D reconstructions are obtained starting from a 3D ultrasound acquisition and printed in resin material in a 1:1 scale and in a magnified 5:1 scale and compared, during the counseling, with a model of a normal fetal heart. Being the fetal reconstruction itself an experimental technique, models were validated by comparing them with both CT/MRI-based 3D models of the same patient after birth and the real anatomy of the fetus's heart during the autopsy run when the family decided to terminate the pregnancy due to the severe condition of the baby.

The same concept can be applied to postnatal counseling. In this case, the 3D patient-specific heart model is obtained from CT or MRI sequences, allowing in most cases to obtain a much more precise model than the fetal one, due to the fact that these imaging techniques have better resolution and allow the usage of contrast medium.

3D technologies such as 3D printed models, Augmented reality (AR) and Virtual Reality (VR) are also utilized for teaching purposes for both undergraduate and cardiac surgery/cardiology residents. Traditionally teaching of CHD is based on textbooks containing bidimensional images, specimen or plastic models, and

bidimensional imaging (CT or MRI) from real patients. When talking about CHDs, what should be considered is the deep connection between anatomy, pathophysiology, clinical features, and treatment required. The first step consists in learning the pathological anatomy; this process appears to be way more challenging than learning the normal anatomy since a deep understanding of the condition is archived only by creating a spatial visualization of the heart with this process that is unlikely to happen based only on 2D images or verbal descriptions. A possible solution for this problem is represented by 3D tools such as printed models or, as stated before, VR or AR. In all these cases students and residents have the opportunity to appreciate the spatial disposition of all heart structures, allowing them to better understand the anatomy of a specific CHD.

VR, which includes the usage of tools such as VR headsets like the Oculus (Facebook Technologies, LLC), allows the student not only to better visualize the external and internal anatomy but also to navigate the heart, giving a deeper understanding of the intracardiac anatomy. To make this teaching method valuable, all models should be developed with attention to detail in order to resemble as much as possible the anatomy of the patient. It's also to be considered that this method comes with some limitations like the fact that, due to technical limitations, it's almost impossible to reconstruct valvular leaflets and other subvalvular tissues, resulting in all models lacking all valves, which can make the usage of the model less effective for teaching purposes. To overcome this limitation, it's possible however to add standard valvular and subvalvular structures during the processing of the model in the CAD software. Also, the coronary anatomy is not always appreciable as long as, to reconstruct the coronary tree, the right amount of contrast medium has to be administered, and the slices shouldn't be thicker than 0.5 mm. As previously described, this limitation can also be solved with standard coronaries added during the preparation of the model, resulting in lower fidelity to the real anatomy. In our center, we developed in 2021 an app called "Congenital heARts" which contains 50 CHD heart models divided into three categories: Preoperative anatomy (30 models), Status post-surgery (10 models), and fetal (10 models). This free app allows all users to explore the anatomy of a specific heart visualizing the model in the smartphone or tablet or using AR. In addition for each CHD or S/P, the main Ecocardiographic-views are available (PLAX, PSAX, 4C for postnatal and S/P models and 3V, 5C, and 4C for fetal ones), in addition to a brief description of

the heart A beta feature is also present, the so-called “Flight mode”, where the users can “fly” inside the heart to better appreciate the internal anatomy.

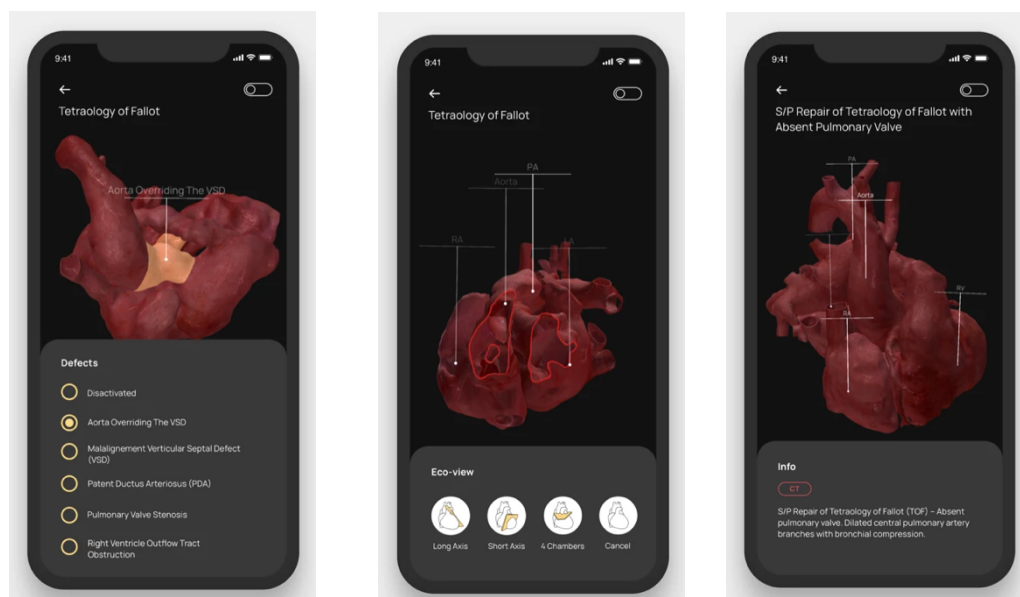


Figure 17 - Some of the "Congenitale heARts" app features. Defects can be highlighted one at the time, ultrasound views are available in addition to a brief description of the case.

For what concerns preoperative surgical planning and training, 3D technologies are rising as an impressive tool to improve surgeons' preoperative performances resulting in faster and safer operations. Even if these technologies are quite recent there are already some studies that demonstrate how surgeons who trained with a 3D model for a specific procedure before actually doing it on the patient have better skills and result in comparison to others who didn't have this opportunity. (52)

Many studies also reported how 3D models helped to prepare the operation beforehand and acquire the knowledge to carry out a perfect operation.

Surgical planning in CHD can be really challenging due to the broad spectrum of conditions and the high variability between patients with the same condition. Nowadays this fundamental step is mainly based on 2D imaging such as Ultrasound and TC with the latter that is not frequently used in order to reduce patient radiation exposure or to avoid contrast medium damages to the body. However, these imaging techniques often result in a suboptimal understanding of the specific morphology with the surgeon that only in the operating room can deeply understand all aspects of the patient's heart defect. In our center, technologies such as 3D printing of patient-specific models and VR are frequently used to determine the best surgical approach prior to real surgery. The utility of the printed model in the

surgical planning for the correction of PAPVR was also validated with a retrospective study showing, besides all limitations, how this method was considered helpful by surgeons (53).

3. Surgical simulation in Congenital Heart surgery

3.1 Premises

Congenital Heart Surgery is one of the most technically demanding surgery due to the wide variety of conditions, the rarity of each, and the dimension of patients' hearts. (54) All these aspects lead to a prolonged learning curve for residents consisting of observation, assistance, and supervised practice in the OR where the surgeon performs operations with increasing complexity in order to learn and improve his/her skills. However, in this kind of learning environment, mistakes can have an important impact on patient outcomes. Furthermore, due to the low surgical exposure of Heart surgeons in training to congenital heart surgery caused mainly by the rarity of these conditions, simulation is emerging as a tool to complement surgical training and skill acquisition.

Simulation supports the concept of surgical practice providing a low-risk, inconsequential environment allowing trainees to repeatedly practice difficult tasks, helping to acquire a specific skill, leading to a more precise operation on the real patient.

Moreover, the fact that simulation offers the possibility to plan more accurately a difficult procedure, in addition to traditional imaging, must be considered and, thanks to its constant development, it's likely that this technology will be extensively used in the future for this purpose.

Nowadays, two approaches are mainly used in simulation: animal and 3D printed simulation

3.2 Animal-based Simulation and wet Lab

Animal-based simulation in congenital heart surgery consists in reproducing a surgical procedure in animals' hearts.

Mavroudis et al demonstrate the effectiveness of neonatal porcine models to replicate CHS procedures. In this case, the trainee was a postgraduate fourth-year cardiothoracic surgical resident with no prior congenital heart surgery experience, and the instructor was a professor of surgery and academic congenital heart surgeon with more than 35 years of experience. All procedures were performed on Neonatal piglets weighing between 2.6 kg and 4.2 kg, humanely sacrificed immediately before the procedures, and constantly under the supervision of a veterinarian. Six different procedures were performed during the training: Norwood Operation, Arterial Switch, Coartectomy with end-to-end anastomosis, Operation for palliation or repair of Tetralogy of Fallot (Including also modified Blalock Taussig shunt placement), Placement of RV to PA conduit, Neonatal Ross Operation; at the end of all procedure, sutures were tested using pressurized saline. Overall, the authors address a crucial problem in simulating complex congenital procedures for surgical residents and demonstrate that a resident with no experience can be coached through these procedures (55).

The advantages of using an animal model are several: first, the anatomic relationship and relative size of structures in a neonatal piglet are very close to what a surgeon encounters in a human. Second, the organic tissue allows the trainee to appreciate tissue qualities in situ. Third, performing simulation on a postmortem model allows the trainee to learn without the concern of cardiopulmonary bypass on a living being. Another positive aspect is that these models incorporate valvular and subvalvular structures that, for now, are lacking in the 3D printed models.

However, despite the positive aspects, the animal-based approach has some negatives that should be considered: to replicate CHD it's necessary to modify the porcine heart significantly, and in some cases, the normal anatomy limits the possibility of reproducing complex defects. Also, the low availability of hearts and the fact that this kind of simulation is limited to a wet lab availability limit its application. Moreover, potential ethical protestation should be considered(54).

3.3 3D printed simulators

In 3D printed simulators, the surgeon performs the procedure on a 3D printed heart obtained by patient-specific data (TC or MRI). These models are applicable for training of both extracardiac and intracardiac procedures and can also be useful in the training of minimally invasive surgery such as ASD closure through a lateral thoracotomy. This new method for training has the advantages of better replicating the anatomy of the CHD and that the model can be produced in many copies allowing more surgeons to operate many times. Another important benefit of this kind of simulation is that it can occur anywhere, allowing the trainee to train at home or in many other places far from the OR (56–58).

Of course, also this type of simulation has some disadvantages: at first, the resin material models are made of remains a limitation, alongside the ability to incorporate valvular and surrounding structures, as currently available imaging modalities do not provide a clear definition of the cardiac valve leaflets and chordae tendinae. Second, only one procedure per model can be performed, and sutures cannot be tested adequately with pressurized saline as in the animal ones. Third, an infrastructure to create the models is necessary; costs of hardware, consumables, and personnel required to design and print the 3D reconstruction should also be taken into consideration.

Besides all that, what should be considered is that nowadays, simulation has the primary aim of allowing residents, both junior or senior, to develop, before the real surgery on the patient, a deep knowledge of all the steps the surgery requires, in addition to improving surgical skills, leading to a much useful and safer surgical practice. Thanks to the rapid evolution of materials and printing techniques, 3D heart models will be able to simulate better not only the anatomy but also the texture of the heart; it's also reasonable to believe that in the future also flow circuits will be included in 3D printed models allowing a much more accurate simulation of the procedures (54).

Besides all limitations, many authors provided a successful demonstration of how 3D- printed models can be used effectively in a variety of simulations in CHS and in some centers, like the Hospital for Sick Kids in Toronto, this method of training has been highly developed, leading to a creation of a successful surgical simulation course where 3D printed heart models are used for the surgical training (Hands-On

Surgical Training, HOST). Since its introduction in 2015, Hands-On Surgical Training (HOST) courses using 3D-printed models have increasingly been popular among surgeons and trainees in congenital heart surgery; most participants of the HOST courses appreciated the educational value of the 3D-printed models in improving their surgical skills. Most of them also strongly agreed that the HOST courses should be included in the curriculum of CHD surgical training (59).

In addition, a dynamic chest wall and operating table simulator have been developed by the same group with the aim of enhancing the heart surgery simulation experience (60).

Yoo et al. have successfully reproduced their course worldwide at multiple institutions highlighting the benefit that 3D- printed simulators can be performed in any location, nullifying the barriers of wet-lab availability. In developing a Heart surgery simulator, Yoo et al underline the importance of not only having accurate 3D heart models but also replicating the conditions, like the position of the surgeon and light exposure, that the surgeon encounters in the OR. Also, Hussain et al reported about the development and validation of an objective, procedure-specific assessment tool for the arterial switch operation in 3D models allowing to incorporate the HOST simulation within curriculums and evolving training internationally; in addition, these checklists can be used by trainees while rehearsing and as a technique for self-assessment. (61)

The same group is now using a new technology to produce their 3D models. Whether in the first place all models were designed and printed using elastic resin in only one print, they have now chanced materials in order to better simulate heart muscles and blood vessels walls. Nowadays, in fact, all their models are produced using 3D printed molds and materials such as PVA: all parts of the heart, including valvular and subvalvular structures, are produced separately and then assembled leading to a much more realistic model for what concerns the texture of all structures. (56,62)

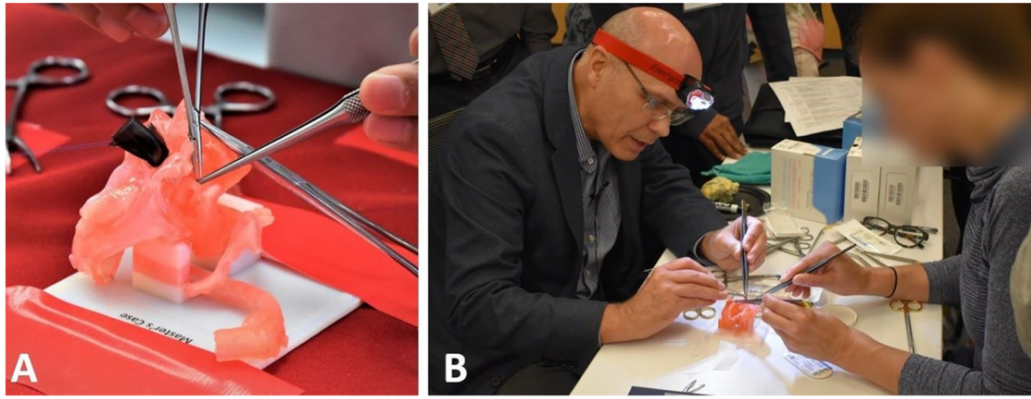


Figure 18 - (A) A surgeon simulating a complex congenital heart surgical procedure on a 3D-printed heart model at the hands-on surgical training (HOST) course. (B) A congenital heart surgeon demonstrating the arterial switch operation on a 3D-printed heart model at the HOST course. Note that the models are stuck to the table at a fixed height forcing the surgeon to sit down preventing them from using their surgical loupes. A simple headlight is used to illuminate the model. The procedure is video recorded for retrospective assessment (not shown). (From “ B. Peel, P. Voyer-Nguyen, O. Honjo, S.-J. Yoo, and N. Hussein, “Development of a dynamic Chest Wall and operating table simulator to enhance congenital heart surgery simulation,” *3D Printing in Medicine*, vol. 6, no. 1, Dec. 2020, doi: 10.1186/s41205-020-00067-4”).

3.4 “Hybrid” simulation

One last type of simulation is the hybrid one, where the usage of animal hearts (mostly Pigs or Cows) and 3D printing are combined. This technique allows the surgeon in training to work on tissues that more resemble human ones while simulating operation using also 3D printed parts like hollow cylinders, for BT Shunt or cavo-pulmonary anastomosis in the third step of Fontan procedure, or pulmonary graft in replicating Ross procedure.

This type of simulation encounters the same negatives described before for animal-based simulation, such as low availability of hearts, need for a wet lab to perform the training, and possible ethical protestation. One other negative aspect consists in the fact that neonatal pigs’ hearts are extremely difficult to find resulting in using adult animals’ hearts that are way bigger in comparison to the ones the surgeon encounters during CHS.

II. AIM OF THE THESIS

4. Rationale of the study

Congenital heart surgery is one of the most technically demanding surgery, with a long training period required to acquire all necessary skills to perform operations ensuring patient safety and positive outcomes. At the same time, however, due to the limited number of centers where this surgery is performed, in association with the relatively low number of patients who undergo these surgical procedures each year, residents' exposure and training in this field is usually limited.

To overcome these limitations, simulation is emerging as a tool to help surgeons develop all skills required to perform this kind of operation with the advantage of being outside the OR in an inconsequential environment.

In addition, to the growing expectation for a perfect patient outcome, simulation tools can also be used to better plan a surgical procedure using patient-specific models.

The constant and rapid improvement of 3D printing technologies and materials has made it possible to develop and print heart models that can be used to simulate all kinds of procedures.

5. Purpose of the study

The aim of the study was to develop a fully 3D printed, multimodal, chest wall simulator to be used in Congenital and acquired heart surgery training. The second target was to also develop procedure-specific models to be used in the simulator with the aim of helping the surgeons in training to develop specific skills.

III. MATERIALS AND METHODS

6. Chest wall simulator development

6.1 Crucial aspects

In order to obtain a valid simulating tool, we decided not only to design procedure-specific models but also a chest wall simulator, offering, by doing so, a more realistic exposure of the surgical field.

In developing the simulator, five different aspects were identified as crucial. First of all, the structure simulating the chest wall should have had to possibility to be secured to a tripod, thus replicating the ergonomics experienced in the OR. By doing so, the trainee can practice and learn about the different positions that should be assumed during each step of the procedure to make it easier. The fact that the tripod can be adjusted in height is also important to grant a comfortable position to the surgeon, in the same way as it happens in the OR.

Another element we considered important was the possibility of simulating different surgical approaches by changing the simulator's position (possibility to roll, pitch, and tilt it) and using specific covers. We designed the simulator with a standard opening at the top of the structure, simulating a median sternotomy. However, this opening can be modified, for what concerns dimensions and position, to allow the simulation of approaches such as mini-sternotomy, right axillary mini-thoracotomy, and left posterior mini-thoracotomy.

One other factor we considered in developing the simulator was to ensure optimal light exposure, allowing the insertion of small LED lamps inside the chest. In addition to optimal light exposure, on the surface of the chest wall also room to attach an external light and a webcam was considered necessary. In designing this tool, we were aiming to allow the trainee to record the procedure in order to watch it after the training to better understand errors and crucial steps of the procedure itself. Furthermore, the presence of a webcam can allow a tutor to live-supervise the procedure while giving advice or correcting errors.

At last, we agreed that the total volume of the simulator had to be small, allowing portability and usability in every environment. By doing so, surgeons can train everywhere without having the limitation of a specific environment to perform all sessions.

6.2 Components design

All components were designed using the software Shapr3D (Siemens®, Parasolid®, Budapest, Hungary) and printed with the printer Formlabs™ Form3L™ (Formlabs, Somerville, MA, USA) using resin materials.

Shapr3D is a solid modeling computer-aided design (CAD) app that provides a complete direct modeling feature set on Apple Pencil compatible iPads. This 3D modeling tool uses a Siemens™ Parasolid™ geometric modeling kernel and D-Cubed™ sketch engine (63). It is compatible with all major desktop CAD software and lets users directly import X_T, STEP, IGES, STL, DXF, DWG, JPG, and PNG files and export X_T, STEP, DWG, DXF, STL, and OBJ files(64). This tool is available for iPad, Mac, and Windows users. In the iPad Pro version, the one used in this study, 80-90% of all modeling is done with the Apple Pencil, except for basic gestures like zoom and pan, which use finger-touch navigation(65). The Apple Pencil enables all other CAD controls. For example, users create a 2D sketch by drawing it in a workspace, extrude a body's volume by tapping on a face and dragging it, or create a fillet by tapping on an edge and dragging it(66).

The graphic user interface of Shapr3D has been designed to be as user-friendly as possible so even personnel with limited or without 3D CAD experience could use this app. In the next paragraphs, I'll explain Shapr3D workflow and tools.

For what concern the workspace, it's possible to identify three lines representing the Cartesian coordinate system (x: red, y: green, z: blue), while on the upper left part of the screen, all tools to import and export models are present. In addition, all tools needed to design the aimed object are located in the same part of the screen.



Figure 19 – Shapr3D’s user interface. Icons to return to the main library, import and export models or objects are visible on the upper left side. Tools to design the model can be found on the middle-left side. On the upper right, orientation tools are present. Also, the Cartesian coordinate system (x: red, y: green, z: blue) is visible.

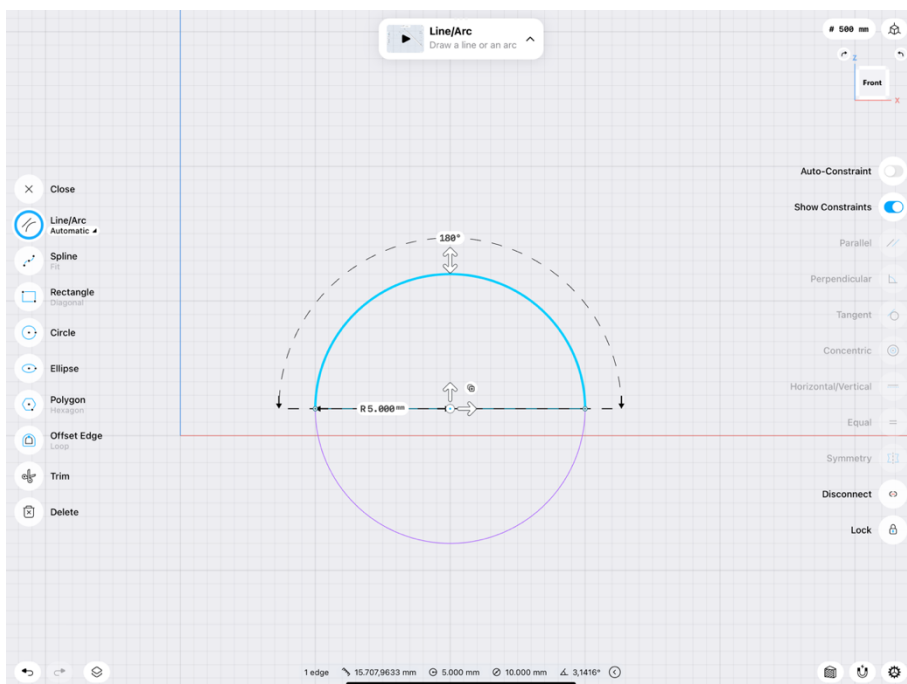


Figure 20 – Example of 2D sketch prior to creating a 3D object. Selecting “Line/Arch” in automatic mode, the app recognizes the user’s intent and automatically switches from drawing lines to drawing arches. Also, geometrical shapes can be selected and added to the sketch.

The first step in designing one object consists in producing a sketch that represents the foundation of the 3D model. All Sketches require the usage of the “Sketch tool” that allows the user to draw lines, arches, or geometrical shapes in a bidimensional space. One interesting aspect is the automatic mode, in which the app recognizes the user intent and switches automatically from drawing lines to drawing arches.

Once a segment or a shape has been drawn, the measure of its length, radius or diagonal can be modified by typing the wanted value in the dimension section. It appears very helpful how this app shows its midpoint/center for each element in the workspace and guides perpendicular or parallel lines to a selected element, thus making it easier to sketch complex or composite objects.

When the sketch has been made, in order to create a 3D object, it’s necessary to pass from the 2D view to the 3D view by simply moving the cartesian coordinate axes with fingers. By doing so, the surface of the obtained shape highlights and can be extruded in different directions thus creating a primitive 3D object. Once the 3D element is designed, all its surfaces can be selected and extruded or modified if needed.

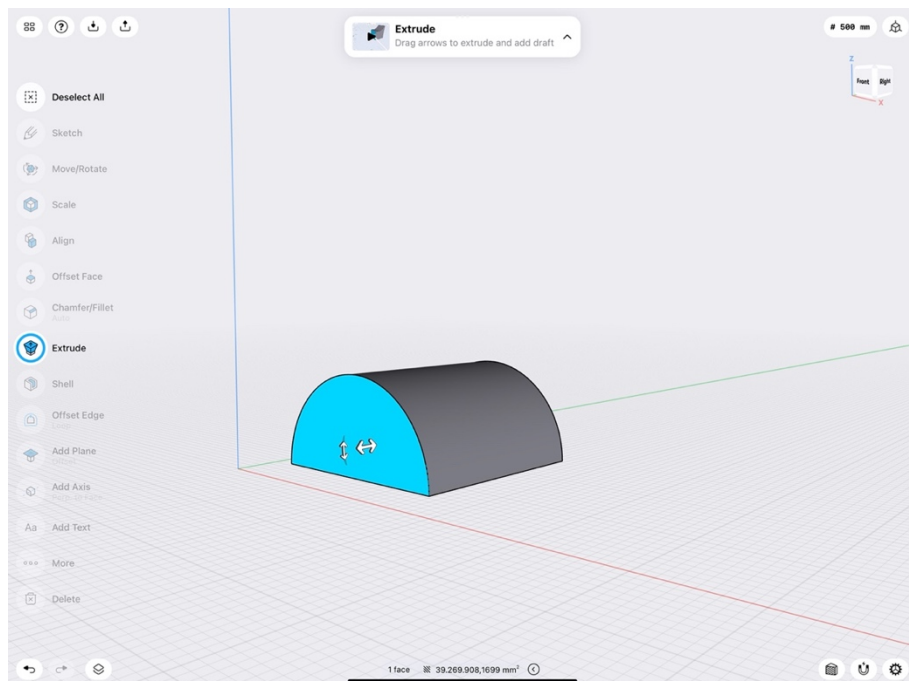


Figure 21 – Extrusion of a 2D sketch to create a 3D object.

By tapping two times on one of the object's faces, it's possible, by switching again to the 2D view, to delineate a second sketch directly on the selected surface and, following the same steps described above, this second surface can be extruded, removing the corresponding volume from the primitive object thus creating hollow structures and cavities.

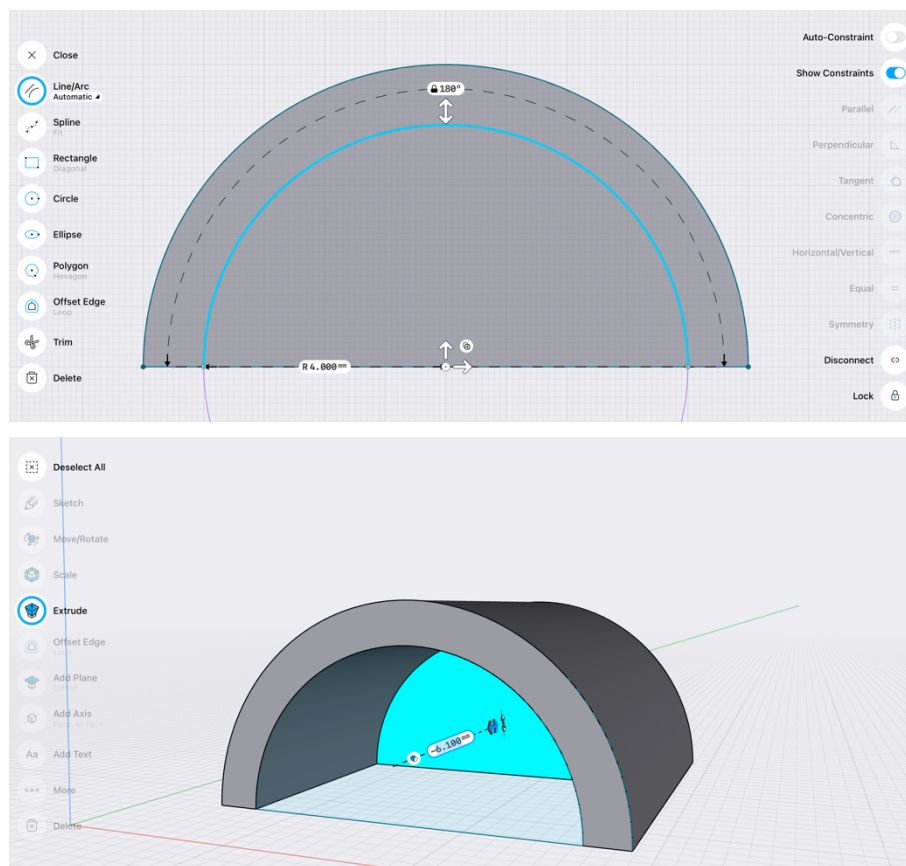


Figure 22 – The two figures above show the “Extrude” tool workflow process to remove part of the object or create a hollow structure. Once a specific surface of the object has been selected with a double finger tap, a second sketch is performed on this surface and then extruded to subtract the corresponding volume.

Once the object has been created, the “Transform” window allows users to execute different actions such as moving/rotating the object, scaling dimensions, translating or rotating it, in addition to aligning its surfaces to a specific plane. The object can also be mirrored, allowing, when designing a model with symmetric parts, to sketch only one half of it, making the whole process way faster.

Many other tools are available by opening the “Tools” window. The most used tools in developing our simulator have been “Extrude”, which allows transforming a 2D surface into a 3D object, “Union”, which let the user join two objects that intersect, in addition to “Subtract”, and the “Split body” tools.

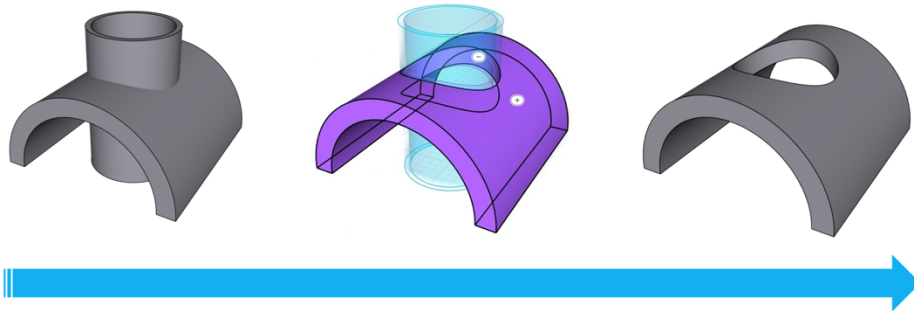


Figure 23 – “Subtract” tool workflow process. Once two objects are intersected, the one to maintain and the one to subtract should be selected for the process to occur. It’s also possible to keep also the object that has been subtracted, leading to the removal of only intersected parts.

Also, edges can be modified in a more round or more flat fashion by selecting the “Chamfer/Fillet” tool and pulling the cursor up or down.

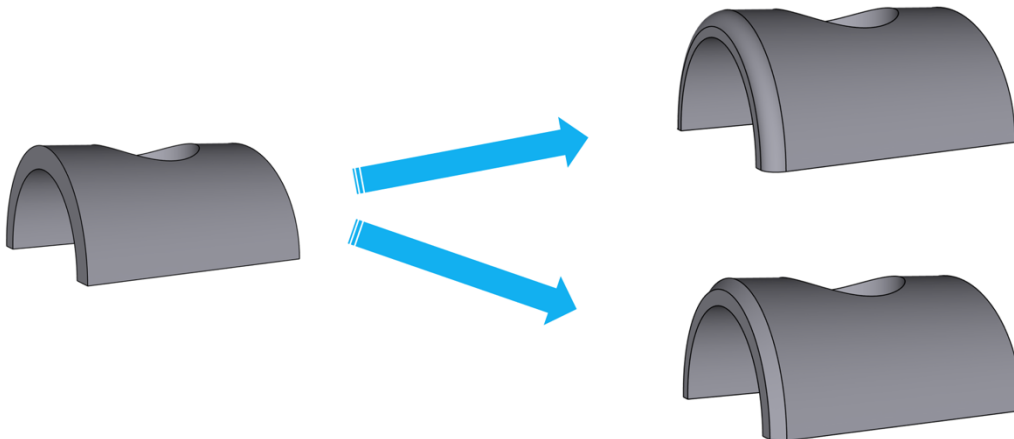


Figure 24 - “Chamfer/Fillet” tool possible results. Once the edge is selected it can be modified in a round or flat fashion.

When the 3D model is ready, it can be exported in many formats, all visible in Fig. 25, for display, AR, further modification, or printing purposes. In this specific case, we exported the model in STL format using otherwise ASCII and not Binary as output language. During the STL export process is also possible to select the resolution of the object itself by adjusting Deviation and Angle tolerances.

Format	Import	Export			
			DXF	✓	✓
X_T (Parasolid)	✓	✓	SVG	✗	✓
STEP	✓	✓	PNG	✓	✓
IGES	✓	✓	JPG	✓	✗
SLDPRT	✓	✗	PDF <small>Single or 1st page only</small>	✓	✓
SLDASM	✓	✗	TIFF	✓	✗
STL	✓ <small>Reference only</small>	✓	BMP	✓	✗
3MF	✗	✓	ICO	✓	✗
SHAPR	✓	✓	RAW	✓	✗
OBJ	✗	✓	GIF <small>Not animated</small>	✓	✗
DWG	✓	✓	USDZ	✗	✓

Figure 25 -Formats available for import and export purposes.

7. Procedure-specific model development

7.1 Low fidelity models

Low fidelity models (see chapter 11) were designed to help surgeons develop skills such as vascular anastomosis or patch placement and suture without printing a whole heart but using instead 3D printed items that schematically represent heart structures.

All these models were developed using the same CAD software utilized for designing the chest wall. These models consisted of two solid platforms (one for CABG simulation and the other for patch placement and anastomosis) aiming to support silicon-like items, printed with Elastic Resin, that resemble heart structures (like ASD/VSD or coronaries) or surgical materials such as bovine pericardial patches.

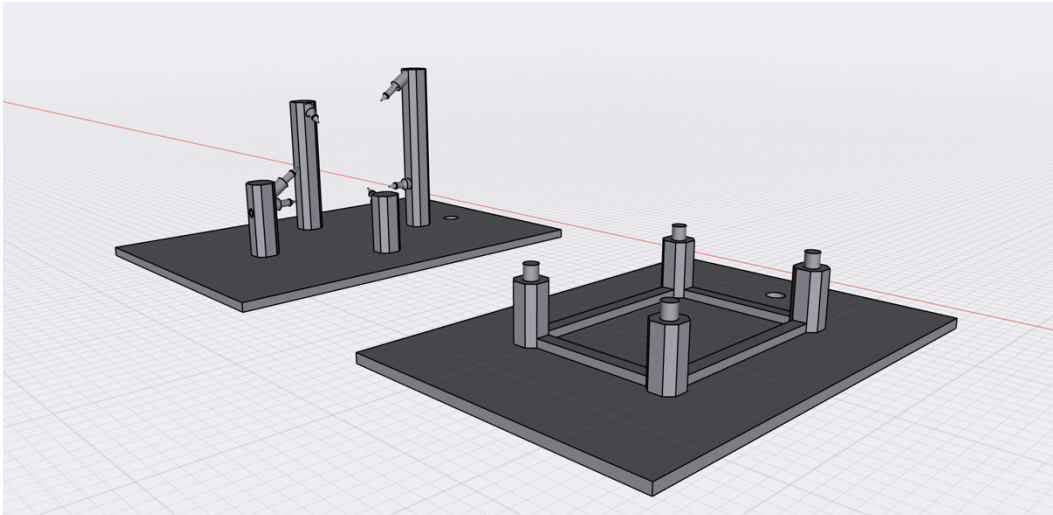


Figure 26 – Low fidelity models. On the left the CABG platform, while on the right the patch placement and anastomosis platform.

7.2 Intermediate fidelity models

Intermediate fidelity models were all developed from real patients whose hearts were reconstructed using the software Mimics inPrint 3.0 (Materialise, Leuven, Belgium) starting from CT or MRI. Materialise’s Interactive Medical Image Control System (Mimics) is a software tool for visualizing and segmenting medical images and rendering 3D objects. Mimics inPrint allows the importation of DICOM image files on the user’s computer or through a PACS interface. The imported images are used to create ROIs (region of interest) with the help of dedicated semi-automated segmentation tools for cardiac, orthopedic, or other applications

In the basic version, only the bone module is available. However, this module has all essential functions, such as the segmentation tool, that allows the reconstruction of all body parts if correctly used. In addition, it’s possible to buy the “Heart module” that can make the heart reconstruction process quicker. This software is designed to be modular; this feature, in addition to the fact that the Graphic user interface is as user-friendly as possible, creates a simple workflow that allows even personnel with limited experience to produce a 3D reconstruction of sufficient quality. The workflow is divided into five steps, both graphically and technically: the segmentation takes place in the first two phases; the third phase, called “Add

Part”, transforms the freshly segmented ROI into a triangulated surface; the last two steps prepare the reconstructed 3D volume to be 3D printed.

Once the image set has been imported into the software, the whole reconstruction process takes place in the main window, which is divided into four viewports; three of those (2D viewports) are used for displaying the medical images in three standard planes (axial, coronal, and sagittal) and the fourth one (3D viewport) shows a preview of the reconstruction during the segmentation process helping the user to better understand what should be done to perfect the reconstruction.

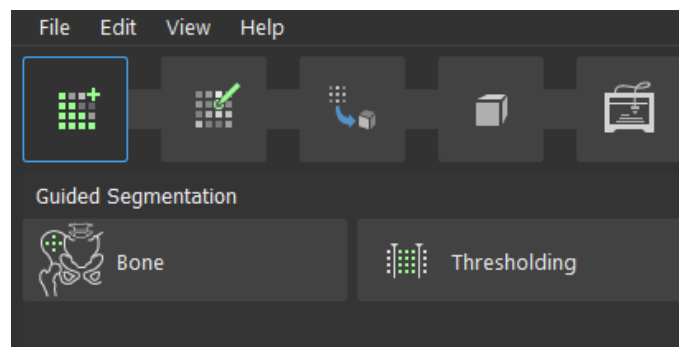


Figure 27 – Creating the ROI through threshold segmentation

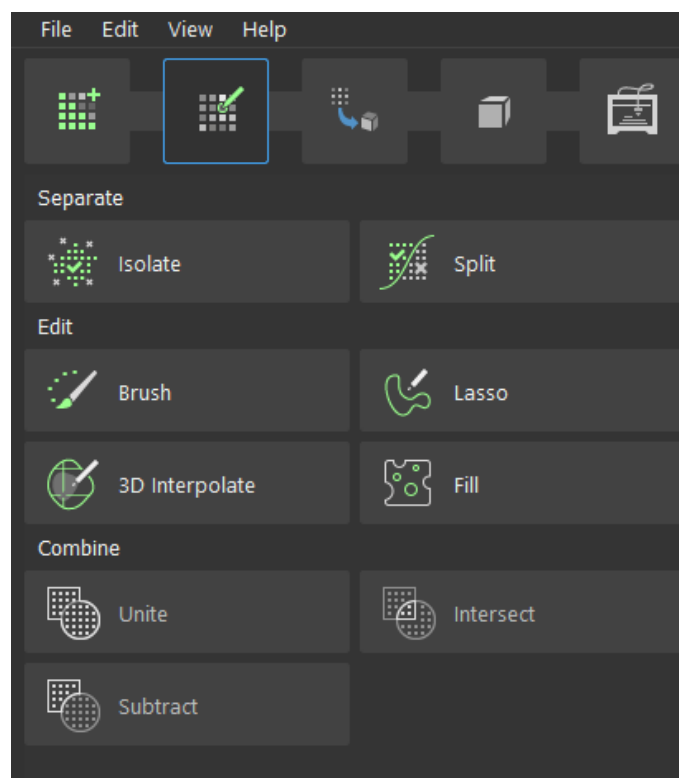


Figure 28 – Editing the ROI using different tools

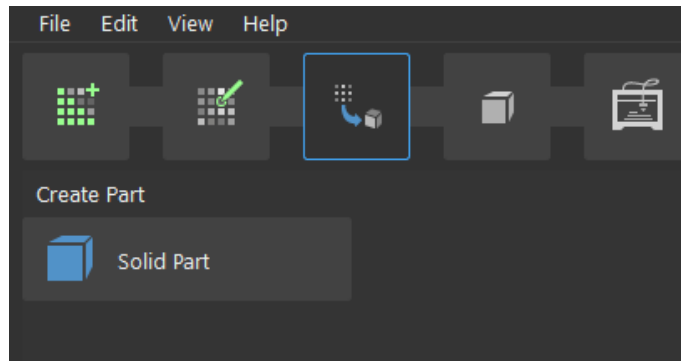


Figure 29 – Add part panel

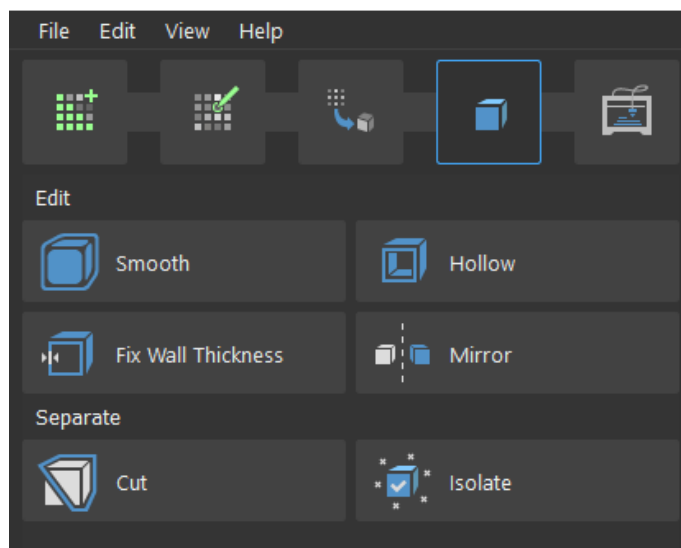


Figure 30 – Edit part panel

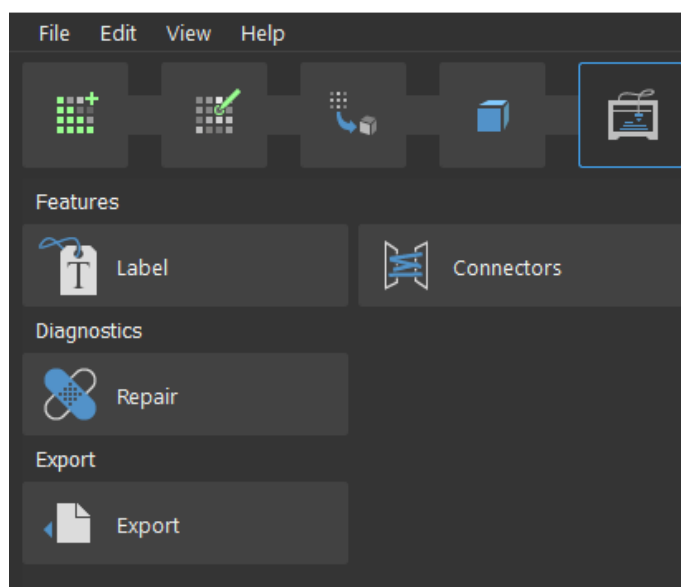


Figure 31 – Preparing the print

The first step at this point consists of Setting the threshold range and selecting the ROI, cropping the segmentation window until only the heart is included. This process allows excluding all other structures, like the ribcage, that have the same pixel intensity value as the blood inside the heart. Since a contrast medium is used, the heart and the great vessels become high-intensity structures such as the sternum and the ribcage, making it potentially challenging to separate them during the mask editing process.

Once this first step is completed, two more modules become available on the upper left part of the main window: the “Edit tool group” and the “Create part” module. In the first one, many tools are available to improve the quality of the reconstruction by dividing structures or erasing unwanted parts.

The “Separate” tool group includes two options: isolating a particular part of the ROI or splitting an ROI into different parts. This tool is mainly used to separate the ribcage and the spine from the heart and the aorta, leaving only vascular structures in the 3D viewport. The edit group tool has many options to edit the ROI. The brush tool edits the selected ROI and can be used both in the 2D and 3D windows as a circular or spherical brush. Before using this option is necessary to choose whether the selected ROI should be added or erased. Other parameters such as diameter can be personalized.

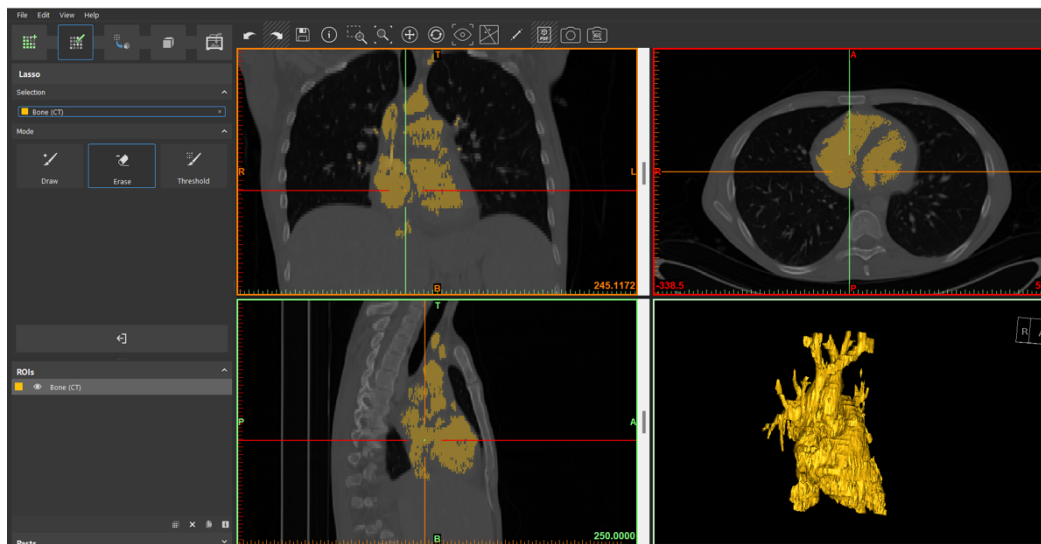


Figure 32 – Mimics Imprint 3.0 (Materialised, Leuven, Belgium) user interface. The DICOM sequence is displayed in three standard planes (Axial, coronal, sagittal) while in the fourth viewport a preview of the 3D reconstruction is available. In the upper part of the user interface all instruments are present.

The “Lasso” tool allows the user to edit the selected ROI in 2D as well as in 3D by using a free-form curve. Also, in this case, the selected area can be added or deleted. The “3D Interpolate” tool allows the user to edit an existing ROI by only marking a few slices in Brush or Lasso Mode. When the user marks an input region in the 2D viewports, a 3D interpolated volume is generated in real-time. The tool is perfect for quickly adding and removing large regions from an ROI. The last tool in this group is the “Fill” tool which allows filling holes in the mask by selecting a specific area or by operating globally in the ROI.

Once the mask has been edited, it can be transformed into a solid part. This process is performed by selecting the “Solid Part” button in the “Add part” panel and requires selecting the mask/ROI to use as input. The object that is generated is a meshed surface.

At this point some CAD tools can be used to edit the generated part to improve the quality of the reconstruction. All tools can be found in the Edit Part panel that is divided into two main operations that can be performed on parts, namely Edit and Separate. The Edit operation has two options: smooth and hollow. Often, generated parts have rough features on their surface like holes and peaks, the Smooth tool removes those features to create a smooth-looking part.

With the Hollow option, a specific thickness can be given to an existing part. In our case, it is used to determine the thickness of the heart walls and arteries, making the model as similar as possible to the reality. The Hollow function can operate in two main directions, outward and inward. Since the generated parts represent the blood pool inside the heart chambers, while the aim is to replicate heart walls, we use only the outward function.

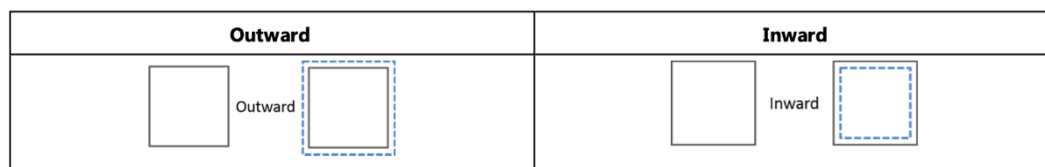


Figure 33 – Schematic image of the “Hollow” mechanism.

The minimum thickness is 1.0 mm, and lower values are not allowed because it would create problems in the printing process.

To ensure that the model's thickness is over 1.0 mm, the “Fix Wall Thickness” tool can be utilized. In this last process, every wall reported as too thin or fragile is

automatically fixed to ensure the best possible printing outcome. In the separate section, two main tools are available, Cut and Isolate. We use only the Cut tool for our purposes, which separates parts or removes part segments. It is mainly used to open windows in the atria or ventricle walls to better appreciate the internal anatomy of the heart .

When the editing part is finally complete, the last step of the workflow is represented by the “Prepare to Print” section. With this step, labels and connectors can be added and the part can be made ready for print.

To improve the overall quality of our models, once this workflow is completed, we export the model in an .stl file and load it into a post-processing open-source CAD software called Meshmixer™ (Autodesk Inc, San Rafael, CA, USA). Thanks to a wide variety of tools (visible in Fig.34), this software allows for editing and perfecting the model. In addition, if necessary, wall thickness can be brought down to less than 1 mm. The final result is then prepped for the printing process (see next Chapter).

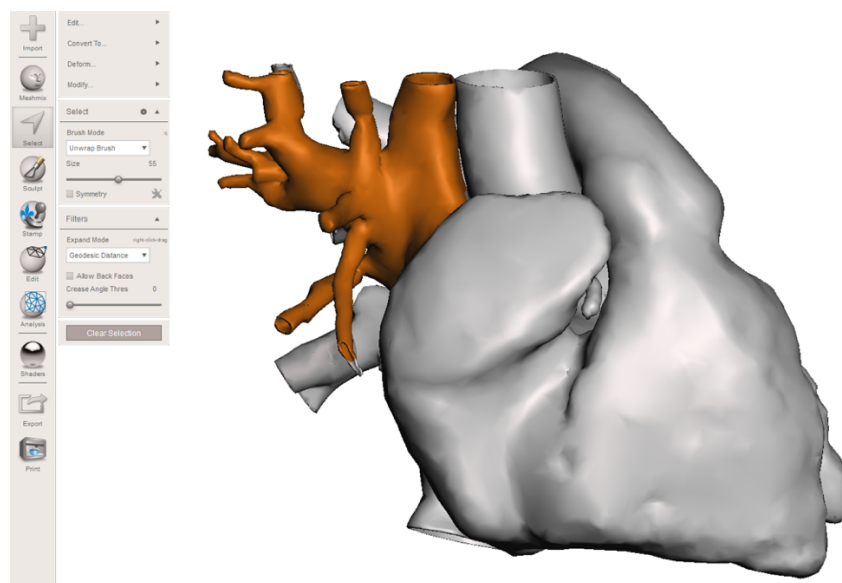


Figure 34 - STL file imported in Meshmixer. All tools available are visible on the left side of the main window. In the picture, it's possible to see the main anomaly of the heart highlighted in orange.

8. Printing process and materials

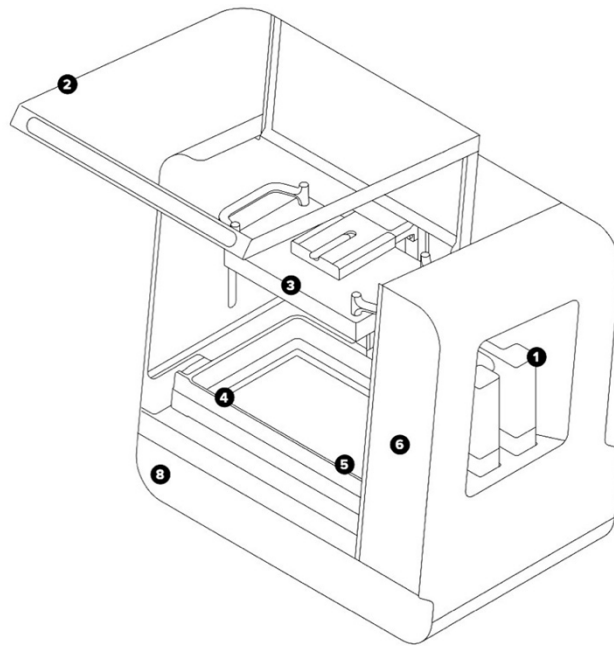


Figure 35 -Our 3D printer, a FormLabs™ Form3L™. (1) Resin cartridge (2) Cover (3) Build Platform (4) Resin tank (5) Mixer (6) Touchscreen display

Our 3D printer is a FormLabs™ Form3L™ (Formlabs, Somerville, MA, USA). This machine uses the Low Force Stereolithography (LFS)™ technology to turn liquid resin into highly precise prints by photopolymerizing each thin layer of resin upon the previous one using a short wavelength laser. The printer is made of four main components: platform, tank, ink cartridges, and finally, the printer itself. The cartridge consists of a disposable container that holds 1L of resin. The Form3L can fit two cartridges at a time to allow printing bigger objects. The resin is automatically delivered into the resin tank, where its level is maintained in a constant volume range. Inside the tank, a mixer is also present to circulate the resin and keep the building area clean from cured residues. The platform is a support structure that provides an attaching surface for the printed item. It moves on the Z-axis thanks to a micrometric stage, and its movement determines the thickness of each layer, which can go from 25 to 300 microns in our printer. Beneath the resin tank, the optical window is present; it consists of a glass plate with an anti-reflective coating that protects the sensitive mirrors inside the printer from dust and other contamination. Below it, the two laser modules are located; the fact that two of these modules are present allows a reduction of the printing time. Each light processing

unit is a 405 nm violet laser (maximum power 250 mW) with an 85-micron laser beam size (FWHM).

Platform and resin tanks are covered by the printer lid, made of metal and an orange-tinted material, which blocks exposure to the lasers and protects the resin from curing due to ambient light.

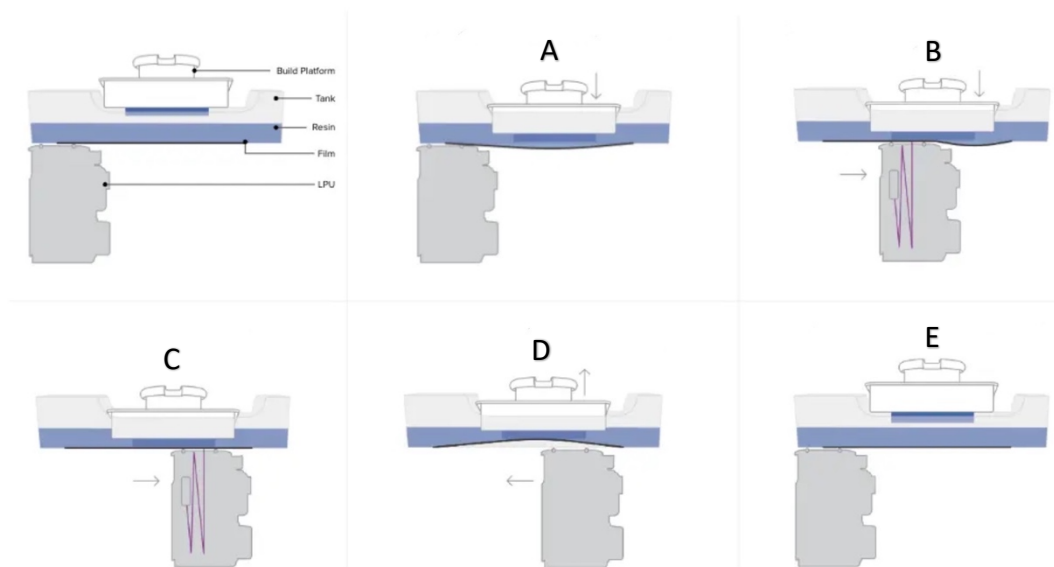


Figure 36 -Printing workflow. (A) Build platform and printed parts lowers into the resin bath (B) Rollers gently squeeze resin out from under the part to generate a thin, even layer of resin (C) The layer is cured and film adheres to the cured material (D) Build platform lifts the liquid resin gently pulling part away from flexible film layer (E) Film relaxes and is ready to print a new layer.

The maximum build volume is 33.5 cm × 20 cm × 30 cm allowing to print bigger objects compared to our other SLA printer, a Formlabs™ Form2™, which allows a maximum printing volume of 14,5 cm x 14,5 cm x 17,5 cm.

Both these printers allow the usage of a wide array of resin, all developed by the same company, to address specific needs. In developing the simulator, two types of resin have been used: the Formlabs Clear Resin™, for printing the chest wall, and the Formlabs Elastic Resin™ to produce the models.

Different resins have different properties and different temperature ranges of operation, requiring the modification of many parameters in the printer when switching from printing with one resin to the other. Fortunately, the printer recognizes the cartridges loaded into it and automatically modifies these parameters allowing an optimal print result.

Clear resin is a rigid PMA like-resin. After proper curing, it becomes very hard, making it suitable for structural purposes. Also, it can be polished to near optical

transparency, making it ideal for showcasing the internal features of an object. We decided to print our simulator using this resin due to the fact that we were aiming to create a resistant structure. Also, pricing has been considered since the elastic resin is more expensive than Clear (see Chapter 14 – Cost Analysis).

On the other hand, Elastic Resin™ is an elastomeric material designed for applications requiring high elongation and high energy return. This resin is suitable for parts that need to bend, stretch, compress, and hold up to repeated cycles without tearing. Elastic is transparent, making it ideal for medical models for simulation or education(67). Printing models with this resin make cutting and suturing possible, enabling the simulation of a specific surgical procedure.

Before loading the object to print via Wi-Fi, it's necessary to prep the .stl file with Preform™, a software also made by Formlabs. This step is essential to define many parameters, such as resin type, layer thickness, and support layout. Apart from a few models, all printed objects come with supports that avoid the collapsing of hanging or fragile parts during the printing process. The software itself automatically defines the support layout but it can also be modified manually. In addition, support density can be set to fit the operator's needs.

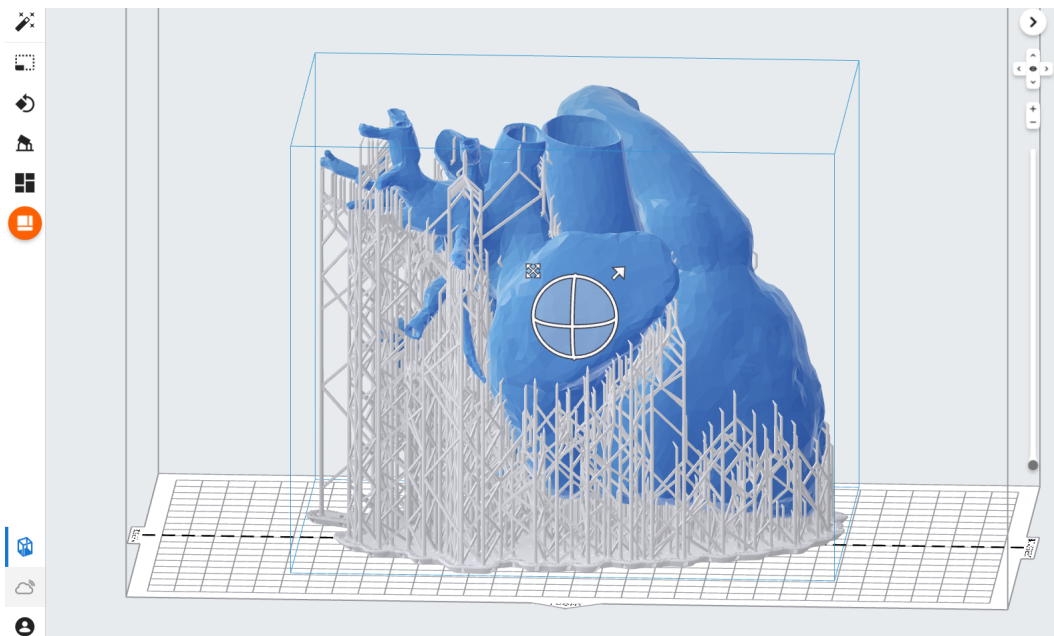


Figure 37 – Model ready to print in PreForm. The model is added to the printing platform and supports are automatically generated by the software.

When the print is completed, the object is detached from the printing platform and washed in an isopropyl alcohol bath (IPA) for 5 to 10 minutes (for more than one cycle if needed) to remove uncured resin that would polymerize spontaneously over time. After the washing process is completed and the model is dried from the IPA, the curing process begins. During this procedure, the model is exposed to UV light for 60-120 minutes, allowing it to reach its maximum strength.

When this step is completed, supports are removed, and the printed object is ready to be used.

IV. RESULTS

9. Chest wall simulator

9.1 Evolution

Our initial idea of the simulator consisted of a multi-modal platform where 3D printed models could be loaded to perform the surgical procedure.

The developing process of the simulator took several months. It started with a Pathfinder version made from wood and metal consisting of a square platform with two small metal rails on top of it where a smaller wooden mobile square-shaped tablet could move back and forward. This element was also equipped with four screw-like vertical elements positioned at 1 cm from each vertex that had the main purpose of stabilizing a third wooden tablet where the 3D-printed heart model was attached. By doing so, the model was stable and could not move while cut, sutured, or retracted. The main platform had a hole in its center, allowing it to be secured to a tripod. The first step at this point was to develop a solid structure to resemble a chest wall to make the simulation more accurate for what concerned heart exposure. The first chest wall we designed was a simple 10 mm thick, half-cylinder with an oval opening at the top thus simulating a median sternotomy with a retractor in place. At the time, however, the dimensions of this item exceeded the maximum printing volume of our printer, a Formlabs Form2. To overcome this limitation, we printed the chest wall in 4 pieces, and we assembled it after the curing process with Lego®-like items that were also printed with the same 3D printer. This step was necessary to evaluate the resin structure's actual resistance and see if, once printed, it could resemble a real patient's chest.

After positive feedback given by pediatric cardiac surgeons of the Pediatric cardiac surgery unit, in addition to the understanding that the resin structure was solid enough for our purposes, we decided to design and print not only the chest wall but also the static and mobile platform at the base of the simulator in order to create a fully printable item.

At this point, we created the first fully printable version (1.0), which consisted of three main parts. At first, a 9.5 mm thick, rectangle-shaped platform with a hole in its center was designed to fit an M6 screw necessary to attach it to a tripod. The dimensions of this platform were 140 x 162.5 x 9.5 mm, making it possible to print this item in one solid piece. The second main element was represented by a half-cylinder, with the same opening as in the pathfinder version; in addition, six pillars were added to the design. These pillars presented three grooves each, one bigger in the lower part to attach this structure to the main platform and two in the middle to allow loading heart models. Having the same printing volume limitation we had for the pathfinder version, we were constrained to divide and print in four parts also this second version of the chest wall and, to make it solid enough after its assembly, eight LEGO-like elements needed to be printed. Due to the complexity of this design and the fact that too many items were needed only to make the simulator stand, this version was never printed, and we started developing the following one. The 2.0 version followed the same rationale as the 1.0 with some improvements in design, stability, and, in addition, a reduction of wall thickness and total weight. In this design pillars were replaced by two “supporting walls” with two levels of grooves, designed to fit different sizes of 3D heart models. In the lower part of these “walls”, an L-shaped structure was present, allowing its insertion in an L-shaped groove placed on the top of the base, thus securing the corresponding half of the chest wall on the platform itself. The improved base platform presented, in addition to lateral grooves, two holes, the first one in the middle, to secure it to a tripod with an M6 screw, and the second, a few centimeters from the anterior edge, to secure, using a resin pin, the tablet with on top the heart model, preventing involuntary movements of the mode itself while performing the procedure.

To improve stability, four small “LEGO-like” items were also printed and used.

In this case, we were able to print the chest wall in only two pieces since a new printer, the Formlabs Form 3L with a more considerable maximum build volume was available. The availability of this printer also made it possible to develop the third and final version.

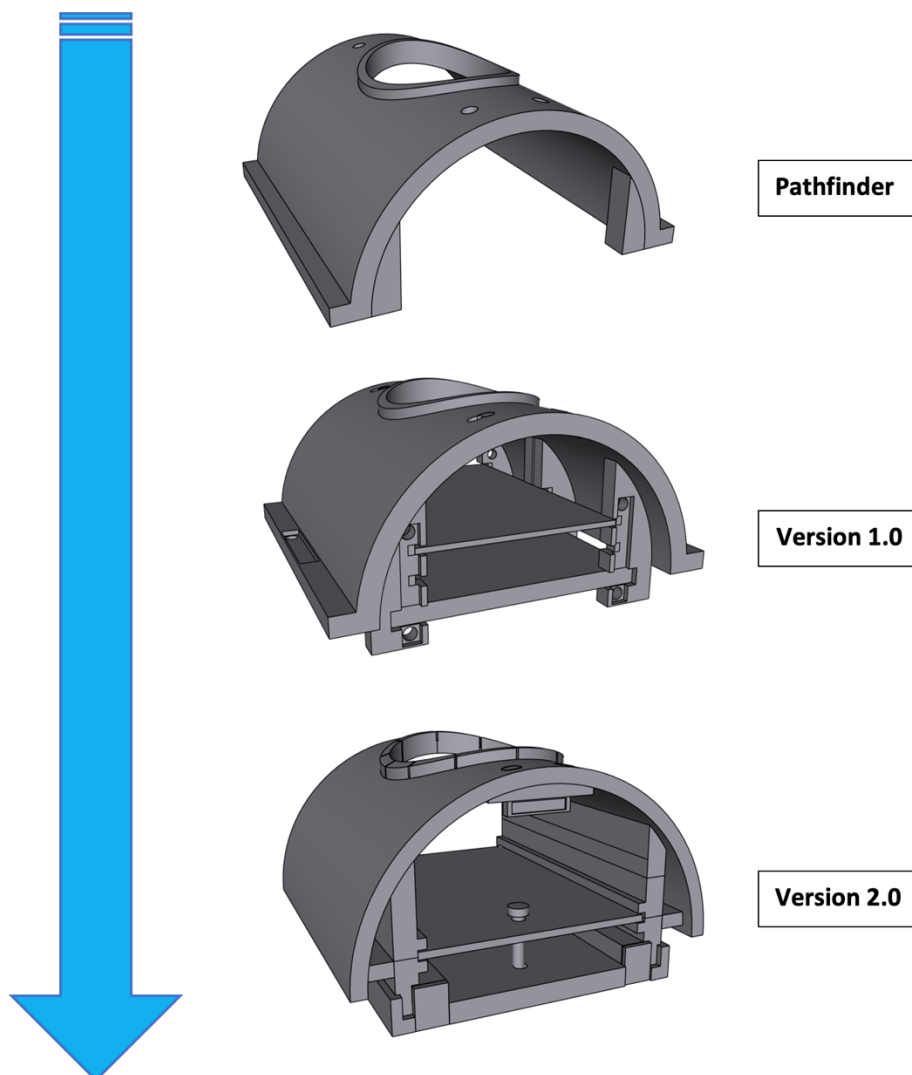


Figure 38 – Evolution of the simulator's design from the first prototype to Version 2.0.

9.2 Final version: “Congenital TrainHeart”

To replicate the pediatric chest wall, we created a half-cylinder with an oval opening thus simulating a median sternotomy with a sternal retractor in place. This structure generates a chest wall cavity where a lower support completes the simulator with two height levels, designed to fit different sizes of 3D printed heart models used during training sessions. This simulator design can be printed in only one piece, improving stability and limiting the need for additional small, printed items like those needed in the previous design.

The 3D-printed models are fixed on a 160 mm x 111 mm, 3.5 mm thick tablet that sits in the chest cavity. The tablet can then be secured to the simulator with a pin to avoid involuntary movements of the models during the procedure. A single hole is

placed under the simulator base to attach it to a tripod with an M6 screw, thus allowing the trainee to perform the surgery in the same position as in the operating room.

At the upper margin of the opening simulating the median sternotomy, a suture retraction ring is placed to accommodate the surgeon's need for sutures to be held securely.

The ring was designed with 12 equally spaced slits around the circumference to allow sutures to be held securely in place.



Figure 39 - Final version of the simulator. The top images show how the simulator appear in the CAD 3D software window while in the bottom image the printed simulator is visible. Inside the chest-wall two led bars are applied to increase light exposure of the model.

9.3 Accessories

In addition to the main simulator body, some additional accessories were also designed to simulate different surgical approaches other than median sternotomy. These items consist of “Covers” that, by attaching to the suture retraction ring, modify the shape, dimensions, and position of the upper opening on the chest wall, thus allowing the simulation of mini-invasive approaches to the heart such as mini-sternotomy (central, upper and lower), left posterolateral mini-thoracotomy, and right axillary mini-thoracotomy. Moreover, thanks to the fact that the simulator can be tilted, a more accurate heart exposure can be archived.



Figure 40 -In this picture the cover for lower/upper mini-sternotomy applied to chest opening is visible. The cover modifies the opening at the top of the chest wall, simulating different surgical approaches.

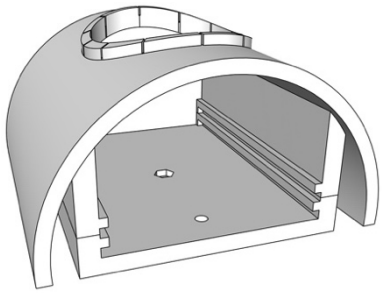
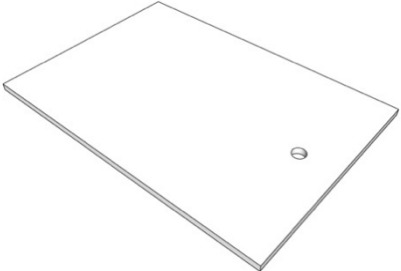
An external suture retraction ring to be placed on top of the cover if many sutures are used and need to be held in place was also developed. While all the covers are printed with elastic resin, making it possible to stretch the opening to reach a better exposure of the target, the external suture retraction ring is printed with clear resin. In this final design, lighting and recording devices can be attached to the chest wall surface to allow surgical procedures to be recorded or live supervised by a tutor. Additional lighting devices are placed inside the chest to provide better illumination.

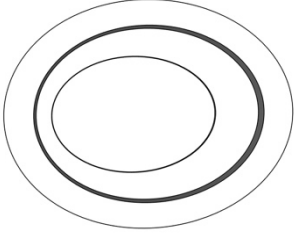
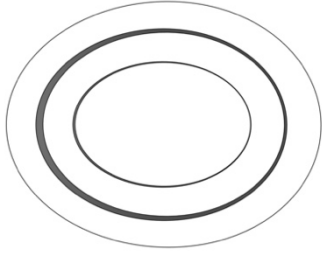
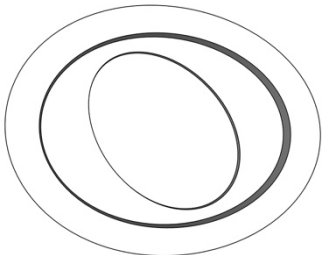
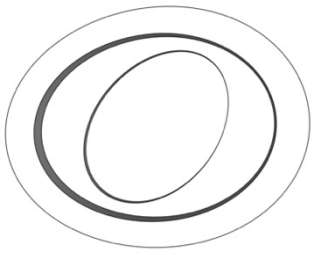


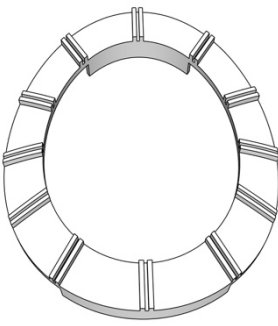
Figure 41 - Congenital TrainHeart attached to the tripod with the external light and webcam allowing surgical procedure to be recorded or live supervised by a tutor.

In the following table, all 3D printable components are summarized.

Table I – 3D printable components

	Item and material	Function
	Simulator's main body - Clear Resin	This structure simulates the chest of the patient approached with a median sternotomy. The simulator can be attached to a tripod enabling height and position adjustments.
	Standard platform - Clear Resin	The standard platform can be inserted at different height levels inside the simulator and supports the different models need to perform the simulation.
	Pin - Clear Resin	The pin can be inserted through the platform and the base of the chest wall simulator thus preventing involuntary movements of the models during the procedure.

	<p>Cover 1: Upper/Lower Mini sternotomy - Elastic Resin</p>	<p>This cover, when applied at the top of the chest wall allows the simulation of an Upper or Lower mini sternotomy approach</p>
	<p>Cover 2: Central Mini-sternotomy - Elastic Resin</p>	<p>This cover, when applied at the top of the chest wall allows the simulation of a central mini sternotomy approach</p>
	<p>Cover 3: Right axillary minithoracotomy - Elastic Resin</p>	<p>This cover, when applied at the top of the chest wall allows the simulation of a right axillary minithoracotomy approach</p>
	<p>Cover 4: left posterolateral minithoracotomy - Elastic Resin</p>	<p>This cover, when applied at the top of the chest wall allows the simulation of a left posterolateral minithoracotomy</p>

	<p>External suture retraction ring</p> <p>-</p> <p>Elastic Resin</p>	<p>This external ring can be placed on the top of the covers if many sutures are used and need to be held in place</p>
---	--	--

9.4 Future directions

Even if the final version described above has already been printed and used for training purposes, many features will likely change in the future since the developing process is still ongoing. Some potential improvements could, in fact affect materials, models used for simulation, and the simulator itself.

A critical feature of our simulator is multimodality, allowing, thanks to different configurations and platforms, to simulate not only different procedures but also different approaches. This aspect comes with the disadvantage of needing a potentially high number of different platforms to simulate all types of procedures, resulting in a reduction of portability, one of the characteristics we defined as crucial in the developing process. What we are aiming to archive in the next future is to develop what we call “a universal platform” where only one tablet comes with the simulator and all supporting items, such as the octagonal pillars (See next chapter), can be re-arranged on the surface to accommodate all types of low fidelity and high fidelity models. We believe we can reach this result by creating a platform with different holes on the surface where all items can be arranged on top of it in various configurations. This modification would increase even more the portability of our simulator while, at the same time, reducing resin consumption leading to a consequent reduction of the total cost for each item. One other improvement regards the structure of the simulator itself: during the first training sessions, surgeons suggested including a surface where to place surgical instruments when not used since, with our latest version, no such structure is present. It’s likely that in the

following versions, such a commodity will be current, increasing the overall experience of the simulation.

In the months to come, the second aspect we will be focusing on is to develop a new valid low and intermediate fidelity model to expand the spectrum of procedures that can be performed with “Congenital TrainHeart”. We are aiming to archive enough models to perform both intracardiac and extracardiac defect correction, allowing the trainee to be prepared for as many types of surgeries as possible, making this simulator a valid tool for surgical training. In addition, in developing new types of models, we are exploring a wide variety of materials in order to improve not only the number but also the quality of our printed hearts. With the constant improvement of materials available and the printing process, we hope to be able soon also to replicate the texture of real tissues.

As stated before, one of the limitations of 3D reconstruction is that valvular and subvalvular structures cannot be adequately visualized and reconstructed, resulting in the absence of all these anatomical features in our 3D printed hearts. We expect in the future, with the evolution of cardiac imaging techniques and 3D reconstruction software, to be able to include them in the models to come.

10. Models and surgical procedures

10.1 Purse strings and central cannulation

One of the basic skills a cardiac surgeon must develop is the ability to establish cardiopulmonary bypass (CBP), connecting the patient to the heart-lung machine. CBP is, in fact, used for both congenital or acquired heart surgery for intracardiac repair and when cardiac mechanical arrest is needed. Two alternatives are available, depending on what kind of surgery the patient needs and what kind of approach the surgeon chooses: central and peripheral cannulation.

The “Central cannulation model” was developed from an ECG gated CT scan acquisition and printed with elastic resin. Once the model is inserted inside the chest wall, the trainee can perform all steps necessary to establish CBP, such as aortic and venous pursestring and cannulation.

The aortic cannulation site is usually located at the level of the pericardial reflection beneath the origin of the innominate artery, thus leaving enough space for the aortic

clamp placement and the cardioplegia cannulation site. Positioning is even more important when procedures are performed on the aortic valve or on the ascending aorta. When the site has been identified, it can be marked with a marking pen. At this point, one or two diamond-shaped pursestring sutures are placed with a 4.0 non-absorbable suture. Even if the resin material all models are made of does not adequately simulate the arterial wall texture and organization, it should be considered that all these sutures should be placed via partial-thickness bites into the tunica media in the adult and into the adventitia in the pediatric patient. Once the pursestring is placed, an 11 blade is used to create a transverse aortotomy to accommodate the cannula. After its insertion, the pursestrings are tightened and secured to the cannula.

For what concerns venous cannulation, both atrial appendage cannulation and bicaval cannulation can be performed with our model. In the former, a single circumferential 4-0-pursestring is placed encircling the right atrial appendage; at this point, a cannula is inserted into the atrium directed towards the inferior vena cava. In the latter two pursestrings are placed in both superior and inferior vena cava while right-angled or straight cannulae are placed into SVC and IVC. Also, caval snares can be placed. In a real patient, this last step is required to minimize both blood return into the surgical field and air entrainment in the CBP circuit.

In addition, also cardioplegia line cannulation and left atrial or ventricular vent positioning can be performed on the model. To allow for an aortic cross-clamp placement, the antegrade cardioplegia cannulation site must be selected proximally to the aortic cannula. In this case, a pledgeted 4-0 polypropylene horizontal mattress suture is placed, allowing for puncture with the cardioplegia needle. Whereas for what concerns left atrium/ventricle venting, a single pursestring should be placed in the right superior pulmonary vein, allowing the venting catheter placement. (68,69)

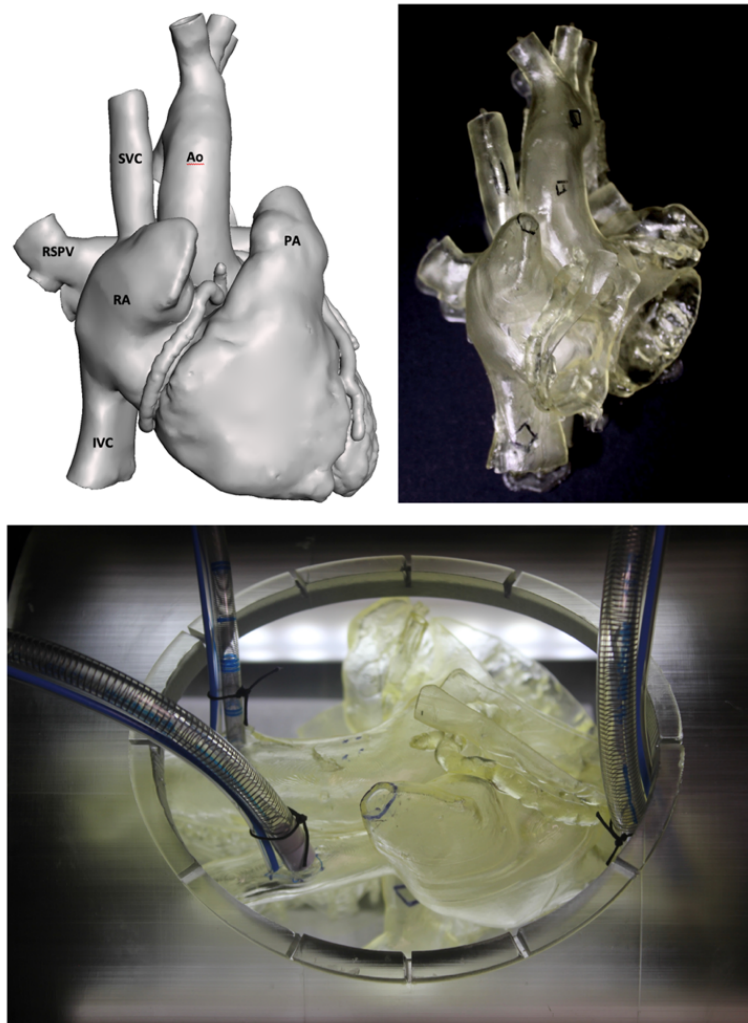


Figure 42 - Cannulation model. In the upper part of the image the 3D model for surgical cannulation is visible. Ventricles are not printed to optimize resin consumption. In the lower part the model inside the simulator with central cannulation performed can be appreciated. SVC: Superior Vena Cava; IVC: inferior Vena Cava; RA: Right Atrium; Ao: Aorta; PA: Pulmonary Artery; RSPV: Right Superior Pulmonary Vein.

10.2 Patch positioning

The “Patch positioning” platform is one of our low fidelity models designed to develop basic surgical skills. This item consists of a variant of the standard tablet, with four octagonal pillars on top of it supporting a rectangle-shape resin patch with an oval hole in its center simulating a schematic ASD or VSD. This patch has four holes in its margin allowing it to be secured to the octagonal pillars, stabilizing it and avoiding unintentional displacement of the patch itself. This platform aims to

close the hole in the center by suturing an oval patch using the same technique needed for ASD and VSD closure. Skills acquired with this model are fundamental to perform the ASD/VSD closure procedure in the intermediate fidelity models (See section 10.4).

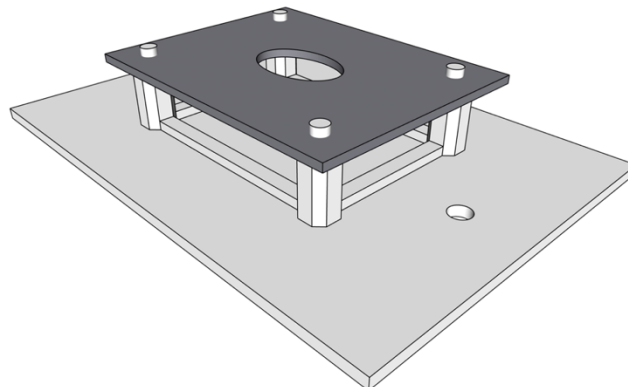


Figure 43- Patch positioning model

10.3 Vascular anastomosis

Vascular anastomosis is one of the basic skills a surgeon should master to control every procedure safely. In congenital heart surgery, this skill is fundamental in all surgeries where an end-to-end or an end-to-side anastomosis is required. In order to allow surgeons to train this skill, we developed a low fidelity model consisting of two cylinders printed with elastic resin that can be anastomosed in an end-to-end or an end-to-side fashion. The first type of anastomosis is generally used in congenital heart surgery when one of the great vessels is transected and needs to be reattached or, in the acquired heart surgery field, for example, in all cases where

the aorta is substituted with a prosthesis due to dilation or dissection. The end-to-side anastomosis is used in many procedures such as the Modified BT shunt placement or the Bidirectional Glenn procedure, where the SVC is connected to the right branch of the pulmonary artery. It's also interesting to underline that in the third surgical step required to reach the Fontan Circulation, both these anastomoses are utilized: the end-to-end type is needed to connect the IVC to the prosthetic conduit whether the end-to-side is employed in the connection of the conduit to the right branch of the pulmonary artery.

It should otherwise be considered that, since the diameter of the printed cylinders is around 2 cm, this model is not suitable for training on coronary anastomosis for which smaller conduits and smaller needles are, in fact, needed; however, a specific platform has been developed for this purpose (see section 10.7).

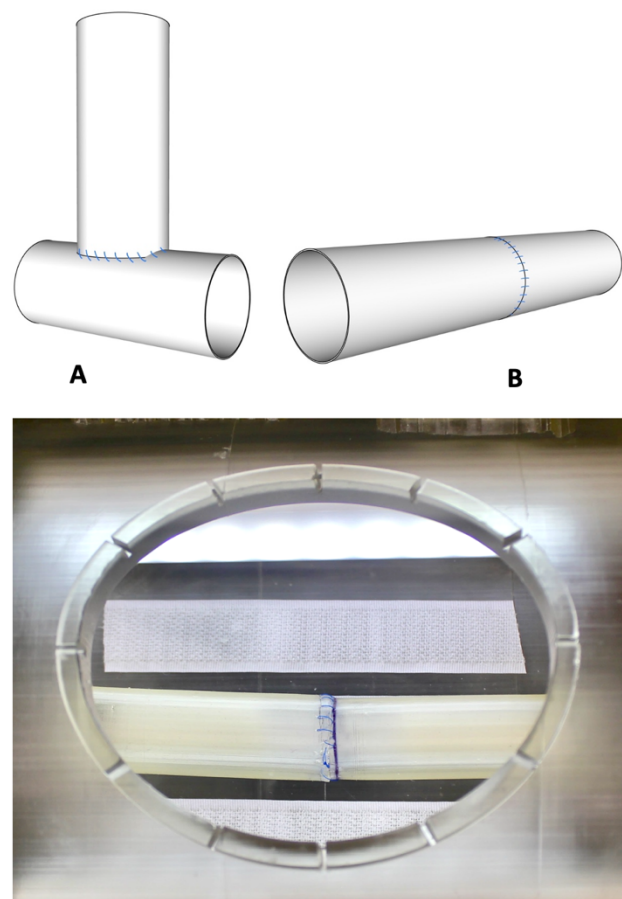


Figure 44 – Vascular anastomosis model. *A: End-to-side anastomosis; B: end-to-end anastomosis. In the bottom image the printed model anastomosed in an end-to-end fashion can be visualized.*

10.4 ASD, VSD closure

Atrial septal defects and ventricular septal defects are both very common congenital heart defects and consist of an anomalous formation of the atrial or ventricular septum resulting in communication between the right and the left chambers of the heart. The “ASD and VSD closure model” was developed from an ECG gated CT scan acquisition of a patient with an ostium secundum ASD. While the Atrial defect was present in the scanned heart, the VSD was added in the developing process. The choice of including both defects allows the execution of two procedures in the same model, thus optimizing both the printing process and resin consumption. In addition, due to the presence of great vessels, cannulation can also be performed, thus simulating all surgical steps.

The model is designed to perform an ostium Secundum ASD closure with a patch, a technique typically used when a large round defect is present; in this case, in fact, direct suturing of the defect can lead to closure under tension or distortion of the normal atrial anatomy.

For what concerns the ventricular septal defect, as stated before, in this model a perimembranous VSD is present. In this case, this platform aims to simulate a VSD closure procedure with a transatrial approach, opening the right atrium and placing the patch through the ostium of the tricuspid valve.

For this kind of procedure, a medial atriotomy is usually performed from the base of the right atrial appendage and extends parallel to the right coronary artery. Once the atrium has been incised, stay sutures are usually placed to guarantee a good exposure of the tricuspid valve orifice. An important limitation of this model is the fact that, due to software limitations, we are still unable to reconstruct and print valvular leaflets. The absence of the tricuspid valve allows better exposure of the interventricular septum, making it easier for the surgeon to reach the defect. Despite this aspect, the procedure in our model is still challenging. However, due to the constant improvement of software quality and materials, we expect to be able soon to integrate AV and semilunar valves in our models, thus increasing the simulation quality. (68,69)

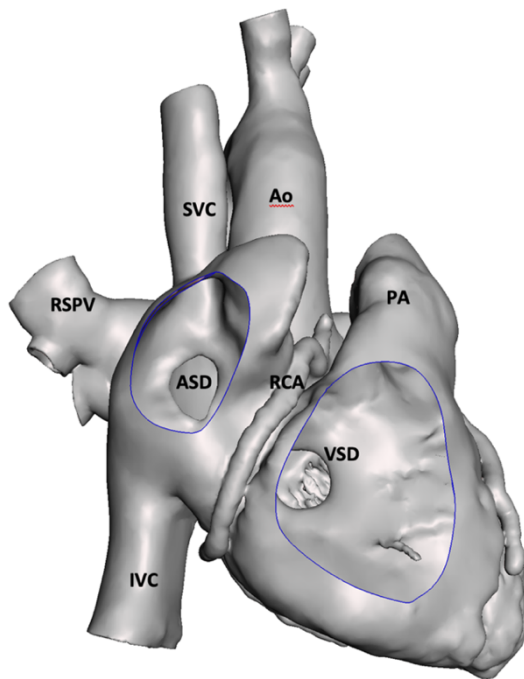


Figure 45 – ASD-VSD model. SVC: Superior Vena Cava; IVC: inferior Vena Cava; RA: Right Atrium; Ao: Aorta; PA: Pulmonary Artery; RSPV: Right Superior Pulmonary Vein; ASD: Atrial Septal defect; VSD: Ventricular Septal Defect; RCA: Right Coronary Artery.



Figure 46 – ASD-VSD model with both atrial and ventricular patch in place. Part of the right atrium was removed to better appreciate the repaired ASD and VSD. A transatrial approach was chosen to repair both defects. Tricuspid valve's leaflets are missing due to printing limitations.

10.5 Sinus venosus ASD

Sinus venosus atrial septal defect is a condition generally associated with Partial Anomalous Pulmonary Venous Connection (PAPVC), where one of the pulmonary veins does not develop correctly, draining blood into the right atrium instead of into the left one. Ninety percent of the PAPVCs are right-sided, seven percent left-sided, and two percent bilateral.(70) Compared to the typical ostium secundum ASD, superior sinus venosus ASD is located more superior and posterior, with the pulmonary vein usually draining at the level of the junction of the SVC and right atrium.

The “Sinus venosus ASD” model was developed from an ECG gated CT scan acquisition and printed with elastic resin with the aim of simulating both Baffle and Warden repair techniques. The first one is performed when the pulmonary vein drain to the cavo-atrial junction area, while the second one is preferred when the pulmonary veins enter in an area up to the SVC or the SVC is smaller than usual, as it usually happens due to the presence of a persistent left SVC.

For what concerns the Baffle repair technique, the first step of the procedure consists of a longitudinal right atrial excision that can extend on the proximal part of the SVC to expose the defect. In doing so, the surgeon must be careful not to damage the sinus node. Of course, in our model, ECG anomalies deriving from damaging the sinus node cannot be detected. Still, the trainee should incise the atrium laterally to better simulate the real exposure of the intracardiac structures. Once the defect has been exposed, a patch is placed and sutured to close the defect and redirect blood flow from the anomalous pulmonary vein into the left atrium. In shaping the patch, it should be considered that a slightly redundant one is preferable to avoid obstruction of the pathway. At the end of the procedure, if the incision of the right atrium has involved the SVC, the atriotomy closure can be augmented with a patch in order to avoid stenosis of the SVC-right atrial junction.

In the Warden procedure, in addition to closing the defect and redirecting blood flow to the left atrium, the SVC is transected and, after its mobilization, it is anastomosed to the right atrial appendage. After transection of the SVC, the cardiac end must be oversewn. Since this model consists of a whole heart, a simulation of cannulation can also be performed before starting with the simulation of the two procedures described above. (68,69)

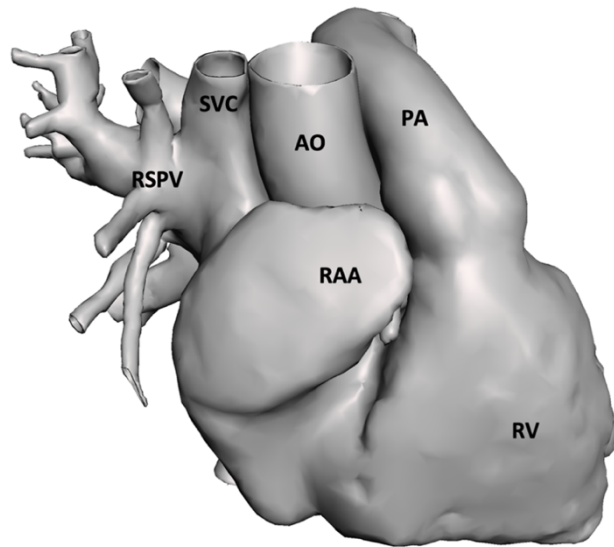


Figure 47 – Sinus venosus Atrial Septal defect model. SVC (Digital): Superior Vena Cava; IVC: inferior Vena Cava; RA: Right Atrium; Ao: Aorta; PA: Pulmonary Artery; RSPV: Right Superior Pulmonary Vein.

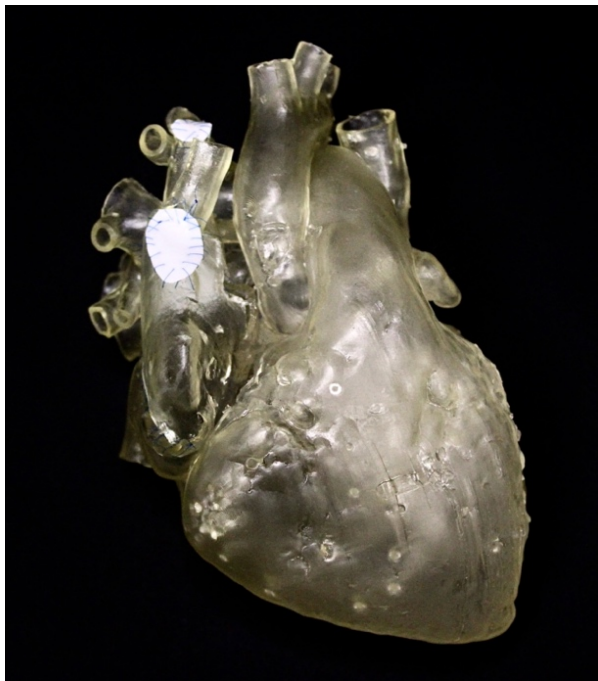


Figure 48 –Printed Sinus venosus Atrial Septal Defect model after Warden procedure. The new position of the SVC is visible in addition to the patch used to enlarge the SVC-atrial junction. This model also presented a Persistent Left superior vena cava draining into the coronary sinus.

10.6 Coarctation of the aorta

Coarctation of the aorta, also called aortic narrowing, is a congenital condition whereby the aorta is narrow, usually in the area where the ductus arteriosus (ligamentum arteriosum after regression) inserts(71). In this condition, the prognosis varies from severe heart failure in infancy to asymptomatic hypertension in older children and adults, while the treatment consists of surgical or transcatheter intervention. For the surgical treatment, many options can be taken under consideration depending on the severity of the pathology itself.

The Aortic Coarctation model was developed from an ECG gated CT scan acquisition and printed with elastic resin. The model includes only the distal half of the aortic arch, pulmonary artery, and the PDA, thus simulating the left posterolateral thoracotomy exposure. In this case, all supports needed to print the aortic coarctation are not removed, requiring the surgeon to mobilize the aorta as it happened in the real surgery. One of the main challenges in developing this model was to find an optimal wall thickness to allow the execution of the procedure and, at the same time, print all structures without internal supports.

Whether many techniques are available to treat this condition, this model was designed for practicing the resection with end-to-end anastomosis. In this technique, after exposure of the aorta and PDA through retraction of the lung and incision of the parietal pleura, the aorta is dissected and mobilized from near structures; sometimes, also ligation and section of intercostal arteries are necessary. At this point, if the Ductus arteriosus is patent, it is ligated; in our model a PDA is present, and this step must be performed before proceeding, thus allowing the surgeon to also train on the PDA ligation and closure. At this point, two claps are placed: an angled clamp should be positioned proximally across the left carotid and the left subclavian artery leaving otherwise the innominate artery patent allowing cerebral perfusion while closing the aortic arch, and the second one distally across the descending aorta. Once claps are in place, the narrowed segment is excised and an end-to-end anastomosis is performed with a double-armed polypropylene suture. When the anastomosis is complete, the distal clamp can be released, and the de-airing process takes place before gently and slowly releasing also the proximal clamp, re-establishing normal blood flow through the aorta. (68,69)



Figure 49 - Coarctation of the aorta. Only the aorta and the Pulmonary artery are printed in this model to optimize resin consumption. The Patent ductus arteriosus is also visible.

10.7 CABG platform for distal anastomosis

Coronary artery bypass graft is a surgical procedure with the aim of restoring blood flow into an obstructed or partially obstructed coronary artery. This surgery is usually performed with a median sternotomy approach and can be “On-Pump”, where the heart is stopped after connecting to the heart-lung machine, and “Off-pump”, with the beating heart. In CABG all main branches of both right and left coronary arteries can be targeted if needed, with the Left anterior descending (LAD), the Posterior interventricular artery (PIVA), and the Left marginal artery (LMA) the most common involved branches. For what concerns the conduit selection, three main grafts are used: Internal thoracic artery (ITA), Radial Artery, and Saphenous vein. Also, the right gastroepiploic artery and the inferior epigastric artery can be utilized.(68,69)

Since this kind of surgery is one of the most common in the acquired heart disease surgery spectrum of procedures, we developed a platform that can be used for

CABG anastomosis training. This Platform, named “CABG platform,” is one of our low fidelity models/platforms and consists of a variation of the standard tablet that comes with the simulator. In this rectangular-shaped tablet, four octagonal pillars of different heights are present on which 3D printed hollow cylinders can be secured, thus simulating coronary arteries.

The tablet is printed with Clear resin, resulting in a solid structure, while the small conduits with a diameter of 3 mm used to simulate both coronary arteries and arterial or venous conduits are printed with elastic resin.

As shown in *Fig.50*, this platform can be set in different configurations, thus simulating the distal anastomosis procedure in three different coronary branches: the left anterior descending artery, the posterior interventricular artery, and the Left Marginal Artery (branch of the circumflex artery). When loading a printed coronary artery in the “C-D configuration”, it’s possible to simulate an end-to-side anastomosis between the LAD and a selected conduit, usually the ITA. Point “C” and point “D” are placed at the same height at a distance of 5 cm, resulting in the conduit being placed parallel to the tablet’s base in a caudocranial direction.

When loading the coronary artery in the “E-F configuration”, it’s possible to simulate an end-to-side anastomosis between the Left Marginal artery, branch of the circumflex artery, and the conduit used for bypassing the obstruction, which is usually represented by the saphenous vein. In this configuration, point “E” and point “F” are placed at a distance of 5 cm but at different heights resulting in the coronary artery being placed at a ninety-degree angle compared to the LAD and tilted 45 degrees from the tablet’s base, thus modifying also the surgeon's approach to the anastomosis.

The last option is represented by the “A-B configuration” which aims to simulate the Posterior descending artery (branch of the left or right coronary artery, depending on the coronary arterial dominance). Also, in this case, point “A” and point “B” are placed at different heights resulting in the coronary artery being tilted 45 degrees from the base of the tablet but, as in the LAD configuration, in a caudocranial disposition. The Posterior descending artery, in fact, in real-life surgery, is usually exposed by moving the apex of the heart in a cranial direction. Therefore, in this platform, point “A” represents the distal part of the PIVA while point “B” its proximal part.

One limitation of this platform is represented by the fact that, since there is no structure to secure the conduit (which is being anastomosed to the simulated coronary artery), the assistant is required to hold the conduit itself while the trainee performs the anastomosis.

In all three configurations, once the coronary artery has been placed on the platform, the anterior wall is incised with a 15-blade scalpel being careful not to damage the posterior wall. At this point, the incision is enlarged with an angled scissor to 4-6 mm for the end-to-side anastomosis (while for the side-to-side the length should be between 3 to 5 mm). The distal end of the conduit is then incised longitudinally for approximately 20% longer than the coronary arteriotomy and is then anastomosed onto the coronary artery using a running 7-0 polypropylene suture.

Another limitation of this platform is the absence of a structure that simulates the aorta, making it impossible to perform the proximal vein graft anastomosis; however, we aim to develop also a high fidelity model for CABG in the future, thus making this possible.

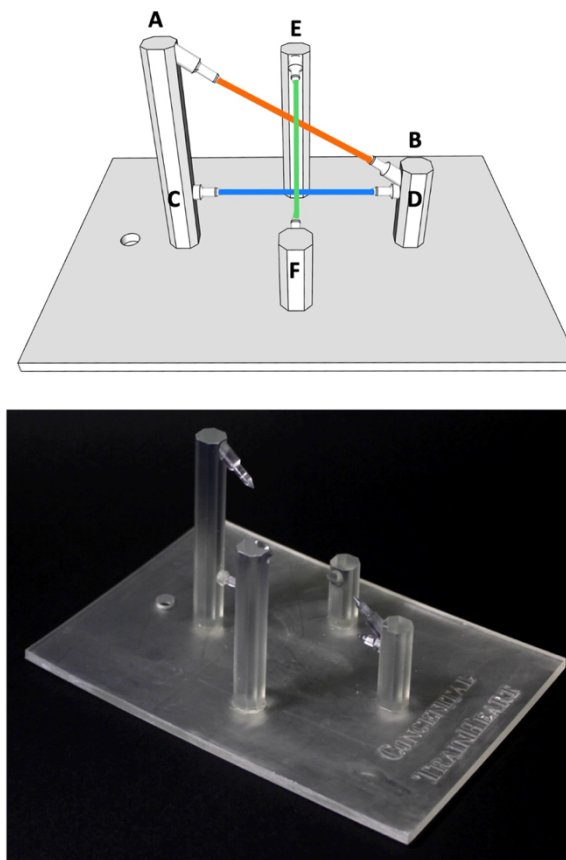


Figure 50 - CABG model. In the upper image the blue line represent the anterior descending coronary artery, the green one the left marginal and the orange the posterior descending artery.

10.8 Surgical aortic valve replacement

In addition to the CABG platform, we created this second model for acquired heart disease training. Aortic valve replacement is one of the most performed heart surgeries in adults since the aortic valve pathology, which includes both Aortic stenosis (AS) and aortic insufficiency (AI), is widespread in the adult/elderly population. AS is more often observed in elderly patients due to the degenerative calcific modification of the AV, with an esteemed 2-7% of the population over 65 years developing this condition. An exception is represented by patients with a bicuspid aortic valve (approximately 1-2% of the population) which appears to be more prone to calcific degeneration, leading to AS at a younger age. One other cause of AS is rheumatic disease, which has been largely eradicated in the western world.

On the other hand, AI can result from primary diseases such as AV calcific degeneration, endocarditis, and congenital anomalies or can be determined by dilation of the aortic root or basal ring as in case of aortic aneurism, aortic dissection, or connective tissue disorders. Both patients with AS and AI can benefit from surgical aortic valve replacement. Regarding aortic valve substitutes, available options are represented by mechanical and biological valves, both with specific risks and benefits.

The AVR model was obtained by designing a hollow cylinder with a dilation on its middle portion, thus simulating the ascending aorta with the aortic root. In the basal part of the aortic root, three cusps reconstructed from a CT scan were added. Also, two coronary arteries were placed at the level of the right and left coronary sinuses. Once the aortic model was ready, we reconstructed a mechanical aortic valve prosthesis from a CT scan. Both the aortic model and the AV prosthesis were printed with elastic resin. Usually, after cardiopulmonary bypass is established and the aorta is cross clamped, an aortotomy is performed to expose the valve. In our model, since only the first tract of the aorta is present, there is no need to perform this step. Once the valve is exposed, leaflets are resected en bloc, and further debridement is performed to eliminate all calcific residues from the annulus. The annulus is then sized, and an appropriate prosthesis is chosen. To implant the prosthesis usually pledgeted ticon 2-0 stitches are used. Four or five pledgets per sinus are normally placed on the aortic side of the annulus and once all sutures are

in place in the sewing ring, the prosthesis is lowered onto the annulus and the sutures are tied. Care should be taken not to obliterate the coronary ostia, which should be visible once the new valve is in place. At this point, the aorta is closed with a 4-0 polypropylene suture, de-airing is performed, and the cross-clamp is then removed. In some cases, it's possible to enlarge the aortic annulus. This additional step is performed by incising the annulus or, in some cases, also the anterior leaflet of the mitral valve; the obtained space is then filled with a diamond-shaped patch made of Dacron or Bovine pericardium.

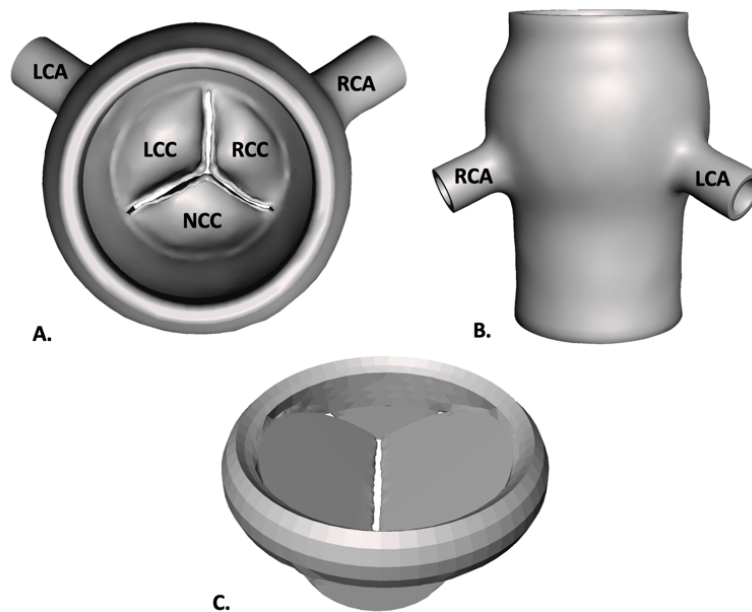


Figure 51 – Aortic root and mechanical valve. Both versions, digital at the top, and printed at the bottom are visible. A: top view of the aortic root. B: frontal view of the aortic root. C: mechanical aortic valve prosthesis. LCA: Left Coronary Artery. RCA: right coronary artery; LCC: left coronary cusp; RCC: right coronary cusp; NCC: non coronary cusp.

Our model allows the trainee to perform leaflet resection, valvular placement, and also annulus enlargement, which are the most challenging steps in this type of surgery. This model is still under development since we aim to reconstruct and print also a bioprosthetic aortic valve. We are also discussing the possibility of incorporating this AV model in a complete 3D printed heart to enhance the fidelity of the simulation requiring the surgeon to perform all steps needed for this surgery, from cannulation to aortotomy, closure, and de-airing. (68,69)

10.9 Surgical Planning

Surgical planning is a fundamental process that takes place before the surgery with the aim of defining all surgical steps required to correct a CHD. For this purpose, in most cases, the image dataset is mainly based on echocardiography, CT scans, and MRI sequences which all provide bidimensional images. In some cases, the software used as image viewer can automatically provide a 3D reconstruction of the heart from CT or MRI sequences; this reconstruction, though, in most cases, is low quality and does not provide a valuable tool to evaluate the anatomical relationship between structures. In this scenario, the surgeon must derive spatial information from 2D imaging, and, most of the time, the procedure is decided directly in the OR when the heart is exposed, and anatomical relationships can be evaluated directly by the surgeon. To improve surgical planning, in our center, since 2019, patient-specific 3D models produced from CT or MRI sequences have been used. These 3D models are usually printed with clear resin and utilized to decide the best approach during surgical planning. Some other times, the model doesn't get printed, and VR is used instead. All these 3D tools help the surgeon to better understand the patient's anatomy allowing for a better planning before the surgery. In patients needing a second surgery, 3D reconstructions are also used in our center to evaluate the relationship between the sternum and cardiac structures, such as the right ventricle or the great vessels. In these cases, in fact, entering the mediastinum with a median sternotomy can be more complex and dangerous due to scar tissue and adhesions that can modify the original disposition of the structure underneath the sternum.

Since the simulator "Congenital TrainHeart" is now available, 3D patient-specific models can now be printed and the procedure can be simulated prior to the real

surgery on the patient's heart. This approach is extremely useful, in particular for rare CHDs; in these cases, in fact, the procedure needed for the correction can be tried at first on the model, helping the surgeon to become confident with every step required for the surgery, increasing the possibility for a successful intervention and resulting eventually in a much quicker surgery so decreasing risks associated with cardiopulmonary bypass time. Studies to assess if this practice can effectively impact patient outcomes will be done in the future, but surgeons who have already tried this approach expressed a positive opinion. As stated in the previous sections, our simulator can simulate many approaches, from median sternotomy to mini-thoracotomy, making it usable in the most varied situations.

Our simulator has been used now in many cases for surgical planning, but we were able to exploit its full potential for one in particular. The patient was a six-year-old girl with a prenatal diagnosis of AVSD complete form. She was born at 39 + 5 w (GA), and after four months she developed bronchiolitis caused by metapneumovirus and, due to her unstable conditions (overlap of cardiogenic and septic shock), she was admitted to the ICU. During the hospitalization, in association with ventilatory and circulatory support, a transesophageal echocardiography was performed, showing the following result: PFO with an accelerated left to right shunt, accelerated blood flow in the pulmonary veins due to the increased perfusion of the lungs and a complete AVSD (Rastelli type A) with a large inlet type VSD partially obstructed by the insertion of the cordae. The VSD also affected the outlet region of the septum. Also, a Double Outlet Right Ventricle was identified. For what concerned valves, the right AV valve showed moderate insufficiency while the left one presented a small mural leaflet due to the presence of two papillary muscles positioned very close to each other and rotated counterclockwise. Aorta and Aortic valves appeared normal with the absence of coarctation.

The AVSD-DORV is an extremely rare condition, with just a few cases diagnosed and treated each year. For this reason, before proceeding with the corrective surgery, the patient underwent a CT scan (executed with contrast medium), and the DICOM files were utilized to obtain a 3D model of the heart. Two copies of the model were then printed with Elastic resin, and the surgery was then simulated two times by cardiac surgeons two days before the real surgery. In this particular case, the procedure consisted of a radical correction of the AVSD by positioning a PTFE

fenestrated patch used to tunnel the LVOT towards the aorta, while the ASD ostium primum type had to be closed using heterologous pericardium. In addition, the cleft on the anterior leaflet of the left AV valve needed to be repaired, and a plasty of the right AV valve was necessary. Due to the absence of the AV valves in the 3D model, only the first part of the procedure could be performed during the simulation; it has otherwise to be considered that the second part of the surgery is a much more common procedure. The surgery on the patient was successful, with post-operative echocardiography showing a residual calibrated VSD, mild residual regurgitation of both right and left AV valves, and no RVOT/LVOT residual obstruction.

During the post-operative recovery in the ICU the patient showed good hemodynamics but developed an infection of the surgical wound. After resolving the infection, the patient was discharged in good general conditions.

This case showed the applicability of the technology we developed in planning surgical procedures for rare cases of CHD.

V. DISCUSSION

11. A new era for Congenital heart surgery training

Congenital Heart surgery is a relatively young specialty and, whether the first decades were dedicated to developing new techniques, the focus nowadays is on perfecting procedures and improving patient outcomes. In this scenario, hands-on surgical training is playing today and will play in the future a fundamental role in surgeons' training in order to improve their skills, reducing, as a consequence, complications deriving from lack of experience. Development and standardization of CHS education will help to create an environment where junior surgeons can clinically mature and improve their technical skills (72–76). Simulation provides a platform whereby deliberate practice can occur without consequences and allows an individual to master a technique in a safe and non-stressful environment.

3D printing technologies for simulation are starting to be extensively used for both training and surgical planning in cardiac surgery. Even if just a few data are available, some studies in this field have already been published. Haoshi et al. (77), for example, reported no mortality, surgical heart blocks, or systemic ventricular outflow obstruction in 20 cases where the surgeon, before the intervention, rehearsed the surgery using a simulator in their center in Osaka; of course, it appears difficult to define if these outcomes are totally due to the simulation, but results like the one shown in this case appear encouraging.

One important center that has been intensively working on 3D printing in the last few years is the “Sick Kids Hospital” in Toronto, where a team led by dr. Yoo has brought important innovation in pediatric cardiac surgery simulation. They, in fact developed many 3D printed heart models in addition to a chest wall simulator(60) and they were also able to organize one of the first courses entirely based on 3D printing, named “HOST-course” (Hands-On Surgical Training). From their experience, as reported by Hussein et al., we know that simulation can positively impact both the surgeon's ability to perform one surgical procedure and the time needed for this purpose. (61)

Therefore, we believe that by developing a simulator that can be used in any environment and the fact that the surgeon can perform complex procedures in an inconsequential environment where instruction, practice, and feedback can be constantly provided and replicated, it will be possible to rehearse operations and teach new techniques for both congenital and acquired heart surgery. Another advantage is that thanks to this tool, surgeons in training can also exercise at home, simulating the OR environment and overcoming the need for a wet lab to train far from the operating table. Wherever the trainee decides to use the simulator, all procedures can be live supervised by a tutor thanks to the webcam attached on the top of the chest wall that allows the surgeon to record the training to identify areas of improvement.

The simulator “Congenital TrainHeart” was patented with the contribution of the University of Padova in December 2021 and first trialed at the “30th annual meeting of the Italian Society of Cardiac Surgery” in Rome with ten cardiac surgeons participating. All surgeons agreed on the fact that this simulator could help in both developing surgical skills and planning a patient-specific procedure. During this event, all surgeons performed a coarctectomy using our “Aortic Coarctation” model. Also, eight simulators were used during the 8th edition of the "International School of Cardiac Surgery" held in Erice, Sicily (Italy) in April 2022. In this case, we decided to bring two different models, the aortic coarctation model and the “CABG platform for distal anastomosis”, allowing participants to train on both congenital and acquired heart disease procedures.

By intensively using this simulator, we hope that residents, both junior and senior, will develop before the real surgery on the patient, a deep knowledge of all the steps the procedure requires, in addition to improving surgical skills, leading to a much more useful and safer surgical practice on the real the patient.

Furthermore, the fact that any 3D model can be fitted inside “Congenital TrainHeart” allows for simulating a wide variety of procedures, from basic purse-string and cannulation to complex CHD surgeries leading not only to a more precise operation but also to a quicker one, both positive aspects for the patient considering how prolonged cross-clamp and cardiopulmonary bypass times appear to be independent predictors of morbidity and mortality (78).

Thanks to the constant development of new 3D heart models, our simulator will be used for a hands-on course for residents as an additional learning tool.

Current limitations in the 3D- printing techniques and materials limit the inclusion of flow circuits with 3D-printed heart models; however, other centers have attempted to overcome this, making it a tangible reality. It is expected that with the ongoing improvements in printing materials, this is the next step in the simulation field.

Thanks to the rapid evolution of materials and printing techniques, 3D heart models will be able to better simulate not only the anatomy but also the texture of the heart walls and arteries allowing a much more accurate simulation of the procedures.

12. Advantages

The fact that “CongenitalTrainheart” was initially designed only for pediatric cardiac surgery simulation led to obtaining a compact item with small overall dimension (175 x 170 x 100 mm). In addition to the low weight, this characteristic allows portability, making it possible for the trainee to move the simulator and train also at home. It should also be considered that the fact that the simulator has been designed with a surface where a webcam can be attached enables live supervision by a tutor that can potentially be anywhere in the world. One other alternative is represented by the possibility of recording the procedure , rewatching it later, alone or with a tutor, to better understand what can be improved, increasing the overall value of the simulation process. Also, if the trainee is performing one specific procedure for the first time, the tutor can explain what needs to be done step by step, leading to a deeper understanding of all steps required. In addition to all these, also surgical planning can benefit from the possibility of live broadcasting a procedure: different surgeons could, in fact, without meeting in person, discuss the best approach to a specific patient while operating on the patient-specific 3D printed heart model, all this, potentially enabling an international team to discuss the most complicate cases for each center.

Whereas this last usage has not been tested yet, in our center, thanks to the number of simulators we have produced so far, residents can already borrow a simulator and some models to train at home.

One other positive aspect of our simulator is the fact that new 3D heart models are constantly produced. This aspect is fundamental since surgeons need to be prepared to face many different conditions. For what concerns the rarest ones, it is in fact

unlikely to be exposed to a sufficient number of cases to master the procedure needed to correct it. The increasing spectrum of models that will be available makes this simulator suitable not only for residents but also for experienced surgeons who want to try a specific surgical procedure before actually performing it in the OR. It should in fact be considered that congenital heart diseases are a broad group of conditions characterized by intra-individual variability, resulting in each surgery being slightly different also between patients with the same condition. In this scenario, the possibility of trying the procedure before operating on the real heart can lead to a better patient outcome.

The versatility of our simulator, in association with the fact that any model can be fitted inside it, also enables training for acquired heart conditions such as CABG or surgical aortic valve replacement.

Costs represent the last positive aspect of our simulator. We were, in fact, able to develop the simulator and models with a limited amount of money. Also, the fact that all items are fully printable with a 3D printer makes it more affordable compared to other 3D simulators available on the market, making it possible for centers with limited funds to take advantage of this product. (See section 11.4 for details).

13. Disadvantages and Limitations

“Congenital TrainHeart” has shown to be a precious tool in surgical training, even if its development is not concluded yet. However, we are aware that some disadvantages and limitations are present.

First of all, model production is not a simple process and is time-consuming. Creating a new 3D model (see section 7.2) can require several hours, depending on the complexity of the anatomy and the quality of the images. Once the STL is ready, it has to be printed for the first time to verify that wall thickness is adequate and that supports needed for printing are positioned correctly. Once the model has been washed in IPA and cured under UV light, a surgeon tries to perform the specific procedure using the model to validate it, allowing its “mass production”. All these steps can require several days, if not weeks, to be completed, making it very difficult to develop more than one model at a time. The same considerations apply to low fidelity models. It should also be considered that if CT/MRI images are not

adequate to extract a 3D model, nothing can be done and it's necessary to wait to find another patient with that same anatomy.

Image resolution is another problem we have to face. As reported in the previous paragraphs, due to image resolution limitations, it's impossible, most of the time, to reconstruct valvular and subvalvular structures, in addition to coronary arteries, that are visible only when the proper amount of contrast medium is used and when 0.5 mm slices are acquired. Due to these limitations, our models come without semilunar and AV valves. The impossibility of including these anatomical features jeopardies the possibility of developing high fidelity models for some CHD, such as the AVSD, where the presence of valve leaflets is fundamental when simulating the surgical correction. In some other cases otherwise, such as for extracardiac defects, all this doesn't represent a problem. One possible solution we are discussing to overcome this limitation consists in designing and printing standard valves and coronaries to apply to our models after the printing process.

One other significant limitation of our 3D models is the material they are made of. The Elastic resin we are using allows to cut, retract and suture the models, but its consistency doesn't resemble cardiac tissues. For this reason, even if the model is anatomically precise, the feeling the surgeon has while performing the surgery is different compared to the one in real life, thus reducing the fidelity of the simulation. We are aware of this limitation, and, even if we believe that the main aim of our simulator is to help surgeons develop a deeper awareness of all steps required in a procedure, we are trying to find new material that better fits our needs. This next step would, in fact, improve the overall quality of the simulation. For example, at the "Sick Kids Hospital" in Toronto, Canada, the elastic resin materials used for their first models have been substituted with materials such as Polyvinyl alcohol (PVA). However, changing the material required a modification also in the production process of the 3D models. In their center, in fact, all parts of the heart, including valvular and subvalvular structures, are produced separately, using 3D printed molds that are filled with PVA and then assembled. Even if the final result is more realistic for what concerns the model's texture, being this process way more complex and time-consuming, it cannot be applied right now to our center due to lack of personnel and facilities and, last but not least, lack of resources.

14. Cost analysis

In order to design a simulator, some type of CAD (Computer Assisted Design) software is mandatory. Our choice was a tablet-based tool called Shapr3D (Siemens®, Parasolid®, Budapest, Hungary) due to the intuitive graphical interface and the simplicity of its usage. For this software, the full license costs between 210 € to 450 € depending on the plan you are purchasing, however, both educational licenses and a 14 days trial versions are also available.

The second cost that must be considered for both the development phase and the production phase is represented by 3D printing itself and it is split between hardware and consumables. There are many different 3D printing technologies available, our choice was a SLA-based printer. In SLA 3D printing, the parts are not immediately ready to use after their creation and they must undergo a cleaning and curing process. Thus, hardware is constituted by the 3D printer and the machines and tools for post-processing. Our printer is a Form3L by Formlabs (Formlabs, Somerville, USA) and has a nominal cost of about 11.000 euros. A wash machine and a curing machine made by Formlabs are also available for purchase, but we decided to use a third-party product that combines both machines into one, the Anycubic Wash and Cure Plus (HongKong AnyCubic Technology Co., HongKong, China), that costs about 250 euros.

The consumables include parts that need replacement after a certain number of uses, such as resin tanks, and substances like photopolymer resin, used as starting material, and isopropyl alcohol (IPA), used as washing solvent.

The resin we used to print all prototypes and that we are still using to produce the final version of the simulator, is the Clear Resin V4™, also made by Formlabs, which costs approximately 120€/L, while isopropyl alcohol is about 5 €/L. As a rule of thumb, five liters of IPA are used to wash parts made with two liters of Clear Resin. Each simulator requires 900 to 1000 mL of resin, we can then estimate a consumable cost of around 150 euros.

To print low and intermediate-fidelity models we use the Elastic Resin V1™. This resin costs 190€/L and due to the fact that each model requires a different amount of material to be printed, the cost can vary between 10 € to 30 € for each item.

In order to develop and print 3D heart models necessary for the surgical simulation, additional costs must be considered such as the price of the reconstruction software.

Medical imaging is also a cost, but in most cases imaging suitable for 3D reconstruction is already acquired for clinical purposes and can be used to create 3D models free of charge.

For our models, the reconstruction was made using the software Mimics inPrint 3.0 (Materialise NV, Leuven, Belgium). Many different license plans are available and we choose a three-year plan that costs about 10.000 euros.

VI. CONCLUSIONS

The development of the simulator “Congenital TrainHeart” can be considered as the peek of our experience in the 3D printing field so far, offering residents a brand-new low-cost learning tool that can support the long learning process needed to acquire all the skills a cardiac surgeon requires. The low production cost of the simulator, in addition to its portability, makes it an accessible tool for all surgeons in training. Even if both simulators and models are still under development, after a few months of usage, they have proven to be a valuable learning tool to improve manual skills required in the OR.

The constant development of new models and the new materials we are exploring will undoubtedly translate in more advanced 3D models in the near future, improving the validity of the simulation.

Moreover, the possibility of creating patient-specific models has proven to help experienced surgeons during the surgical procedure, especially when a CHD is rare and the surgeon has a limited experience in that specific surgery. Also, thanks to all the accessories we developed, not only procedures in median sternotomy, but also mini-invasive approaches can be rehearsed.

The development of this simulation represents the starting point for developing an annual course for residents where the main surgical procedures, for both congenital and acquired heart diseases, are taught by experienced surgeons and rehearsed by surgeons in training.

With training limitations being a global problem for congenital heart surgeons, it is expected that simulators like these will be increasingly utilized in surgical training worldwide to improve surgical skills resulting in better patient outcomes.

BIBLIOGRAPHY

1. Bruneau BG. The developmental genetics of congenital heart disease. *Nature* [Internet]. 2008 Feb 21;451(7181):943–8.
2. Warnes CA. The adult with congenital heart disease: Born to be bad? Vol. 46, *Journal of the American College of Cardiology*. 2005. p. 1–8.
3. Pierpont ME, Basson CT, Benson DW, Gelb BD, Giglia TM, Goldmuntz E, et al. Genetic basis for congenital heart defects: Current knowledge - A scientific statement from the American Heart Association Congenital Cardiac Defects Committee, Council on Cardiovascular Disease in the Young. Vol. 115, *Circulation*. 2007. p. 3015–38.
4. Jenkins KJ, Correa A, Feinstein JA, Botto L, Britt AE, Daniels SR, et al. Noninherited risk factors and congenital cardiovascular defects: Current knowledge - A scientific statement from the American Heart Association Council on Cardiovascular Disease in the Young. *Circulation*. 2007 Jun;115(23):2995–3014.
5. Moretti A, Caron L, Nakano A, Lam JT, Bernshausen A, Chen Y, et al. Multipotent Embryonic *Isl1*⁺ Progenitor Cells Lead to Cardiac, Smooth Muscle, and Endothelial Cell Diversification. *Cell*. 2006 Dec 15;127(6):1151–65.
6. Tzahor E. Wnt/ β -Catenin Signaling and Cardiogenesis: Timing Does Matter. Vol. 13, *Developmental Cell*. 2007. p. 10–3.
7. Garg V, Muth AN, Ransom JF, Schluterman MK, Barnes R, King IN, et al. Mutations in *NOTCH1* cause aortic valve disease. *Nature*. 2005 Sep 8;437(7056):270–4.
8. Stalsberg H, DeHaan RL. The precardiac areas and formation of the tubular heart in the chick embryo. *Dev Biol*. 1969 Feb;19(2):128–59.
9. Tam PP, Parameswaran M, Kinder SJ, Weinberger RP. The allocation of epiblast cells to the embryonic heart and other mesodermal lineages: the role of ingression and tissue movement during gastrulation. *Development*. 1997 May;124(9):1631–42.
10. Inagaki T GMVSG. Regulative ability of the prospective cardiogenic and vasculogenic area of the primitive streak during avian gastrulation. In 1993. p. 57–8.
11. Kirby ML, Waldo KL. Neural crest and cardiovascular patterning. *Circ Res*. 1995 Aug;77(2):211–5.

12. Besson Iii WT, Kirby ML, van Mierop LHS, Robert J, Ii T. Effects of the size of lesions of the cardiac neural crest at various embryonic ages on incidence and type of cardiac defects [Internet].
13. Waldo KL, Kumiski D, Kirby ML. Cardiac neural crest is essential for the persistence rather than the formation of an arch artery. *Dev Dyn*. 1996 Mar;205(3):281–92.
14. Nishibatake M, Kirby ML, van Mierop LH. Pathogenesis of persistent truncus arteriosus and dextroposed aorta in the chick embryo after neural crest ablation. *Circulation*. 1987 Jan;75(1):255–64.
15. Kirby ML, Gale TF, Stewart DE. Neural crest cells contribute to normal aorticopulmonary septation. *Science*. 1983 Jun 3;220(4601):1059–61.
16. Kirby ML, Hunt P, Wallis K, Thorogood P. Abnormal patterning of the aortic arch arteries does not evoke cardiac malformations. *Developmental Dynamics*. 1997 Jan;208(1):34–47.
17. Thiene G, Frescura C. Anatomical and pathophysiological classification of congenital heart disease. In: *Cardiovascular Pathology*. 2010. p. 259–74.
18. Osler W. *The Principles and Practice of Medicine*. D. Appleton and Company, editor. 1893.
19. Taylor AJ, Cerqueira M, Hodgson JM, Mark D, Min J, O’Gara P, et al. ACCF/SCCT/ACR/AHA/ASE/ASNC/NASCI/SCAI/SCMR 2010 Appropriate Use Criteria for Cardiac Computed Tomography. A Report of the American College of Cardiology Foundation Appropriate Use Criteria Task Force, the Society of Cardiovascular Computed Tomography. *J Am Coll Cardiol*. 2010 Nov 23;56(22):1864–94.
20. Lee J, Kim TH, Lee BK, Yoon YW, Kwon HM, Hong BK, et al. Diagnostic accuracy of low-radiation coronary computed tomography angiography with low tube voltage and knowledge-based model reconstruction. *Sci Rep*. 2019;9(1):1308.
21. Lawley CM, Broadhouse KM, Callaghan FM, Winlaw DS, Figtree GA, Grieve SM. 4D flow magnetic resonance imaging: role in pediatric congenital heart disease. Vol. 26, *Asian Cardiovascular and Thoracic Annals*. SAGE Publications Inc.; 2018. p. 28–37.
22. Bichell DP, Geva T, Bacha EA, Mayer JE, Jonas RA, del Nido PJ. Minimal access approach for the repair of atrial septal defect: the initial 135 patients. *Ann Thorac Surg*. 2000 Jul;70(1):115–8.
23. Cherup LL, Siewers RD, Futrell JW. Breast and pectoral muscle maldevelopment after anterolateral and posterolateral thoracotomies in children. *Ann Thorac Surg*. 1986 May;41(5):492–7.

24. Laussen PC, Bichell DP, McGowan FX, Zurakowski D, DeMaso DR, del Nido PJ. Postoperative recovery in children after minimum versus full-length sternotomy. *Ann Thorac Surg*. 2000 Feb;69(2):591–6.
25. Rashkind WJ, Miller WW. Creation of an atrial septal defect without thoracotomy. A palliative approach to complete transposition of the great arteries. *JAMA*. 1966 Jun 13;196(11):991–2.
26. Jacobs JP, O'Brien SM, Pasquali SK, Jacobs ML, Lacour-Gayet FG, Tchervenkov CI, et al. Variation in outcomes for risk-stratified pediatric cardiac surgical operations: an analysis of the STS Congenital Heart Surgery Database. *Ann Thorac Surg*. 2012 Aug;94(2):564–72.
27. Jacobs JP, O'Brien SM, Pasquali SK, Jacobs ML, Lacour-Gayet FG, Tchervenkov CI, et al. Variation in outcomes for benchmark operations: An analysis of the society of thoracic surgeons congenital heart surgery database. *Annals of Thoracic Surgery*. 2011 Dec;92(6):2184–92.
28. Jacobs JP, O'Brien SM, Pasquali SK, Kim S, Gaynor JW, Tchervenkov CI, et al. The importance of patient-specific preoperative factors: an analysis of the society of thoracic surgeons congenital heart surgery database. *Ann Thorac Surg [Internet]*. 2014; 98(5):1653–9.
29. Vinocur JM, Menk JS, Connett J, Moller JH, Kochilas LK. Surgical volume and center effects on early mortality after pediatric cardiac surgery: 25-year North American experience from a multi-institutional registry. *Pediatr Cardiol*. 2013 Jun;34(5):1226–36.
30. Kempny A, Dimopoulos K, Uebing A, Diller GP, Rosendahl U, Belitsis G, et al. Outcome of cardiac surgery in patients with congenital heart disease in England between 1997 and 2015. *PLoS One*. 2017 Jun 1;12(6).
31. Spector LG, Menk JS, Knight JH, McCracken C, Thomas AS, Vinocur JM, et al. Trends in Long-term Mortality after Congenital Heart Surgery. *J Am Coll Cardiol [Internet]*. 2018 May 29;71(21):2434.
32. Zachow S, Zilske M, Hege HC. Konrad-Zuse-Zentrum für Informationstechnik Berlin ZIB-Report 07-41 (Dezember 2007) 3D reconstruction of individual anatomy from medical image data: Segmentation and geometry processing. 2007.
33. McCue T. Significant 3D Printing Forecast Surges To \$35.6 Billion. Accessed June 10, 2020. <https://www.forbes.com/sites/tjmccue/2019/03/27/wohlers-report-2019-forecasts-35-6-billion-in-3d-printing-industry-growth-by-2024/#5f496a9d7d8a>.
34. Petzold R, Zeilhofer HF, Kalender WA. Rapid prototyping technology in medicine--basics and applications. *Comput Med Imaging Graph*. 1999 Oct; 23(5):277–84.

35. He W, Tian K, Xie X, Wang X, Li Y, Wang X, et al. Individualized Surgical Templates and Titanium Microplates for the Fort i Osteotomy by Computer-Aided Design and Computer-Aided Manufacturing. *Journal of Craniofacial Surgery*. 2015 Sep 1;26(6):1877–81.
36. Derby B. Printing and prototyping of tissues and scaffolds. *Science* [Internet]. 2012 Nov 16;338(6109):921–6. Available from: <https://pubmed.ncbi.nlm.nih.gov/23161993/>
37. Kasza KE, Rowat AC, Liu J, Angelini TE, Brangwynne CP, Koenderink GH, et al. The cell as a material. *Curr Opin Cell Biol*. 2007 Feb; 19(1):101–7. Available from: <https://pubmed.ncbi.nlm.nih.gov/17174543/>
38. Murphy S v., Atala A. 3D bioprinting of tissues and organs. *Nat Biotechnol*. 2014; 32(8):773–85. Available from: <https://pubmed.ncbi.nlm.nih.gov/25093879/>
39. Skardal A, Mack D, Kapetanovic E, Atala A, Jackson JD, Yoo J, et al. Bioprinted amniotic fluid-derived stem cells accelerate healing of large skin wounds. *Stem Cells Transl Med* [Internet]. 2012 Nov 1;1(11):792–802. Available from: <https://pubmed.ncbi.nlm.nih.gov/23197691/>
40. Cui X, Breitenkamp K, Finn MG, Lotz M, D’Lima DD. Direct human cartilage repair using three-dimensional bioprinting technology. *Tissue Eng Part A* [Internet]. 2012 Jun 1;18(11–12):1304–12. Available from: <https://pubmed.ncbi.nlm.nih.gov/22394017/>
41. Duan B, Hockaday LA, Kang KH, Butcher JT. 3D bioprinting of heterogeneous aortic valve conduits with alginate/gelatin hydrogels. *J Biomed Mater Res A*. 2013 May;101(5):1255–64. Available from: <https://pubmed.ncbi.nlm.nih.gov/23015540/>
42. Norotte C, Marga FS, Niklason LE, Forgacs G. Scaffold-free vascular tissue engineering using bioprinting. *Biomaterials*. 2009 Oct;30(30):5910–7. Available from: <https://pubmed.ncbi.nlm.nih.gov/19664819/>
43. Chang R, Nam J, Sun W. Direct cell writing of 3D microorgan for in vitro pharmacokinetic model. *Tissue Eng Part C Methods*. 2008; 14(2):157–66. Available from: <https://pubmed.ncbi.nlm.nih.gov/18544030/>
44. Xu F, Celli J, Rizvi I, Moon S, Hasan T, Demirci U. A three-dimensional in vitro ovarian cancer coculture model using a high-throughput cell patterning platform. *Biotechnol J*. 2011 Feb; 6(2):204–12. Available from: <https://pubmed.ncbi.nlm.nih.gov/21298805/>
45. Barron JA, Ringeisen BR, Kim H, Spargo BJ, Chrisey DB. Application of laser printing to mammalian cells. In 2004. p. 383–7.
46. Brown TD, Dalton PD, Hutmacher DW. Direct writing by way of melt electrospinning. *Adv Mater*. 2011 Dec 15; 23(47):5651–7. Available from: <https://pubmed.ncbi.nlm.nih.gov/22095922/>

47. Saidy NT, Shabab T, Bas O, Rojas-González DM, Menne M, Henry T, et al. Melt Electrowriting of Complex 3D Anatomically Relevant Scaffolds. *Front Bioeng Biotechnol.* 2020 Jul 24;8. Available from: <https://pubmed.ncbi.nlm.nih.gov/32850700/>
48. Dalton PD, Woodfield TBF, Mironov V, Groll J. Advances in Hybrid Fabrication toward Hierarchical Tissue Constructs. *Advanced science (Weinheim, Baden-Wurttemberg, Germany).* 2020 Jun 1;7(11). Available from: <https://pubmed.ncbi.nlm.nih.gov/32537395/>
49. West JL & HJA. J.A. Polymeric biomaterials with degradation sites for proteases involved in cell migration. In 1999. p. 241–4.
50. Noor N, Shapira A, Edri R, Gal I, Wertheim L, Dvir T. 3D Printing of Personalized Thick and Perfusable Cardiac Patches and Hearts. *Advanced science (Weinheim, Baden-Wurttemberg, Germany) [Internet].* 2019; 6(11). Available from: <https://pubmed.ncbi.nlm.nih.gov/31179230/>
51. Asulin M, Michael I, Shapira A, Dvir T. One-Step 3D Printing of Heart Patches with Built-In Electronics for Performance Regulation. *Advanced science (Weinheim, Baden-Wurttemberg, Germany).* 2021 May 1; 8(9). Available from: <https://pubmed.ncbi.nlm.nih.gov/33977062/>
52. Sekhar A, Sun MR, Siewert B. A tissue phantom model for training residents in ultrasound-guided liver biopsy. *Acad Radiol [Internet].* 2014; 21(7):902–8. Available from: <https://pubmed.ncbi.nlm.nih.gov/24928159/>
53. Guariento A, Cattapan C, Chemello E, Bertelli F, Padalino M, Reffo E, et al. 3D reconstruction for preoperative planning of partial anomalous pulmonary venous return. *Kardiol Pol.* 2021 Nov 30;79(11):1271–3. Available from: <https://pubmed.ncbi.nlm.nih.gov/34643265/>
54. Hussein N, Honjo O, Haller C, Hickey E, Coles JG, Williams WG, et al. Hands-On Surgical Simulation in Congenital Heart Surgery: Literature Review and Future Perspective. *Seminars in Thoracic and Cardiovascular Surgery.* 2020 Mar 1;32(1):98–105.
55. Mavroudis CD, Mavroudis C, Jacobs JP, DeCampi WM, Tweddell JS. Simulation and Deliberate Practice in a Porcine Model for Congenital Heart Surgery Training. *The Annals of Thoracic Surgery.* 2018 Feb 1;105(2):637–43.
56. Yamada T, Osako M, Uchimuro T, Yoon R, Morikawa T, Sugimoto M, et al. Three-Dimensional Printing of Life-Like Models for Simulation and Training of Minimally Invasive Cardiac Surgery. 2017.
57. Raemer DB. Simulation in cardiothoracic surgery: A paradigm shift in education? Vol. 138, *Journal of Thoracic and Cardiovascular Surgery.* 2009. p. 1065–6.

58. Ribeiro IB, Ngu JMC, Lam BK, Edwards RA. Simulation-Based Skill Training for Trainees in Cardiac Surgery: A Systematic Review. Vol. 105, *Annals of Thoracic Surgery*. Elsevier USA; 2018. p. 972–82.
59. Hussein N, Honjo O, Haller C, Coles JG, Hua Z, van Arsdell G, et al. Quantitative assessment of technical performance during hands-on surgical training of the arterial switch operation using 3-dimensional printed heart models. *Journal of Thoracic and Cardiovascular Surgery*. 2020 Oct 1;160(4):1035–42.
60. Peel B, Voyer-Nguyen P, Honjo O, Yoo SJ, Hussein N. Development of a dynamic Chest Wall and operating table simulator to enhance congenital heart surgery simulation. *3D Printing in Medicine*. 2020 Dec;6(1).
61. Hussein N, Honjo O, Haller C, Coles JG, Hua Z, van Arsdell G, et al. Quantitative assessment of technical performance during hands-on surgical training of the arterial switch operation using 3-dimensional printed heart models. *Journal of Thoracic and Cardiovascular Surgery*. 2020 Oct 1;160(4):1035–42.
62. Yoo SJ, Hussein N, Peel B, Coles J, Arsdell GS van, Honjo O, et al. 3D Modeling and Printing in Congenital Heart Surgery: Entering the Stage of Maturation. Vol. 9, *Frontiers in Pediatrics*. Frontiers Media S.A.; 2021.
63. Shapr3D Brings Direct 3D Modeling (and Sketching) to iPad Pro - SolidSmack [Internet]. Available from: <https://www.solidsmack.com/cad/shapr3d-parametric-3d-modeling-app-ipad-pro/>
64. The World's Most Intuitive 3D Design App | Shapr3D [Internet]. [cited 2022 Mar 29]. Available from: <https://www.shapr3d.com/>
65. Why Shapr3D Changes the iPad Pro Story From Toy to Tool. Available from: <https://architosh.com/2018/03/why-shapr3d-changes-the-ipad-pro-story-from-toy-to-tool/>
66. Pro CAD on an iPad Pro? | Engineering.com [Internet]. Available from: <https://www.engineering.com/story/pro-cad-on-an-ipad-pro>
67. Using Elastic 50A Resin. Available from: https://support.formlabs.com/s/article/Using-Elastic-Resin?language=en_US
68. Thomas L. Spray, Michael A. Acker. Rob & Smith's - Operative Cardiac Surgery. Sixth Edition. CRC Press, editor. 2019.
69. Frank W. Sellke, Pedro J. del Nido, Scott J. Swanson. Sabiston & Spencer - Surgery of the Chest. 9th ed. Elsevier, editor. Vol. Volume 1-2. Philadelphia; 2016.

70. Alsoufi B, Cai S, van Arsdell GS, Williams WG, Caldarone CA, Coles JG. Outcomes after surgical treatment of children with partial anomalous pulmonary venous connection. *Ann Thorac Surg.* 2007 Dec; 84(6):2020–6. Available from: <https://pubmed.ncbi.nlm.nih.gov/18036929/>
71. Groenemeijer BE, Bakker A, Slis HW, Waalewijn RA, Heijmen RH. An unexpected finding late after repair of coarctation of the aorta. *Neth Heart J [Internet].* 2008;16(7–8):260–3. Available from: <https://pubmed.ncbi.nlm.nih.gov/18711614/>
72. Beckerman Z, Mery CM. Teaching congenital heart disease: A new era? *The Journal of Thoracic and Cardiovascular Surgery.* 2017 Jun 1;153(6):1541.
73. Karl TR, Jacobs JP. Paediatric cardiac surgical education: Which are the important elements? *Cardiology in the Young.* 2016 Dec 1; 26(8):1465–70.
74. Dearani JA. Invited Commentary. *The Annals of Thoracic Surgery.* 2018 Feb 1;105(2):643–4.
75. cardiovascular SHS in thoracic and, 2020 undefined. Does practice make perfect? pubmed.ncbi.nlm.nih.gov/; Available from: <https://pubmed.ncbi.nlm.nih.gov/31400401/>
76. Burkhart HM. Simulation in congenital cardiac surgical education: We have arrived. *Journal of Thoracic and Cardiovascular Surgery.* 2017 Jun 1;153(6):1528–9. Available from: <http://dx.doi.org/10.1016/j.jtcvs.2017.03.012>
77. Hoashi T, Ichikawa H, Nakata T, Shimada M, Ozawa H, Higashida A, et al. Utility of a super-flexible three-dimensional printed heart model in congenital heart surgery. *Interactive Cardiovascular and Thoracic Surgery.* 2018 Nov 1;27(5):749–55.
78. Al-Sarraf N, Thalib L, Hughes A, Houlihan M, Tolan M, Young V, et al. Cross-clamp time is an independent predictor of mortality and morbidity in low- and high-risk cardiac patients. *Int J Surg.* 2011;9(1):104–9. Available from: <https://pubmed.ncbi.nlm.nih.gov/20965288/>

Ringraziamenti

“Circondati di persone che credono nei tuoi sogni, che sostengono le tue idee, che incoraggiano le tue ambizioni, che fanno esaltare il meglio di te.”

A tutti coloro che hanno creduto in me

A chi mi seguirà nel viaggio che sta per iniziare

GRAZIE